UAB
Universitat Autònoma de Barcelona

Proteomic insights into the immune response of rice plants to M. oryzae infection

María Ribaya Muñoz

UNIVERSIDAD AUTÓNOMA DE BARCELONA
Facultad de Biociencias
Doctorado en Biología y Biotecnología Vegetal

Ph. D. Thesis

Proteomic insights into the immune response of rice plants to *M. oryzae* infection

María Ribaya Muñoz
Barcelona, November 2023

UAB
Universitat Autònoma
de Barcelona

CRAG
CENTRE FOR RESEARCH
IN AGRICULTURAL GENOMICS

UNIVERSIDAD AUTÓNOMA DE BARCELONA
Facultad de Biociencias
Doctorado en Biología y Biotecnología Vegetal

Proteomic insights into the immune response of rice plants to *M. oryzae* infection

Dissertation presented by María Ribaya for the degree of Doctor of Biology and Plant Biotechnology by the *Universitat Autònoma de Barcelona*.
This work was performed at the Center for Research in Agricultural Genomics.

Dr. Blanca San Segundo
Thesis director

Dr. Roser Tolra Pérez
Tutor

María Ribaya Muñoz
Author

A mis mentores, Juan Antonio y Adrián

From the depths of my heart, I want to express my profound gratitude to all of you. This journey has been a remarkable one, not only for the knowledge gained but for the extraordinary souls I've had the privilege to meet along the way. You have been the guiding lights that have made this path truly special.

“A ti podría decirte
que para mí
cualquier lugar
es mi casa
si eres tú
quien abre
la puerta.”

Elvira Sastre

Index

Abbreviations

ABA	Abscisic acid
BIC	Biotrophic interfacial complex
CA buffer	Apoplast extraction buffer
CBB	Coomassie brilliant blue staining
CDPK	Calcium-dependent protein kinase
CEBiP	Chitin elicitor-binding protein
D14	SL receptor DWARF 14
DAMPs	Damage-associated molecular patterns
DTT	Dithiothreitol
EIHM	Extra-invasive hyphal membrane
ET	Ethylene
ETI	Effector-triggered immunity
FDR	False discovery rate
FRET	Fluorescence resonance energy transfer
GO	Gene Ontology
HR	Hypersensitive response
InsP	Inositolphosphates
JA	Jasmonic acid
MAPK	Mitogen-activated protein kinase
MAPKK	Mitogen-activated protein kinase kinase
MAPKKK	Mitogen-activated protein kinase kinase kinase
MDH	Malate dehydrogenase
miRNAs	microRNAs
MOPS	3-(N-morpholino) propanesulfonic acid
NERICA	New Rice for Africa

OsCERK1	Rice chitin elicitor receptor kinase 1
P1BS	Phosphoinositide-binding site
PAMPs	Pathogen-associated molecular patterns
PEPRs	PEP receptors
PEPs	Plant elicitor peptides
PHO1	PHOSPHATE1
PHO2	Phosphate over accumulator 2
PHR	PHOSPHATE STARVATION RESPONSE transcription factors
PHT	Phosphate Transporter
PR	Pathogenesis-related proteins
PROPEPs	Precursor Peps
PRRs	Pattern recognition receptors
PSI	Phosphate starvation-induced
PSR	Phosphate Starvation Response
PTI	PAMP-triggered immunity
ROS	Reactive oxygen species
RuBisCO	Ribulose-1.5-bisphosphate carboxylase/oxygenase
SA	Salicylic acid
SDEL1	RING-finger ubiquitin E3 ligase
SLs	Strigolactones
TLCK	Tosyl-L-lysyl-chloromethane hydrochloride
TPCK	Tosyl phenylalanyl chloromethyl ketone
Xoo	*Xanthomonas oryzae*

Summary

Plants face a constant array of environmental stresses, including biotic and abiotic challenges, which significantly impact crop yields. Biotic stresses originate from living organisms such as fungi, oomycetes, bacteria, viruses, nematodes, insects, and weeds, while abiotic stresses encompass factors like salinity, drought, extreme temperatures, flooding, radiation, nutrient limitations, and heavy metal toxicity. Given their immobile nature, plants have developed intricate mechanisms to confront these stresses, involving the activation of signal transduction pathways and subsequent transcriptional reprogramming of gene expression. In this context, plants in their natural habitat continually grapple with both biotic and abiotic stresses, significantly compromising their productivity. Research efforts have primarily centered on understanding plant responses to individual stressors. When plants experience a combination of stress factors, it can lead to complex outcomes due to crosstalk between the respective signaling pathways. Over the course of evolution, plants have developed intricate mechanisms to combat pathogen infections, resulting in a substantial body of literature and data detailing the transcriptional reprogramming of gene expression in response to pathogen attack. There is also evidence to suggest that plant immune responses can be post-translationally regulated through protein phosphorylation. However, our understanding of the specific proteins and phosphorylation events involved in the crosstalk between pathogen-induced signaling pathways and nutrient signaling in plants remains limited. Furthermore, the nutritional status of a plant has been shown to influence disease resistance. Phosphorus is an essential nutrient for plant growth and development. Plants acquire this nutrient from the soil in the form of inorganic phosphate (Pi). The low bioavailability of Pi in agricultural soils

represents a limiting factor for plant growth. Consequently, Pi fertilizers are routinely used in modern agriculture to optimize crop yields, leading to a scenario of Pi excess in many agricultural ecosystems. At the molecular level, a large effort has been made to understand how plants adapt to Pi limiting conditions through the so called Phosphate Starvation Response (PSR). Less information is available on adaptive mechanisms to Pi excess in plants.

In this Ph. D. Thesis, we investigated the effect of Pi on the response of rice plants to pathogen infection at the proteomic level, as well as Pi-mediated mechanism underlying disease resistance/ susceptibility in rice. In **Section 1** we described the dual impact of phosphate content in rice leaves on both the rice plant and the fungal pathogen *Magnaporthe oryzae*. The accumulation of phosphate negatively affected the presence of Pathogenesis-Related (PR) proteins in the plant, leading to susceptibility. Simultaneously, there was an increase in the expression of fungal effectors. **Section 2**, described how, in Low-Pi plants, the leaf apoplast was enriched with proteins associated with plant defense reactions, aligning with observed resistance against *M. oryzae*. Further, in **Section 3**, a phosphoproteomic analysis was conducted, where we showed that High-Pi plants undergo substantial modifications in response to *M. oryzae* infection, whereas Low-Pi plants maintained a basal level of phosphorylation under both mock and infected conditions. For **Section 4**, we explored the involvement of *OsPBZ1* gene in defense response. We found that *OsPBZ1* plays a pivotal role in the rice's defense response to pathogen infection, with its expression being influenced by Pi content. CRISPR/Cas9-mediated mutagenesis of *OsPBZ1* alters blast resistance in a Pi-dependent manner, suggesting a complex interplay between *OsPBZ1*, Pi availability, and susceptibility. Finally, in **Section 5** we analyzed FRET-live imaging sensors as a tool for real-time detection of Pi by live cell imaging, showcasing their effectiveness in monitoring phosphate

changes induced by various stimuli in rice plants. Further investigations are needed to understand molecular interactions and signaling pathways involving phosphate and rice's defense.

General introduction

1. Rice

1.1 Agronomic importance of rice

Cereals, like wheat, maize, and rice, account for 60% of the global daily nutrient intake, making rice one of the most important crops in the world. Rice serves as a major food crop for over half of the world's population. Since the 1960s, the Green Revolution has led to increased agricultural yields and has facilitated the cultivation of new crops in different parts of the world. The development of high-yielding varieties and the application of fertilizers has revolutionized agriculture. Due to these progresses, India was able to double its production of wheat and rice, thus alleviating the impact of the Great Bengal famine of 1943. In Asia, the International Rice Research Institute (IRRI) introduced the first high-yielding rice variety, IR8, which was generated through breeding in 1966 (Estudillo *et al*., 2023). At present, the three largest rice producer countries are China, India, and Indonesia. China produces about four times more rice than Indonesia, although Indonesia has a higher yield per unit area **(Figure 1)**.

The use of fertilizers in rice cultivation, while helping to boost rice production, has also led to negative effects on the environment by increasing soil and water pollution (Fakhar *et al*., 2022). Other contaminants affecting rice crops are heavy metals such as arsenic, which is a potent carcinogenic contaminant. When arsenic is present in irrigation waters and/or soils, it negatively impacts agriculture and food safety. In rice, arsenic tends to accumulate in grains and enters the food chain, thus, posing a human health risk (Singh & Srivastava, 2023).

On the other hand, the climate crisis poses new challenges to food security due to increases in temperature, drought stress, intense storm events, and rises in sea levels, among others (Shahzad *et al*.,

2021). These challenges, combined with the continuous growth of the world's population, require a significant increase in food production. To address this need, new strategies are being developed, such as the use of varieties that can withstand abiotic stresses, such as drought or salinity, or biofortified varieties, which have a higher nutritional value. In 2019, Golden Rice, a rice variety genetically modified to produce beta-carotene, was approved for direct use as food and feed in the Philippines (Malik & Maqbool, 2020).

Biotic stresses, such as pathogen infection, also pose a threat to rice yields. Blast disease caused by the fungus *Magnaporthe oryzae* causes up to 30% yield losses in rice production (Wilson & Talbot, 2009). Traditional breeding and chemical treatments are being used to address this problem. Probenazole and spermidine, which function as inducers of plant defense mechanisms, are used to protect rice plants from the rice blast fungus (Iwai *et al*., 2007; Moselhy *et al*., 2016). The wide use of these chemicals might lead to the development of resistance in the pathogen and/or cause side effects on non-target organisms and the environment. Therefore, New strategies for improving crop production while reducing harmful side effects need to be developed.

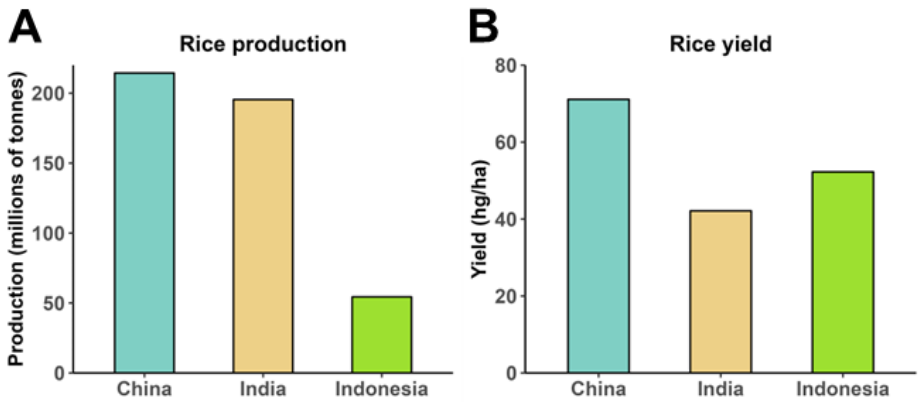

Figure 1. **Rice production and yield in the main rice producing countries. A)** Rice production in millions of tons (Mt). China is the world's leading producer of rice, followed by India and Indonesia. **B)** Rice yield in hg/ha. China has the highest rice yield. Source: FAOSTAT stats 2021.

1.2 The rice plant

Rice is the common name for the *Oryza* genus, a member of the *Monocotyledonae* class and the *Poaceae* or *Gramineae* family of grasses. Among cereals, rice has the smallest genome, with about 430 Mbp in 12 chromosomes, which has promoted its use as a plant model. *Oryza* genus has 23 wild rice species identified, representing ten genomes: AA, BB, CC, EE, FF, GG for diploids and BBCC, CCDD, HHKK, and HHJJ for tetraploids (Jacquemin *et al*., 2013; Atwell *et al.*, 2014). Of these, only two, belonging to the AA diploids, have been domesticated: Asian rice (*Oryza sativa*) and African rice (*Oryza glaberrima*) (Garris *et al.,* 2005).

O. sativa was first domesticated in the Pearl River region of China around 14.000 years ago, and originated from two different ancestral wild rice populations, *Oryza rufipogon* and *Oryza nivara* (Chen *et al*., 2019). *O. glaberrima* was domesticated in the inland delta of the Upper Niger River around 3,000 years ago from the wild ancestor *Oryza barthii* (Stein *et al*., 2018). *O. sativa* includes five subspecies: *aromatic rice, aus, indica, temperate japonica,* and *tropical japonica,* the two major groups of cultivated rice being *indica* and *japonica*. Whereas *indica* varieties are mainly cultivated in tropical environments, *japonica* subspecies are grown in temperate regions.

Based on genome data, there are different hypotheses about the origin and diversification of domesticated rice from its wild species attributed to distinct genome clustering (Huang & Han, 2015; Civáň & Brown, 2017; Choi *et al*., 2017). *O. sativa* cultivars are more widespread than *O. glaberrima* because they have higher yields. However, African rice has resistance to biotic stresses such as rice yellow mottle virus, nematodes, and other weeds, and to abiotic stresses such as drought, acidity, and iron toxicity (Brar & Singh, 2011). The New Rice for Africa

(NERICA) breeding program aims to cross *O. sativa* and *O. glaberrima* to leverage complementary effects of both traits. NERICA cultivars have contributed to improving agricultural development and food security in Africa (Arouna *et al*., 2017). The adoption of NERICA varieties has now expanded and they are also being used by breeders in varietal improvement programes in Bangladesh, China, India and several other countries globally (https://www.africarice.org/nerica).

Rice is a very flexible/adaptable plant that grows well under both flooded and rainfed conditions. The rice anatomy is shown in **Figure 2**. The rice plant has round and hollow stems, flat leaves, and panicles at the top of the plant. The plant comprises vegetative organs: roots, stems, leaves, and reproductive organs; the latter is the panicle. Panicles are composed of primary ramifications (small branches) with secondary branches carrying the spikelets. One single panicle can bear between 50 and 500 spikelets.

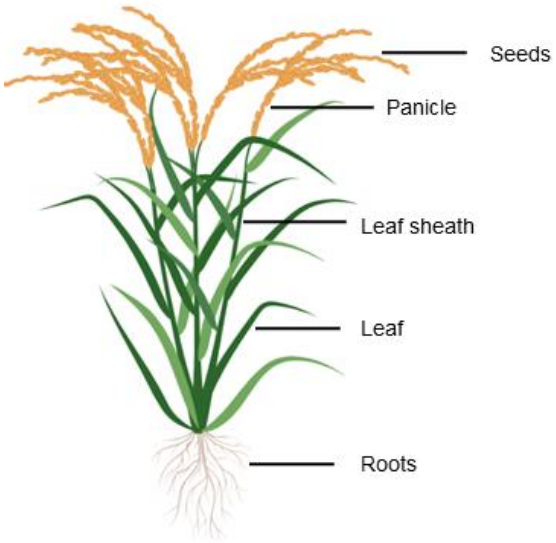

Figure 2. The rice plant anatomy. Illustration of an adult rice plant

1.3 Rice as a model for research

Rice is the model plant for functional genomics studies in monocotyledonous species (cereals). Genome sequences for both *japonica* and *indica* subspecies (Nipponbare and 93-11, respectively) were made available in 2002 (Goff *et al*., 2002, Yu *et al*., 2002). The "3,000 rice genomes" project (3K RGP) was a collaborative effort by researchers from the Chinese Academy of Agricultural Sciences (CAAS), the International Rice Research Institute (IRRI), and the Beijing Genomics Institute (BGI). The project sequenced the genomes of 3,024 rice varieties from 89 countries (Li *et al*., 2014). In addition to the genome sequences, there are extensive collections of expressed sequence tag (EST) and several mutant resources are available, such as: POSTECH Rice Insertion Database (http://cbi.khu.ac.kr/), Rice Mutant Database (http://rmd.ncpgr.cn/), Taiwan Rice Insertion Mutant (http://trim.sinica.edu.tw), Oryza Tag Line from Génoplant (http://oryzatagline.cirad.fr/) (Wang *et al*., 2013; Wei *et al*., 2013; Lo *et al*., 2016; Ram *et al*., 2019). Efficient protocols for rice transformation have been developed, including *Agrobacterium*-mediated transformation (Sallaud *et al*., 2003). This makes rice as a valuable model for understanding the genetic basis of traits associated with development and yield, or tolerance to biotic and abiotic stresses in cereal research.

In recent years, genome editing technologies have allowed researchers to make precise changes in a plant genome. This has paved the way for new possibilities for crop improvement, such as the development of plants that are resistant to herbicides, with improved productivity or more tolerant to abiotic or biotic stress. In particular, the CRISPRCas9 technology has expanded the range of possible genome

editing modifications, enabling high specific targeting for rice improvement (Miao *et al*., 2013; Lowder *et al*., 2015; Hu *et al*., 2016).

2. Rice pathogens

2.1 Major pathogens of rice

Rice is susceptible to a variety of bacterial and fungal diseases that are responsible for important yield losses and also pose a threat to food safety. The most important bacterial disease of rice is bacterial blight, which is caused by the bacterium *Xanthomonas oryzae pv. oryzae*. Bacterial blight is a widespread disease that is found in warm, humid areas around the world. The disease can cause wilting of seedlings, yellowing and drying of leaves, and can even result in the death of entire rice plants. Another important bacterial disease of rice is bacterial leaf streak, which is caused by the bacterium *Xanthomonas oryzae pv. oryzicola*. Bacterial leaf streak is a less severe disease than bacterial blight, but it can still cause significant yield losses (Niño-Liu *et al.*, 2006; Raj *et al.*, 2019).

Regarding fungal pathogens, *M. oryzae* is the most devastating fungal pathogen of rice, which is responsible for significant losses in rice production worldwide (discussed in **Section 2.2**). Rice is also affected by other fungal pathogens, such as *Rhizoctonia solani*, *Gibberella fujikuroi*, causing sheath blight and bakanae, respectively (Singh *et al*., 2019; Singh & Sunder, 2012). *Rhizoctonia solani* is a necrotrophic soil fungus that can cause a variety of diseases in rice, including sheath blight. The fungus infects rice plants through the roots and can spread to the leaves and stems. A disease of increasing economic importance is Bakanae (“foolish seedling” in Japanese), caused by one or more seed-borne *Fusarium* species, mainly *F. fujikuroi*. *Fusarium* species can infect rice plants from the seedling stage to the mature stage, with

severe infection of rice seeds (Iqbal *et al*., 2011). In addition to causing disease, *Fusarium* species also produce mycotoxins in rice grains. Mycotoxins are toxic compounds that can pose serious food safety concerns for both animal and human health (Munkvold, 2017). In Japan, for example, the disease has been estimated to cause losses of up ~10–20% due, but it can also reach more than 70% under severe infection (Fiyaz *et al*., 2014). Phenotypic lesions on rice leaves caused by bacterial and fungal diseases are shown in **Figure 3.**

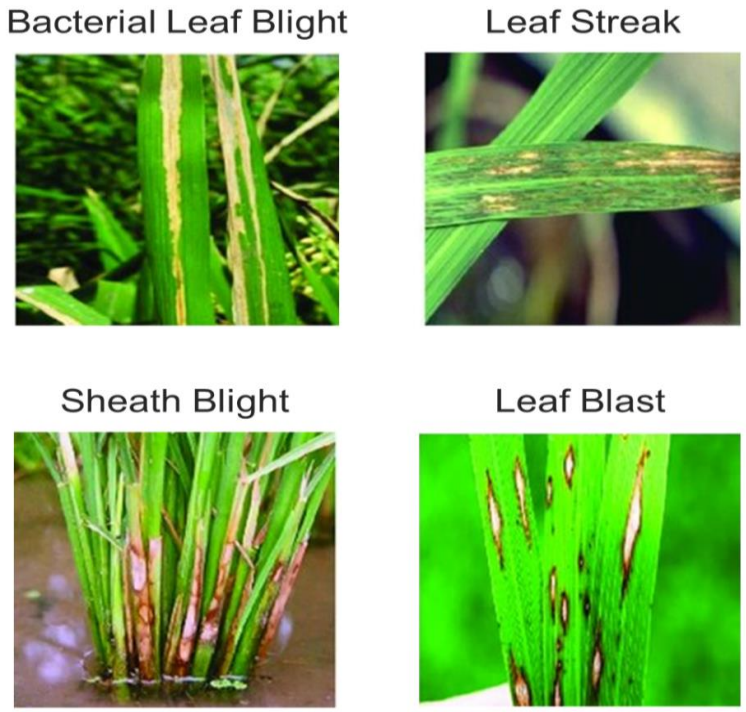

Figure 3. Rice leaf diseases. Bacterial Leaf Blight cause by *Xanthomonas oryzae pv. Oryzae*; leaf streak caused by the bacterium *Xanthomonas oryzae pv. oryzicola;* Sheath Blight caused by *Rhizoctonia solani, and* Leaf Blast caused by *Mangaporthe oryzae*. Taken from Simhadri *et al*., 2023.

There are several strategies that can be used to manage bacterial and fungal diseases of rice. These strategies include the use of resistant varieties, crop rotation, and the application of agrochemicals. However,

the development of new and effective control strategies is essential to mitigate the economic and food safety risks posed by these diseases.

2.2 *Magnaporthe oryzae*

Magnaporthe oryzae causes blast disease in several gramineous crops like maize, wheat, and rice. In rice, it can affect different tissues, leaves, leaf collars, necks, and panicles. The first records of rice-infecting strains date from 7000 years ago in the Middle Yangtze Valley of China (Couch *et al*., 2005). Blast disease is responsible for approximately 30% of rice production losses globally. Based on its scientific and economic relevance, the rice blast fungus *M. oryzae* was ranked at the top of the list of phytopathogenic fungi (Dean *et al*., 2012).

M. oryzae has a hemibiotrophic lifestyle that first starts with a biotrophic phase and then turns into necrotrophic. (Wilson & Talbot, 2009; Fernandez & Orth, 2018). Infection of rice leaves is initiated when a *M. oryzae* spore sticks to the leaf surface from which a germ tube develops and grows on the leaf surface. Germ tubes develop melanized appressoria to physically penetrate the plant tissue **(Figure 4)**. From the appressorium a penetration peg emerges that penetrates the plant cuticle and cell wall and enters into the epidermal cell, becoming an invasive hypha. During this stage, invasive hyphae are thin, tubular structures that grow inside the plant cell surrounded by the host plasma membrane, known as extra-invasive hyphal membrane (EIHM). As the bulbous intracellular invasive hyphae develops, an extended dome-shaped structure forms, known as the biotrophic interfacial complex (BIC) **(Figure 4)** (Mosquera *et al*., 2009; Khang *et al*., 2010). While growing, invasive hyphae change from thin tubular to bulbous untill they

completely fill the plant cell and then move through plasmodesmata to the adjacent cells. The pathogen's growth causes the host vacuole to collapse, leading to host cell death, which corresponds with the necrotrophic phase. The fungus continues expanding in the tissue and both phases occur at the same time in different cells (Kankanala *et al.*, 2007). Blast lesions are diamond-shaped with brown borders that appear on the leaf surface after several days of infection **(see Figure 3)**. From these lesions, the fungus spreads to other plants by sporulating.

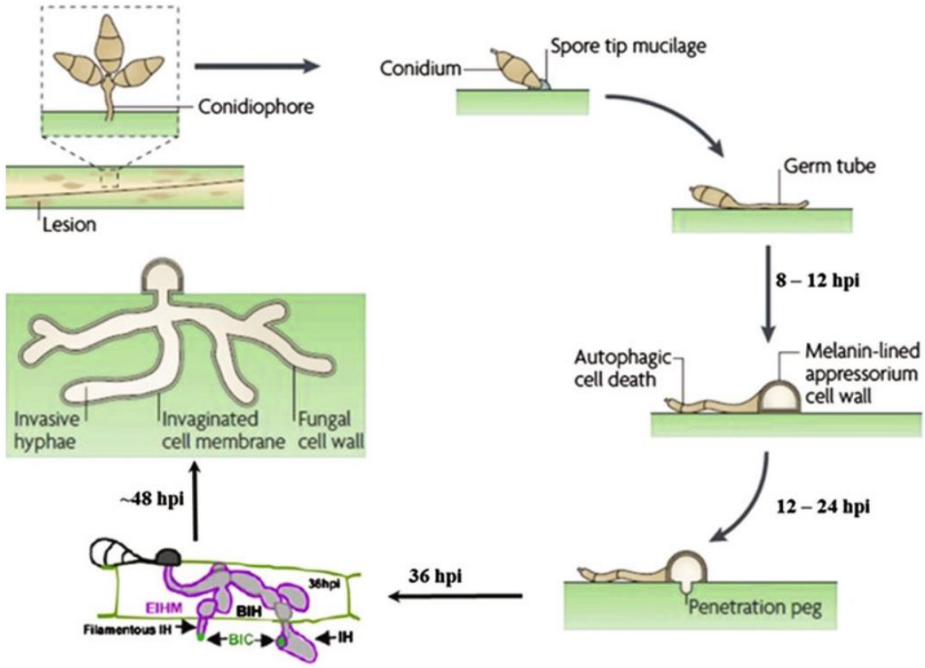

Figure 4. Infective life cycle of *M. oryzae* adapted from Wilson and Talbot (2009) and Mosquera *et al.* (2009). The figure has been adjusted to include the biotrophic phase of the life cycle, which includes the development of bulbous invasive hyphae, biotrophic-interfacial complexes (BICs) surrounded by the extra-invasive hyphal membrane (EIHM).

During infection, the pathogen can deploy diverse strategies to invade the plant tissue, including the production of effector proteins capable of promoting virulence (Devanna *et al*., 2022). Based on their

localization *in planta*, *M. oryzae* effectors have been classified as apoplastic and cytoplasmic effectors. Effectors that accumulated between the EIHM and the fungus cell wall are the apoplastic affectors (Kankanala *et al*., 2007; Mosquera *et al*., 2009; Mentlak *et al*., 2012; Yi & Valent, 2013). Cytoplasmic effectors accumulate at the BIC structure of bulbous invasive hyphae before being translocated to the host cytoplasm of living rice cells (Mosquera *et al*., 2009; Khang *et al*., 2010). Recent studies have shown that *M. oryzae* also secretes effectors through the BIC which are then delivered to the host cell nucleus (Lee S. *et al*., 2023). Some examples of apoplastic effectors are BAS4, and Slp1, while PWL2, BAS1, and AvrPiz-t are cytoplasmic effectors (Khang *et al*., 2010; Park *et al*., 2012; Giraldo & Valent, 2013). *M. oryzae* effectors might have diverse functions that facilitate host tissue invasion (Guo *et al.,* 2019). *M. oryzae* effectors include: avirulence factors (Avr), BAS (Biotrophy-Associated Secreted proteins) effectors, cell host death suppressors and cell death inducers (e.g., *Magnaporthe oryzae* snodprot1 homolog, MSP1) (Wang *et al.,* 2016). As the *M. oryzae* genome has been sequenced, the identification of effector genes and their function during the infection is increasing (Dean *et al*., 2005).

3. The plant immune system

Plants have evolved multiple mechanisms to perceive and respond to pathogen infections which rely on numerous changes at the biochemical, physiological, and molecular levels. Plant defense mechanisms include passive defenses such as cell wall and some pre-existing toxins and enzymes, and inducible responses (i.e., activated under pathogen attack).

To prevent infections, plants have evolved a multi-tiered immune system (Nobori & Tsuda, 2019). The first layer is initiated by the recognition of conserved pathogen-associated molecular patterns (PAMPs), previously known as elicitors, through pattern recognition receptors (PRR) located at the cell surface, a phenomenon referred to as PAMP-triggered immunity (PTI) or basal defense (Jones & Dangl, 2006). The activation of PRR triggers the immediate phosphorylation and activation of Receptor-like kinases and subsequent signaling pathways. Among others, PTI components include the production of reactive oxygen species (ROS), Ca^{2+} influx, the reinforcement of the cell wall, and activation of protein phosphorylation, which encompass phosphorylation/dephosphorylation cascades serving as critical signaling pathways. Phosphorylation events are important factors in controlling immune responses as described below (General Introduction, **Section 5.2**). Mitogen-activated protein kinases (MAPKs) and Calcium-dependent Protein Kinases (CDPKs) are key participants in these cascades **(Figure 5)** (Jones & Dangl, 2006; Erickson *et al*., 2022). PTI responses also include the production of antimicrobial compounds and accumulation of Pathogenesis- Related (PR) proteins (van Loon, 1985; van Loon *et al*., 1994; Ali *et al*., 2018). The most well-characterized PTI model in rice is the chitin elicitor binding protein (CEBiP) and chitin elicitor receptor kinase 1 (CERK1) interaction with chitin (a component of the cell wall, or PAMP) (Shimizu *et al*., 2010).

During PTI, the plant is also able to sense internal host molecules known as damage-associated molecular patterns (DAMPs) to trigger defense responses (Pastor-Fernández *et al*., 2023). Plant elicitor peptides (PEPs) are DAMPs that can be released during pathogen invasion (Tabata and Sawa, 2014). PEPs are short acid peptides produced by a wide range of plant species in response to stress or infection. These PEPs are produced via the cleavage of their

precursor PEPs (PROPEPs) which are a component of the plant's innate immune response. The majority of PROPEPs can be transcriptionally induced upon pathogen infection or wounding. Mature Peps are released from the C-termini of PROPEPs through metacaspase-mediated cleavage and relocated to the apoplast. PEPs are examples of proteins without an N-terminal secretion signal. Once in the apoplast they are perceived by PEP receptors (PEPRs), which are located in the plant cell membrane, to elicit typical PTI responses. Metacaspases, together with Peps and PEPRs, have emerged as key molecules of innate immunity and are potential targets for breeding and improving crop immunity (Garcia *et al*., 2023).

To counteract this innate defense, pathogens deliver effector proteins into the host cell that can inhibit the PAMP-PRR interaction or downstream signaling. Microbial effectors, or the biochemical consequences of their activity, are in turn recognized by host Resistance (R) proteins. The direct or indirect recognition of effectors by R proteins results in the so-called effector-triggered immunity (ETI) (Jones & Dangl, 2006; Deslandes & Rivas, 2012; Pel & Pieterse, 2013). *R* genes encode mainly for proteins from the nucleotide-binding leucine-rich repeat receptor (NB-LRR) family **(Figure 5)**. ETI is associated with more sustained and robust immune responses that leads to localized cell death and hypersensitive response (HR) (Ding *et al*., 2022). On the other hand, effective defense responses also depend on a number of factors. The timing of the response, the plant's nutritional status, and the environmental conditions, all play a role in shaping the plant's defense response (Ding *et al*., 2022; Gorshkov & Tsers, 2022).

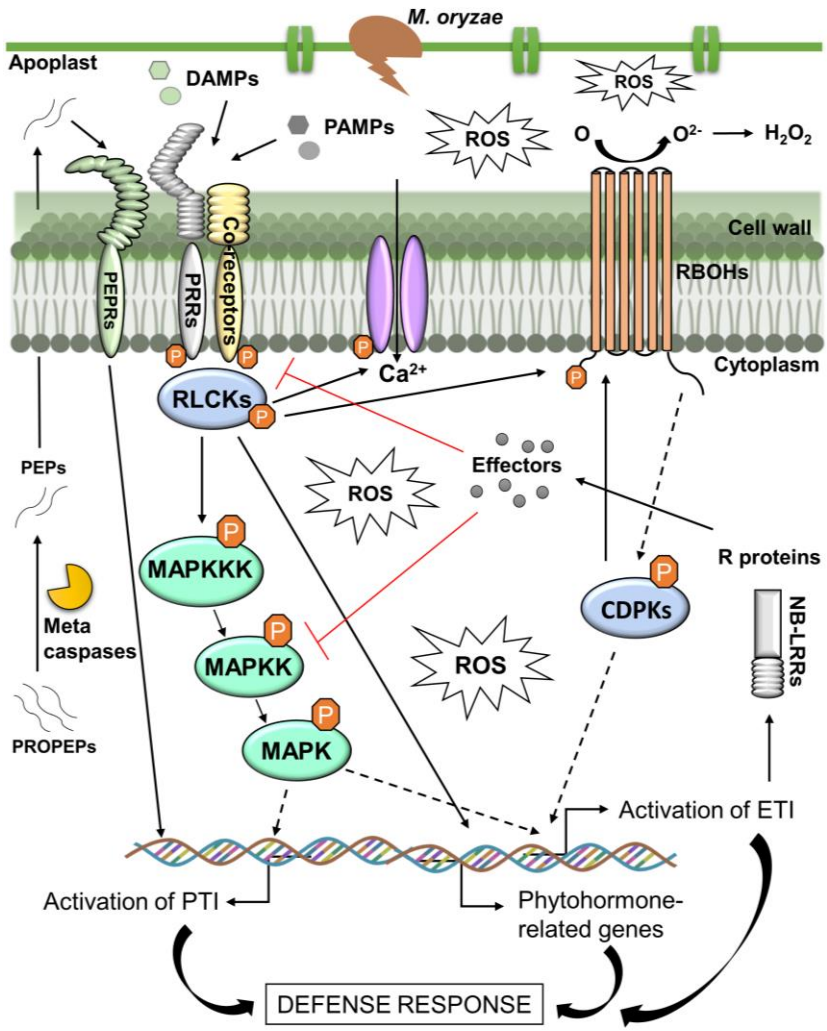

Figure 5. Schematic representation of plant immune response. Upon recognition of PAMPs, cell surface localized PRRs recruit co-receptors to form receptor complexes and activate downstream RLCKs, which subsequently phosphorylate downstream components (e.g., RBOHD, CDPKs, MAP kinases). This recognition triggers a ROS burst, Ca^{2+} influx, activation of MAP kinase cascades, transcriptional reprograming and phytohormone production. Other components such as DAMPs and PEPs also contribute to plant immunity. Microbial effectors are recognized by R proteins and trigger ETI. Solid arrows indicate direct effects, dashed arrows indicate indirect effects and red arrows negative effects. Abbreviations: Calcium-regulated kinases (CDPKs), Damage-associated molecular patterns (DAMPs), Mitogen-activated protein kinase (MAPK), Nucleotide-binding leucine-rich repeat receptor (NB-LRR), Pathogen-associated molecular patterns (PAMPs), PEP receptors (PEPRs), Plant elicitor peptides (PEPs), precursor Peps (PROPEPs), Pattern recognition receptors (PRRs), Respiratory burst oxidase homologs (RBOHs), Receptor-like cytoplasmic kinases (RLCKs), Reactive oxygen species (ROS).

Plants and pathogens are engaged in a constant battle of wits. This is a dynamic process in which the plant's defense mechanisms are constantly evolving, and the pathogen is constantly under pressure to adapt (Jwa *et al*., 2017; Kou *et al*., 2019; Gorshkov & Tsers, 2022). During plant-pathogen co-evolution, the pathogen develops strategies to suppress the plant's immune system and/or to evade the plant's defense response. The susceptibility (S) genes of plants are target genes for phytopathogens. These genes are important for other developmental functions, so they are maintained through evolution. However, phytopathogens have evolved to suppress the action of these genes, enabling them to penetrate and spread into the host (Liu *et al*., 2021). Resistance mediated by *R* genes faces this problem, as resistance can be broken down over time (Wu *et al*., 2019).

Plant hormones play a crucial role in plant immunity. They are involved in complex networks that allow plants to respond to different types of stresses. These networks can act antagonistically or synergistically, depending on the specific stress. Salicylic acid (SA), ethylene (ET), jasmonic acid (JA), and abscisic acid (ABA) are the most well-studied plant hormones involved in plant immunity. Typically, pathogens that need a living host (biotrophs) are more sensitive to SA-mediated responses, while pathogens that kill the host cell (necrotrophs) are generally affected by ET-JA mediated responses (Zhou & Zhang, 2020; Aerts *et al*., 2021). Furthermore, SA (and SA-derivatives) can move from local infected tissue to distal tissue, inducing the systemic acquired resistance. After systemic acquired resistance activation, the plant may become broadly resistant to different pathogens for an extended period. Pathogens can also hijack the hormone signaling network for their own benefit, e.g., by disrupting phytohormone biosynthesis/signaling pathways or diminishing plant immune responses. Additionally, several studies have demonstrated that

pathogens can generate phytohormone-mimicking molecules to alter host immune responses. (Zhang *et al*., 2018).

3.1 Pathogenesis-related proteins

Pathogenesis-related (PR) proteins are a diverse group of proteins that accumulate in plants in response to a variety of stresses, including pathogen infection. They are defined as "*Proteins encoded by the host plant but induced only in pathogenic or related conditions*". Most PR proteins accumulate either in the apoplast or the vacuole. Acidic PR proteins are usually secreted to the extracellular space, and basic PR proteins are generally transported to the vacuole (Buchel & Linthorst, 1999). The presence of PR proteins in the apoplast during pathogen infection suggests that they are important for active defense against disease early during infection.

PR proteins are currently classified into 19 major families based on their amino acid sequence, biochemical, or serological features (van Loon, 1985; van Loon *et al*., 1994, 2006; Ali *et al*., 2018). Some PR proteins have antimicrobial activity, and they are distinguished by their distinct mode of action **(Table 1)** (Kaur *et al*., 2022). Summarizing, PR1 presents antifungal activity, PR2 are hydrolytic β-1,3-glucanases, PR3, 4, 8, and 11 are chitinases **(Table 1)**. PR5 are classified as thaumatin-like proteins, and PR6, 7, and 9 are proteinase inhibitors, endo-proteinase, and peroxidase respectively. PR10 proteins (in particular the PR10 family member *OsPBZ1*) has been shown to exhibit ribonuclease activity and is required for cell death progress in plants (Kim *et al*., 2011) **(Table 1)**. PR12 are plant defensins; PR13, plant thionins; and PR14, lipid transfer proteins. PR15 and PR16 belong to the oxalate oxidase protein family and PR17 are secretory proteins with antifungal and antiviral function. PR18 are classified as carbohydrate oxidases and PR19 proteins bind to fungal cell wall glucans altering cell wall structure,

leading to morphological distortion of hyphae **(Table 1)** (Kaur *et al*., 2022).

Table 1. Classification, properties, and source of PR proteins. Adapted from Kaur *et al*., 2022.

PRProteins	Property/function	Source	Reference
PR1	Antifungal	*Nicotiana. tabacum*	Antoniw *et al*., 1980
PR2	β-1,3-glucanases	*N. tabacum*	Antoniw *et al*., 1980
PR3	Class I, II, IV, V, VI, VII Chitinases	*N. tabacum*	Van Loon 1982
PR4	Class I, II Chitinases	*N. tabacum*	Van Loon 1982
PR5	Thaumatin-like proteins	*N. tabacum*	Selitrennikoff 2001
PR6	Proteinase inhibitor	*Solanum lycopersicum*	Green & Ryan 1972
PR7	Endoproteinase	*S. lycopersicum*	Vera & Conejero 1988
PR8	Class III Chitinase	*Cucumis sativus*	Métraux *et al*., 1988
PR9	Peroxidase	*N. tabacum*	Lagrimini *et al*., 1987
PR10	Ribonuclease-like proteins	*Petroselinum crispum*	Somssich *et al*., 1986
PR11	Class I Chitinase	*N. tabacum*	Melchers *et al*., 1994
PR12	Defensin	*Raphanus raphanistrum*	Terras *et al*., 1995
PR13	Thionin	*Arabidopsis thaliana*	Epple *et al*., 1995
PR14	Lipid-transfer protein	*Hordeum vulgare*	García-Olmedo *et al*., 1995
PR15	Oxalate oxidase	*Hordeum vulgare*	Zhang *et al*., 1995
PR16	Oxidase-like	*H. vulgare*	Wei *et al*., 1998
PR17	Antifungal and antiviral	*N. tabacum*	Okushima *et al*., 2000
PR18	Carbohydrate oxidases	*Helianthus annuns*	Custers *et al*., 2004
PR19	Antimicrobial protein	*Pinus Sylvestris*	Sooriyaarachchi *et al*., 2011

The PR10 family is one of the less characterized families among PR proteins. They are described as small acidic proteins of about 19 kDa (Linthorst & van Loon, 1991). *PR10* expression is induced by pathogen infection and by the defense-related hormones SA and JA, as well as by abiotic stresses such as salt, drought, and phosphate starvation (Sinha *et al*., 2020; Lopes *et al*., 2023). Induction of *PR10* expression by pathogen infection in different plant species (e.g., potato, tobacco or rice) suggest that PR10 proteins play a role in plant immunity, but the exact mechanisms by which these proteins exert their function remains poorly understood (Matton & Brisson, 1989; Midoh & Iwata, 1996; McGee *et al*., 2001). Ribonuclease activity has been described for some PR10 proteins (Liu *et al*., 2006, Xie *et al*., 2010; Huang *et al*., 2016; Sinha *et al*., 2020).

Constitutive expression of certain *PR* genes in transgenic plants either alone or in combination (e.g., chitinases, β-1,3-glucanases, PR1, defensins, thionins, PR10) has been shown to decrease disease severity after infection by fungal pathogens (Alexander *et al.,* 1993; Broglie & Broglie, 1993; Jach *et al.,* 1995, Ali *et al.,* 2018, Lopes *et al.,* 2023).

3.2 The apoplast in plant immunity

The apoplast is the extracellular matrix of the plant cell wall and the intercellular spaces where the apoplastic fluid circulates (Agrawal *et al*., 2010). In the early stages of infection, the apoplast serves as a site of interaction between molecules derived from plants and those secreted by pathogens. The apoplast acts as a bridge that perceives and transduces signals from the environment to the symplast, with the nature of these interactions also dependent on the lifestyle of the

pathogen (Gupta *et al*., 2015). This highly dynamic compartment serves as the molecular battlefield that contributes to either the success of the infection or to plant resistance.

On the other hand, pathogens have the capacity to create environments suitable for their proliferation in the host, including the suppression of plant immunity and the promotion of water and nutrient availability. The importance of nutritional susceptibility, including increased water and nutrient availability in the apoplast, is emerging (El Kasmi *et al*., 2018; Gentzel *et al*., 2022). However, the distinction between defense suppression and nutritional susceptibility is ambiguous. During PTI, the plant host reduces the apoplastic sugar and amino acids to avoid pathogen development (Yamada *et al*., 2016; Naseem *et al*., 2017). Additionally, apoplast hydration can be assessed as a symptom of plant disease against certain pathogens (mainly bacteria), as water availability triggers pathogen growth (Freeman & Beattie, 2009; Beattie, 2011).

Not all pathogens rely on apoplast hydration in the same way. For example, fungi use apoplast water to generate mechanical pressure for penetration, while viruses are typically transmitted through plasmodesmata rather than the apoplast. Research on apoplast hydration is limited, but current findings suggest that its contribution to the plant defense response may vary depending on the pathosystem. The factors of nutritional susceptibility and apoplast hydration are interconnected: an increase in carbon sources and solutes negatively impacts water potential, as observed in the interactions of between *Pseudomonas syringae* and *Arabidopsis thaliana*, and *Pantoea stewartii* and maize (Wright & Beattie, 2004; Gentzel *et al*., 2022).

The availability of nutrients in the apoplast is a dynamic process that is modulated by both the host plant and the pathogen. For instance,

the host can decrease the sugar content in the apoplast by inhibiting its transport, while the pathogen can activate transporters or degrade cell walls to increase carbonate compounds, facilitating cell penetration. In rice plants, the transcriptional activation of the sugar transporter gene *SWEET* promotes growth of *Xanthomonas oryzae*. In contrast, the bacterial pathogen *Pseudomonas syringae pv. tomato* is able to degrade cell walls in *A. thaliana*, thus, increasing the availability of nutrients like pectins and amino acids, that the pathogen uses to fuel its growth. These findings suggest that the availability of nutrients in the apoplast might determine the outcome of plant-pathogen interactions (El Kasmi *et al*. 2018, Gentzel *et al*., 2022).

In the rice-*Magnaporthe* interaction, the fungus secretes diverse proteins into the apoplast to facilitate host tissue colonization. These proteins include cell wall degradation enzymes, antioxidant and stress-related proteins, protease/peptidases, and effector proteins (Guo & Cheng, 2022). Rice plants recognize these signals through PRRs, leading to an increase in cytoplasmic Ca^{2+} concentration, activation of ROS production, and the induction of defense-related genes. In the rice-*Magnaporthe* interaction, there are also mechanisms in apoplastic immunity related to the control of redox and pH levels in the apoplast (Delaunois *et a*l., 2014). It appears that the composition of the apoplastic fluid is continuously changing and understanding the role of the apoplast in plant-pathogen interactions, will open new avenues for the development of strategies to protect plants from disease.

4. Abiotic stress in plants

Abiotic factors are non-living environmental factors that can affect plant growth and productivity. These factors include drought,

salinity, heat, cold, chilling, freezing, nutrients, light intensity, ozone, nutrient deficiencies/excess, and heavy metals, among others.

Both drought and salinity represent major abiotic stresses in plants (Sharma *et al*., 2019). Drought-induced crop yield losses are likely to outnumber losses from all other sources combined. The severity of a drought depends on the occurrence and distribution of rainfall, evaporative demand, and moisture storing capacity of soils. Drought-stressed plants diminish both their shoot growth and metabolic demands (Ahluwalia, 2021). Salt stress can impose osmotic stress and ion toxicity on crop plants, leading to reduced growth and yield (Wang *et al*., 2022). Salinity is caused by the accumulation of salts in the soil or groundwater as a result of natural processes, through human activities, or the use of salt-rich irrigation water on soils with poor drainage.

Heat stress and cold stress are also important abiotic stresses in plants. In nature, plants must adapt to temperature variations (e.g., high temperature, chilling and freezing conditions). To survive lethal conditions like cold stresses, plants acquire chilling and freezing tolerance by undergoing a process known as acclimation (Kerbler & Wigge, 2023). When plants experience heat stress, there are declines in seed germination rate, photosynthetic efficiency, and overall yield. The rising temperatures around the world are becoming a major concern in modern agriculture. Nutrient stress, e.g., deficiency or excess of nutrients, also negatively affect plant growth and productivity. Within the scope of abiotic stresses, research in this Ph.D. thesis will be on the study of nutrient stress.

4.1. Nutrient stress in plants

Plant nutrition has been the subject of extensive research due to its significant implications for plant growth and productivity (Pandey, 2018). Nutrients can be classified into macronutrients and

micronutrients. Macronutrients are those that are required in higher quantities and include nitrogen (N), phosphorus (P), potassium (K), calcium (Ca), sulfur (S), and magnesium (Mg). Micronutrients, also known as trace elements, include iron (Fe), boron (B), chlorine (Cl), manganese (Mn), zinc (Zn), copper (Cu), molybdenum (Mo), and nickel (Ni). All nutrients must be incorporated in a fine-tuned, regulated manner and properly distributed throughout the plant's body to maintain an adequate metabolic state. An imbalance in any of these elements can have a severe impact on plant metabolism. As a result, plants have developed highly specialized mechanisms to maintain nutrient homeostasis. However, modern agricultural practices often disrupt these natural nutrient recycling mechanisms due to the overuse of fertilizers, which is aimed at maintaining crop yields. Several studies have linked the nutritional status of plants to disease resistance (Val-Torregrosa *et al*., 2021) (discussed below, **Section 4.3**).

4.2 Phosphate stress

Phosphorus (P) represents a critical macronutrient essential for plant growth and development. It assumes key roles as a constituent of nucleic acids, phospholipids, and participates in vital enzymatic reactions and intricate signal transduction cascades, notably protein phosphorylation. Moreover, P is a fundamental component of adenosine triphosphate, the ubiquitous cellular energy cofactor pivotal to biological processes. Within the realm of plant nutrition, P is absorbed by the roots primarily in the form of inorganic phosphate (Pi). Despite the typically abundant presence of Pi in soil, its limited bioavailability poses a substantial constraint on plant growth, necessitating the application of fertilizers to sustain crop production (Hinsinger *et al*., 2011). This scarcity of accessible P can be attributed to its propensity to form

insoluble complexes with various cations—like aluminum and iron in acidic soil conditions, and calcium and magnesium in alkaline soil environments. Additionally, P supplied in the form of fertilizers tends to be predominantly retained by the soil, rendering it unavailable to plants that lack specific adaptations. Alarmingly, global reserves of P are depleting rapidly, with projections suggesting the depletion of soil P reserves by the year 2050 (Cordell *et* al., 2011).

Under Pi limiting conditions, plants activate the Phosphate Starvation Response (PSR) to enhance Pi acquisition (Chiou & Lin, 2011; Paz-Ares *et al.,* 2022). Phenotypic changes, such as a modification of root structure, increasing the ratio of surface area to volume, also take place under Pi-deficiency to maximize Pi uptake (Lynch, 1995). At the molecular level, Pi acquisition is enhanced by: i) secreting phosphatases to increase the concentration of available Pi in the soil; ii) increasing the number of Pi transporters at the root-soil interface); and iii) exchanging Pi between organs and subcellular compartments, as mobilization of Pi is stored in the vacuole (Versaw & Garcia, 2017; Bhadouria & Giri, 2022; Ravelo-Ortega *et al*., 2022). In the plant, the vacuole serves as a primary Pi reservoir. Under adequate Pi supply, up to 95% of intracellular Pi is stored in the vacuole (Bucher & Fabiańska, 2016). Recently, vacuolar located SPX-MFS domain-containing proteins have been characterized to mediate Pi transport across the tonoplast. (Guo *et al*., 2023).

Adaptive mechanisms to Pi-deficient conditions are mainly regulated through the function of PHOSPHATE STARVATION RESPONSE (PHR) transcription factors (Puga *et al*., 2017; Chien *et al*., 2018) **(Figure 6)**. When Pi levels are optimal, SPX domain-containing proteins form specific complexes: SPX1 and SPX2 bind to PHR1, whereas SPX4 associates with PHR2. These interactions effectively prevent PHR1 and PHR2 from binding to the promoter regions of target

genes, resulting in the downregulation of Phosphate Starvation Induced (PSI) genes (Wang *et al*., 2014) **(Figure 6A)**. The orchestration of these interactions is mediated by inositol polyphosphates (InsP), acting as signaling molecules that can either promote or inhibit the formation of SPX protein-transcription factor complexes, thereby fine-tuning the plant's response to phosphate availability (Wild *et al*., 2016). Conversely, in Pi-limiting conditions, strigolactones (SLs) come into play as crucial regulators. Strigolactones regulate the interaction of D14-SDELs-SPX4, leading to the degradation of SPX4 under Pi-limiting conditions. This degradation, in turn, enables PHR2 to bind to its target genes for the activation of the Phosphate Starvation Response (PSR) **(Figure 6B)** (Gu *et al*., 2023). Strigolactones are thus instrumental in shifting the plant's molecular response towards phosphate conservation when it becomes scarce. Another strategy developed by Pi-starved plants is an increase in RNAses and phosphatase activities, these enzymes being involved in metabolic Pi recycling (Tadano & Sakai, 2012; Gho *et al*., 2020).

Various microRNAs (miRNAs) play a key role in plant Pi homeostasis regulation (Paul *et al*., 2015). These short non-coding RNAs orchestrate post-transcriptional gene silencing, impacting developmental processes and responses to environmental stress (Llave *et al*., 2002; Brodersen *et al*., 2008). The role of miR399 in the Phosphate Starvation Response (PSR) is well-established (Fujii *et al*., 2005; Chiou *et al*., 2006; Hsieh *et al*., 2009; Puga *et al*., 2017; Ham *et al*., 2018). When the plant detects low Pi levels, PHR1 triggers the expression of MIR399, leading to the downregulation of Phosphate over accumulator 2 (PHO2), which encodes a ubiquitin E2 conjugating enzyme responsible for Pi transporter degradation **(Figure 6B)**. Consequently, the accumulation of miR399 alleviates negative post-transcriptional control, facilitating increased Pi uptake via PHT1 family

Pi transporters **(Figure 6B)**. MiR399 also acts as a long-distance signaling molecule, moving from shoots to roots to regulate Pi homeostasis during Pi deficiency (Fujii *et al*., 2005; Aung, 2006; Chiou, 2006). Additionally, PHO2 influences the degradation of PHOSPHATE1 (PHO1), involved in Pi loading into the xylem for root-to-shoot Pi translocation (Liu *et al*., 2012). This miR399/PHO2 module exhibits a conserved role in controlling phosphate homeostasis in both Arabidopsis and rice plants.

MiR827 plays a significant role in the Phosphate Starvation Response (PSR), with its regulation in rice controlled by *OsPHR2* **(Figure 6)**. This miRNA targets two distinct rice genes, *OsSPX-MFS1* and *OsSPX-MFS2*. Notably, the SPX domain, which is found in various Pi transporters and signaling proteins in plants, is a key feature of these genes (Secco *et al*., 2012). In Arabidopsis, their counterpart, *AtPHT5*, has already been characterized as a Pi influx transporter into the vacuole (Liu *et al*., 2016). Given the similarities between *OsSPX-MFS1*, *OsSPX-MFS2*, and *AtPHT5*, as well as their shared localization at the rice tonoplast, there is a strong indication that they may function as vacuolar phosphate transporters (Lin *et al*., 2010, 2018). Consequently, it has been proposed that miR827 in rice contributes to Pi compartmentalization and storage (Lin *et al*., 2010, 2018; Wang *et al*., 2012; Liu *et al.,* 2016).

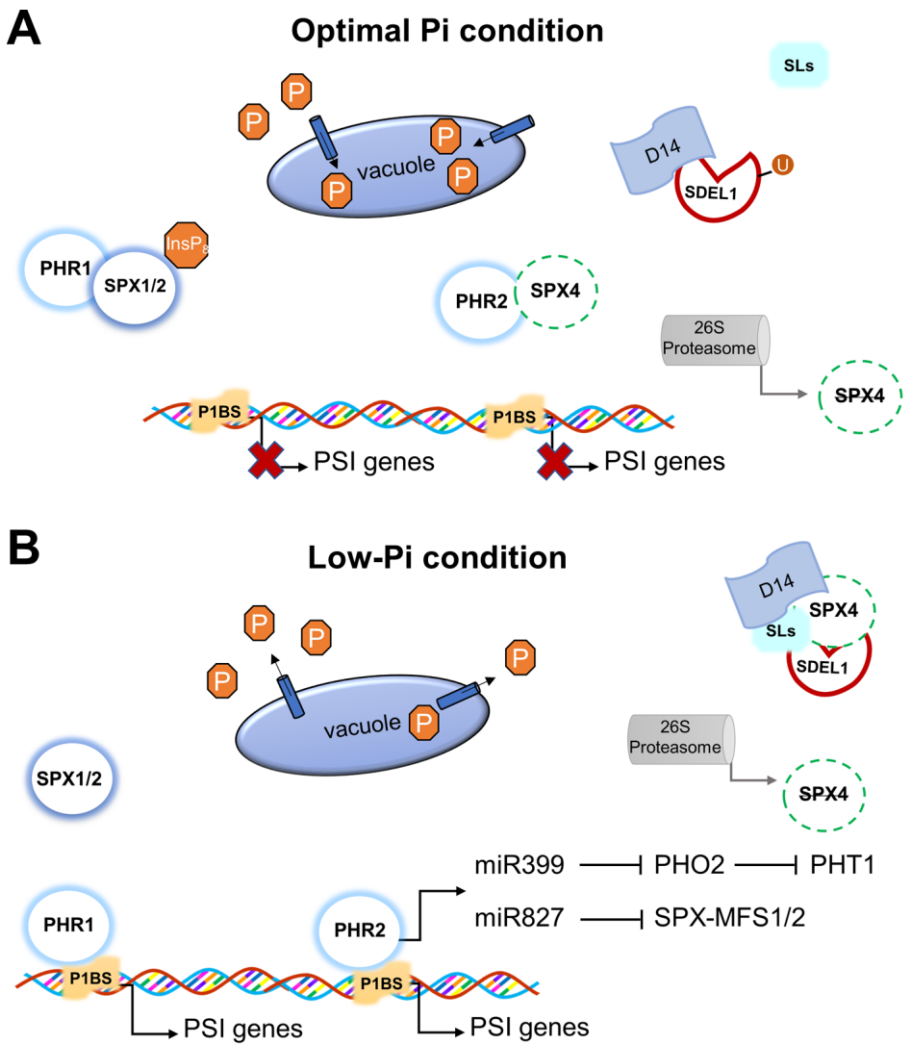

Figure 6. Schematic representation of Pi response in rice. A) Low-Pi condition. In the absence of InsP molecules, PHR1 is free and binds to P1BS. SLs regulates the interaction of D14-SPX4-SDEL1 complex, enabling PHR2 to bind to the P1BS, inducing the expression of PSI genes. Abbreviations: Phosphate (P), inositolphosphates (InsP), PHOSPHATE STARVATION RESPONSE transcription factors (PHR), strigolactones (SLs), Phosphate starvation-induced (PSI), phosphoinositide-binding site (P1BS), microRNAs (miRNAs), *PHO2* (Phosphate over accumulator 2), Phosphate Transporter (PHT), SL receptor DWARF 14 (D14), RING-finger ubiquitin E3 ligase (SDEL1). **B)** Optimal Pi condition. High cellular Pi levels drive InsP, which triggers the interaction between SPX1/2 factors and PHR1, suppressing the activation of PSI genes. PHR2 controls the expression of *MIR399* and *MIR837*, that target PHO2 and SPX-MFS1/2 respectively. When SDEL1 is ubiquitinated, SLs cannot bind to D14-SDEL1 complex and cytosolic SPX4 interacts with PHR2 to sequester PHR2 from targeting to the nucleus, thus, reducing PSI gene expression.

Pi excess in the soil can influence root development, leading to a reduction in primary root growth and lessened meristematic activity (Shukla *et al*., 2017). Excessive Pi accumulation leads to toxicity at the tip of rice leaves, mainly in older leaves (leaf tip necrosis). Compared with adaptive responses to Pi deficiency, our knowledge on mechanisms involved in plant adaptation to Pi excess is less well-characterized. To note, Pi fertilizers are commonly used in modern farming to maximize crop yields, leading to a scenario of Pi excess in agricultural ecosystems. Excessive use of fertilizers not only has a negative economic impact, but also causes several environmental problems due to soil pollution and water eutrophication, while raising serious concerns about food safety and animal health. Thus, understanding the molecular mechanism of plant adaptation to high-Pi conditions will provide useful information to design strategies for sustainable crop production.

4.3 Impact of nutrient stress on plant immunity

In nature, plants are simultaneously exposed to combinations of biotic and abiotic stresses. However, most studies that aim to determine the effects of environmental stress have been performed on plants exposed to individual stresses. The plant response may vary depending on whether it is subjected to just one single stress or a combination of stresses, as some of the signaling pathways that plants activate to address one type of stress might have a positive or negative impact on the other stress (Suzuki *et al*., 2014; Saijo & Loo, 2020). As an example, high supply of nitrogen has been associated with an increased severity of the rice blast disease, a phenomenon referred to as Nitrogen-Induced Susceptibility (Ballini *et al*., 2013). On the other hand, copper, a fungicide and bactericide widely used in agriculture (Bordeaux mixture),

not only has a direct effect on microbial pathogens, but also has an effect on the host plant through the activation of MAPK signaling for the upregulation of rice defense genes (Yuan *et al*., 2010). Additionally, our group reported that high Fe treatment of rice plants promotes both the expression of defense genes and enhanced resistance to *M. oryzae* infection (Peris-Peris *et al*., 2017). Altogether, these results support the existence of links between nutrient signaling and immune signaling in plants.

Regarding Pi nutrition, emerging evidence supports the existence of crosstalk between the Pi starvation and immune responses in *Arabidopsis* plants (Castrillo *et al*., 2017; Chan *et al*., 2021). Our group has described that high Pi excess compromises the expression of immune responses and enhances susceptibility to infection by *M. oryzae* in rice plants (Campos-Soriano *et al*., 2020). Thus, the indiscriminate use of Pi fertilizers might have an adverse effect on the rice plant by increasing the likelihood of blast disease. Clearly, there is the need to develop eco-friendly technologies to maintain rice production while reducing the use of Pi fertilizers and agrochemicals.

The impact of nutrient stress on disease resistance is, however, difficult to predict as different results have been observed depending on the host plant, the type of pathogen and the fertilization treatment. Contrary to what is observed in rice, in *Arabidopsis thaliana* Pi accumulation confers resistance against infection by fungal pathogens (Val-Torregrosa *et al*., 2021; Val-Torregrosa *et al*., 2022).

4.4 Phosphate biosensors in plants

Genetically encoded fluorescent sensors, or biosensors, are versatile tools that have shed light on a wide range of cellular processes

(Chen *et al*., 2017). These biosensors can monitor ions, metabolites, or enzymatic activity in real time, and visualize them in their native cellular context (Pendin *et al*., 2017). One class of biosensors uses Fluorescence Resonance Energy Transfer (FRET) for measuring and detecting changes in Pi levels. FRET is a phenomenon in which nonradiative energy is transferred from an excited donor fluorophore to an acceptor molecule in close proximity. These Pi biosensors are composed of two fluorescence proteins that are covalently linked to a sensing domain. The sensor undergoes a conformational change in response to the interaction with, or absence of, a target molecule (ligand) with the sensing domain, which can be quantified by measuring FRET efficiency **(Figure 7)**. A variety of FRET-based sensors have been generated in plants for the analysis of metabolites such as glucose, sucrose (Deuschle *et al*., 2006; Chaudhuri *et al*., 2008, 2011), the amino acid glutamine (Yang *et al*., 2010) or pH (Gjetting *et al*., 2012). FRET-based Pi sensors can be used for live cell imaging, a process that is helpful for studying cellular processes at the organ level, either in plants or animals (Lalonde *et al.,* 2005; Okumoto *et al.,* 2012).

Pi FRET-based sensors (named as Fluorescent Indicator Protein for inorganic Phosphate, FLIPPi) are genetically encoded fluorescent sensors that consist of chimeric genes formed by a cyan fluorescent protein (eCFP) fused to the *Synechococcus* Pi binding protein (PiBP), and an enhanced yellow fluorescent protein (cpVenus) that act as FRET partners (Gu *et al*., 2006). In *Arabidopsis*, such Pi sensors have been successfully used to monitor cytosolic Pi dynamics in root cells in response to Pi deprivation and resupply (Mukherjee *et al*., 2015; Assunção *et al.,* 2020). Differences in Pi content between developmental zones of the *Arabidopsis* root, with notable changes in FRET ratio detected in the transition zone, have been described using FLIPPi biosensors (Banerjee *et al*., 2016; Sahu *et al*., 2020).

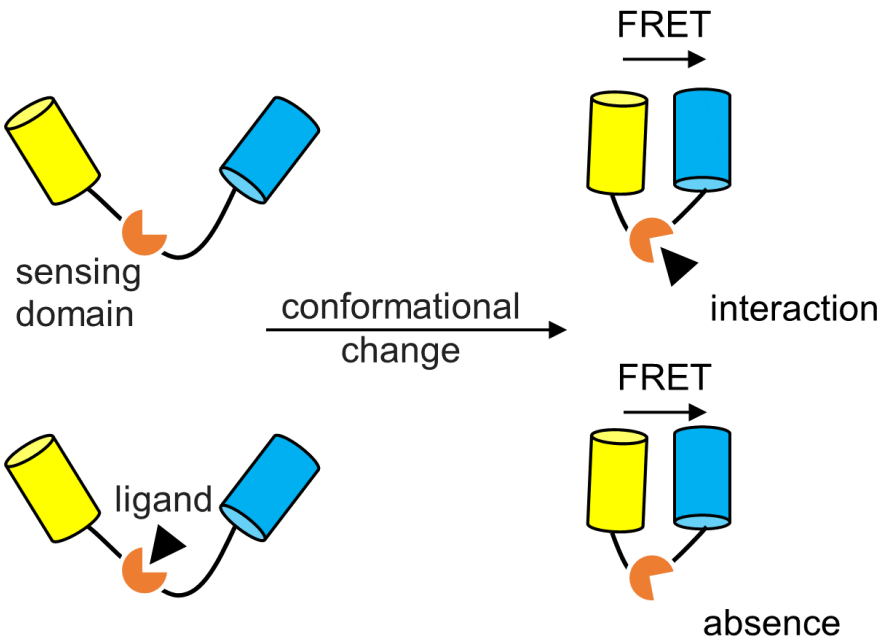

Figure 7. FRET biosensor scheme. The interaction with, or the absence of, the ligand (such as Pi) with the sensing domain causes a conformational change, leading to an increase in FRET.

5. Application of proteomics to the analysis of plant responses to pathogen infection

The omics revolution has ushered in a new era of plant biology research, providing a powerful tool to gain a broad perspective of changes at different levels of biological organization (genomics, transcriptomics, proteomics, metabolomics, ionomics, phenomics). In plants, genomics and transcriptomics offer a platform for studying stress responses, including the regulatory networks governing such stress responses. However, a more comprehensive understanding of stress responses in a particular plant species requires the characterization of its proteome.

Proteomics allows the identification and characterization of proteins involved in a variety of processes, including plant development and responses to environmental stress. Advances in protein separation and mass spectrometry analysis provide highly sensitive quantification of protein abundances and diversity in plant tissues. Two-dimensional gel electrophoresis (2-DGE) coupled with mass spectrometry (MS) laid a foundation for proteomics. These techniques enable the comparison of protein profiles among different samples through the quantification of protein spots. Label-based protein quantification strategies were developed, such as two-dimensional fluorescence difference in gel electrophoresis (DIGE), isotope-coded affinity tags (ICATs), isobaric tags for relative and absolute quantitation (iTRAQs), tandem-mass tags (TMTs), and stable isotope labeling with amino acids in cell culture (SILAC). More recently, label-free quantitative proteomic approaches have been successfully applied in genome-wide proteomics investigations (Katz *et al*., 2010; Wang *et al*., 2010). Factors such as sample purity and the coverage of protein databases remain major

bottlenecks in the proteomics analysis of plant proteomes, including those in plant-microbe interactions.

In addition to the identification of proteins, proteomic studies also allow for the estimation of the relative and absolute abundance and post-translational modifications of proteins, and protein-protein interactions. Among post-translational modifications, phosphoproteomics might provide valuable information on the dynamics and status of protein phosphorylation that can regulate plant responses triggered by biotic stress (Sharma *et al*., 2020). Furthermore, proteomics can help to identify new biomarkers of stress, which can be used to monitor plant health and to develop early warning systems for stress. Since the early 2000s, several proteomic studies have been conducted in plant-microbe interactions, including the rice/*M. oryzae* interaction (reviewed by Wei *et al*., 2023). A proteomic approach was used to investigate the impact of nitrogen deprivation in rice plants during *M. oryzae* infection (Konishi *et al*., 2001).

In recent years, the importance of the study of the apoplast proteome has progressively increased. Several studies have described the apoplast proteome (or secretome) during rice-pathogen interactions, such as during infection by *M. oryzae, Cochliobolus miyabeanus, Zymoseptoria tritici,* or in response to treatment with elicitors (Kim *et al*., 2009; Shenton *et al*., 2012; Kim *et al*., 2014; Yang *et al*., 2015; Kim SG *et al*., 2013; Liu *et al*., 2022). More studies are still needed to identify the full range of apoplastic proteins in plant-pathogen interactions.

5.1 Protein phosphorylation in plant cell signaling

Protein phosphorylation is an important cellular regulatory mechanism as many enzymes and receptors are activated/deactivated

by phosphorylation and dephosphorylation events, by means of kinases and phosphatases. Kinases create a covalent bond between a phosphate group and the hydroxyl group of a specific amino acid, and phosphatases reverse the reaction by removing the phosphate group. The balance of these two enzymes regulates the amount of phosphorylation residues found in a specific process. In plants, the most common amino acids found to be phosphorylated are serine (80–85%), threonine (10–15%), and tyrosine (0–5%) (Li & Liu, 2021). Plant genomes contain approximately twice the number of kinases as mammalian genomes. In rice, there are 1,512 (subsp*. japonica*) and 1,403 (subsp*. indica*) annotated kinases. Moreover, more than three million phosphorylation sites have been predicted in rice (Lin *et al*., 2016). The P(3)DB (http://www.p3db.org/) site provides a resource of protein phosphorylation data from multiple plant species (Gao *et al*., 2009).

Protein phosphorylation is important for regulating many essential reactions in a multitude of biological processes as it can modify the biochemical activity, interactions, localization, and stability of proteins (Lenman *et al*., 2008). Protein phosphorylation events in plants can also regulate reactions toward abiotic and biotic factors. Phosphorylation cascades are commonly used for the transduction or transmission of signals (Friso & van Wijk, 2015). Additionally, protein phosphorylation can define other post-translational modifications such as ubiquitination or sumoylation (Vu *et al*., 2018). Usually, the change in the phosphorylation status of a protein involves a change in its biological function.

On the other hand, the precise editing of phosphorylation sites in proteins has the potential to revolutionize crop improvement. By targeting specific phosphorylation sites, we can manipulate the activity of proteins involved in a variety of important processes, such as growth,

development, and stress response (Zhang *et al*., 2023). This could lead to the development of crops that are more productive, nutritious, and resilient to diseases.

5.2. Protein phosphorylation in plant immunity

Protein kinases play an essential role in regulating early responses during pathogen infection. When plants are treated with a general inhibitor of serine/ threonine kinases, early defense signaling events are abolished (Peck, 2003). The main phosphorylation pathways identified in biotic stress response involve mitogen-activated protein kinases (MAPKs) and calcium-dependent protein kinases (CDPKs) (Marcec *et al*., 2019; Manna *et al*., 2023).

The MAPK cascades play essential roles in growth and developmental regulation, as well as biotic and abiotic stress responses, and phytohormone signal transduction and responses (Manna *et al*., 2023). Highly conserved signal transduction modules are implicated in the plant response to biotic stress (Chen *et al*., 2021). MAPKKKs phosphorylate and activate MAPKKs, the activated MAPKKs subsequently phosphorylate MAPKs, and finally the activated MAPKs phosphorylate a large number of specific downstream substrates (e.g., transcription factors, chromatin remodeling factors, kinases or other enzymes) (Jagodzik *et al*., 2018). MAPK cascades that are activated by ROS also regulate ROS production by feedback mechanisms (Jalmi & Sinha, 2015).

Changes in cytosolic Ca^{2+} concentrations are one of the earliest cellular responses observed following pathogen challenges. The interplay between Ca^{2+} and ROS is bidirectional: the cytosolic Ca^{2+}

content is regulated by ROS, and Ca^{2+} is crucial for ROS production (Gaupels *et al*., 2017). In this process, CDPKs respond to pathogen-induced alterations in Ca^{2+} levels, and at the same time, they modulate the activity of RBOHDs that produce ROS, thus, creating a positive feedback loop (Gilroy *et al*., 2016).

In rice, CALCIUM-DEPENDENT PROTEIN KINASE 18 (CPK18) and MITOGEN-ACTIVATED PROTEIN KINASE 5 (MPK5) mutually phosphorylate. When phosphorylated, MPK5 suppresses defense gene expression, increasing susceptibility to blast disease (Xie *et al*., 2014). In the dephosphorylated resting state, CPK4 promotes the degradation of RLCK176 and negatively regulates defense responses while promoting plant growth and development (Wang *et al*., 2018b). CPK4 phosphorylation, however, prevents RLCK176 (RECEPTOR-LIKE CYTOPLASMICKINASE 176) degradation and positively contributes to plant immunity. It is also known that *OsCPK4* overexpression enhances resistance to the rice blast fungus *M. oryzae* (Bundó and Coca, 2016). Probably, the phosphorylation state of the protein is responsible for the double-face protein functionality. In other studies, it was reported that IPA1 (Ideal Plant Architecture 1) becomes phosphorylated early during infection leading to activation of *OsWRKY45* expression and resistance to *M. oryzae* infection. Later on, however, IPA1 dephosphorylates to avoid yield reduction (Wang *et al*., 2018).

Due to the importance of protein phosphorylation in plant defense against pathogens, large-scale identification of phosphorylated proteins has been carried out in rice, but none of these studies focused on the combination of abiotic and biotic stress. Therefore, more research is needed to fully understand the role of phosphorylation in plant immunity.

OBJECTIVES

The general aim of this PhD thesis was to investigate the effect of phosphate in disease resistance in rice, in particular resistance to the rice blast fungus *M. oryzae*, from a proteomics perspective. The specific objectives were:

-Objective 1: To determine the effect of Pi treatment on the accumulation of defense-related proteins in rice leaves during infection by *M. oryzae*, and to characterize Pi- mediated alterations in the proteome of the leaf apoplast in response to pathogen infection **(Sections 1 and 2)**.

-Objective 2: To investigate the phosphorylation status of rice proteins during infection by *M. oryzae* **(Section 3)**.

-Objective 3: To determine the functional implication of *OsPBZ1*, a member of the PR10 family of PR proteins, in blast resistance using the CRISPR/Cas9 system for genome editing **(Section 4)**.

-Objective 4: To evaluate the feasibility of using FLIPPi biosensors to assess alterations in Pi content in rice tissues, and its use to examine the plant response to treatment with elicitors of immune responses **(Section 5)**.

Results

Section 1 - Pi nutrition influences resistance to the rice blast fungus *M. oryzae*

1. Pi nutrition influences resistance to the rice blast fungus *M. oryzae*

1.1 Phosphate treatment has an effect on the accumulation of Pathogenesis-Related proteins during infection of rice plants with the blast fungus *M. oryzae*

Pathogenesis-Related (PR) proteins form a heterogenous group of proteins that accumulate in plant tissues during pathogen infection, some of these PR proteins exhibiting antimicrobial activity (Lopes *et al*., 2023). Previously, our group reported that treatment with high-Pi of rice plants is accompanied by a weaker induction of *OsPR1a* and *OsPBZ1* expression during infection and increased blast susceptibility (Campos-Soriano *et al.,* 2020).

In this work, we examined the effect of Pi treatment on the accumulation of PR proteins. Plants were grown under two contrasting Pi conditions: Low Pi (0.025mM) and High Pi (2.5 mM Pi) (henceforth High-Pi and Low-Pi plants). That plants perceive and respond to Pi treatment, was confirmed by measuring Pi content in leaves. High-Pi plants accumulated ten times more free Pi than Low-Pi plants **(Figure 1.1)**.

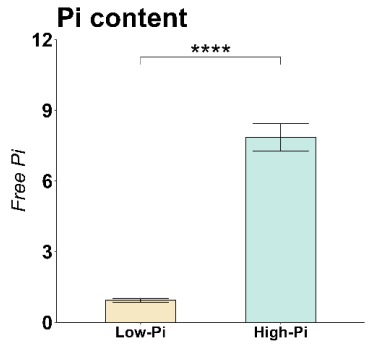

Figure 1.1. Accumulation of Free Pi in leaves of High-Pi and Low-Pi rice plants. Free Pi content in leaves of 3 weeks-old rice plants grown under Low- or High-Pi conditions for 15 days. Bars represent mean of four biological replicates with three plants per replicate ± *SEM* (*t* test, ****$p < 0.0001$).

High-Pi and Low-Pi plants at the three- to four-leaf stage were spray-inoculated with *M. oryzae* spores. Western blot analysis served to examine the accumulation of proteins belonging to different families of PR proteins, namely PR1, PR2 and PR10 (PBZ1) in leaves at different times after inoculation with *M. oryzae* spores (24, 48 and 72 hpi). Of them, PR1 and PBZ1 are usually considered as marker genes of the induction of rice defense responses (Midoh & Iwata, 1996; Agrawal *et al*., 2001), while the PR2 family comprises proteins with chitinase activity (Mauch *et al*., 1988). To assess the phenotype of resistance/susceptibility to infection, a set of plants was allowed to continue growth under the same experimental conditions (Low-Pi and High-Pi, mock-inoculated and *M. oryzae*-inoculated).

Results obtained by western blot analysis of leaf protein extracts are presented in **Figure 1.2**. Pathogen-induced accumulation of PR10 and PR2 was clearly observed at 72 hpi, in both Low-Pi and High-Pi plants (**Figure 1.2**, infected *vs.* mock, each time and condition). Pathogen-induced accumulation of PR1 occurred at an early time point (24 hpi, in Low-Pi and High-Pi plants). Intriguingly, at 48 hpi, PR10 accumulated at a higher level in mock-inoculated leaves than in *M. oryzae*-infected leaves of Low-Pi plants. Most probably, treatment with low Pi provokes a stressful situation in the plant that has an effect on PR10 accumulation in the absence of pathogen infection. Further investigation is required to clarify this aspect. An interesting finding was that all three PR proteins accumulated at a much lower level in High-Pi plants compared with low-Pi plants, also under infection conditions **(Figure 1.2)**.

Blast resistance of High-Pi and Low-Pi plants was determined at 7 days after infection with *M. oryzae*. As shown in **Figure 1.3**, treatment with High-Pi increased blast susceptibility as revealed by visual inspection and quantification of the lesion area in the *M. oryzae*-infected

leaves. Thus, the observed phenotype of susceptibility to *M. oryzae* infection correlates well with a weaker accumulation of PR proteins during *M. oryzae* infection in High-Pi plants.

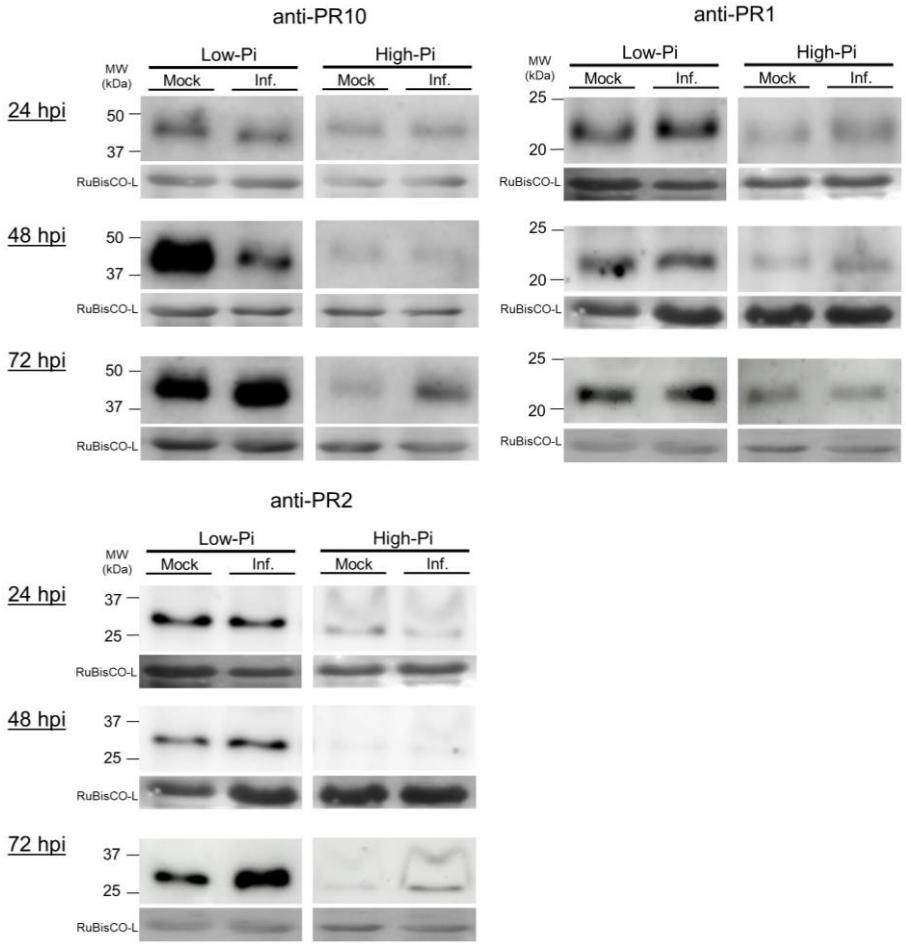

Figure 1.2. Accumulation of PR proteins in leaves of High-Pi and Low-Pi rice plants. Total protein extracts (10 µg) were separated by 12% SDS-PAGE and transferred onto nitrocellulose membrane. The accumulation of PR proteins was examined at the indicated time points (24, 48 and 72 hpi). Blots were probed with antibodies against rice PR1, PR10 or PR2 proteins. For detection of PBZ1, we used an antibody against rice PR10 proteins (or anti-PR10). Detection of inmunological reactions was performed using the secondary antibody, horse rabbit peroxidase (HRP)-labelled donkey anti-Rabbit IgG (H+L) (Thermo Fisher Scientific) and visualized on an Amersham ImageQuant™ 800 CCD imaging system. The large subunit of RuBisCO-L (Ribulose-1,5-bisphosphate carboxylase-oxygenase) served as loading control after Ponceau Red staining.

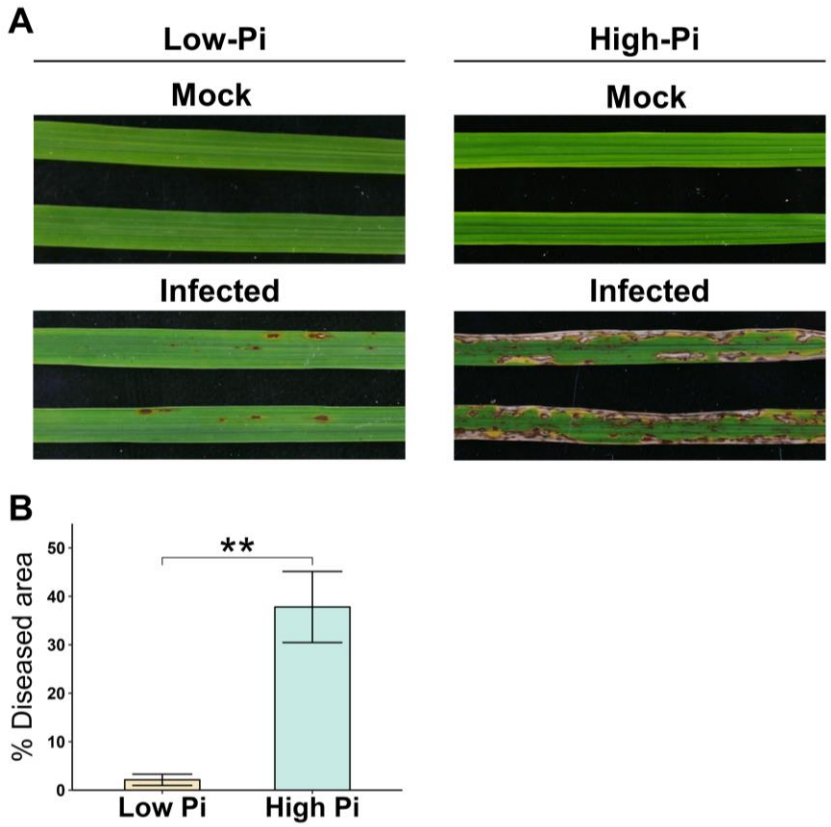

Figure 1.3. Susceptibility to *M. oryzae* infection in rice plants grown under high Pi supply. **A)** Rice plants were grown under High-Pi or Low-Pi conditions for 15 days and inoculated with a suspension of *M. oryzae* spores (5× 105 spores/ml), or mock-inoculated. Disease symptoms were examined in the youngest developed leaf (3rd leaf) at 7 days post-inoculation (dpi). **B)** Percentage of diseased area at 7 dpi (n=10) was determined by image analysis (APS Assess 2.0). Results from one representative experiment of four independent experiments with similar results are presented. (t test, $^{**}p < 0.01$).

Collectively, these results support that Pi accumulation in rice leaves is an important factor in determining susceptibility or resistance to infection by the blast fungus. Treatment with high Pi is associated with a lower accumulation of PR proteins during infection and enhanced susceptibility to *M. oryzae* infection. Contrary to this, treatment with Low Pi notably reduces rice blast disease, most probably, through a basal accumulation of certain PR proteins (e.g., PR10 proteins) in the absence of pathogen infection.

1.2 Pi accumulation in rice leaves influences the expression of *M. oryzae* effectors

Knowing that treatment of rice plants with high Pi enhances blast susceptibility, we investigated whether Pi accumulation, in addition to negatively affect host defense responses, might also influence the production of *M. oryzae* effectors, hence, fungal pathogenicity. To gain insight into this issue, we examined the *in planta* expression of *M. oryzae* effectors during infection in Low- and High-Pi rice plants. They were: *PWL2, BAS1, BAS3* and *BAS4* (MGG_04301, MGG_04795, MGG_11610 and MGG_10914, respectively). These effectors are produced during the biotrophic phase of the infection process. Of them, PWL2 and BAS1 accumulate at the BIC structure of *M. oryzae* invasive hyphae before being translocated to the cytoplasm of rice cells (cytoplasmic effectors) (Zhang & Xu, 2014). BAS3 accumulates in the regions where the invasive hyphae cross at the cell wall to neighboring cells (Mosquera *et al*., 2009). As for BAS4, this effector is secreted into the EIHM compartment surrounding the invasive hyphae but do not enter the rice cytoplasm (apoplastic effector) (Mosquera *et al*., 2009). The expression of *M. oryzae* effectors was examined during biotrophic invasion of rice leaves (e.g., 18, 27, 40, and 48 hpi).

Early during biotrophy (18, 27 hpi), expression of all four effectors was similar in Low- and High-plants **(Figure 1.4)**. At later times of infection, however, these effectors were expressed at significantly higher levels in High-Pi plants compared to Low-Pi plants. At 40 hpi, all four effector genes showed a great difference in their expression in High-Pi plants compared to Low-Pi plants **(Figure 1.4)**. These results indicate that the expression of *M. oryzae* effectors, at least the four fungal effectors here examined, is affected by Pi content in rice leaves. Stronger expression of effector genes in High-Pi plants during the

biotrophic phase of *M. oryzae* infection, both cytoplasmic and apoplastic effectors, is expected to promote host tissue invasion.

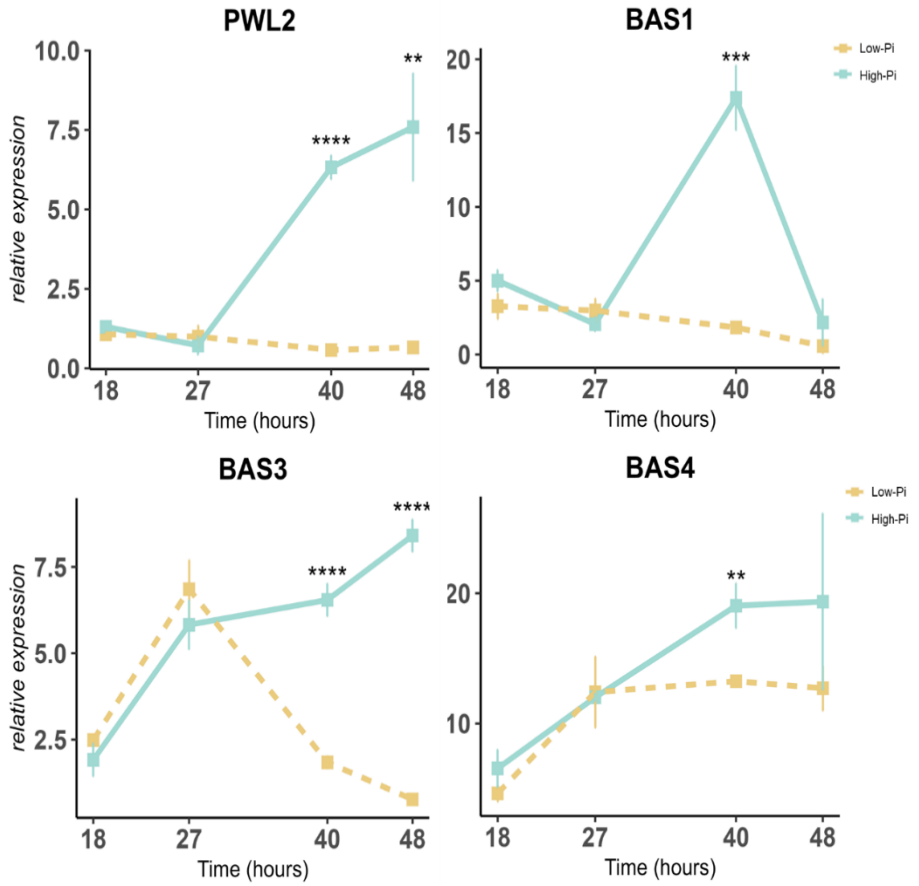

Figure 1.4. Expression of *M. oryzae* biotrophic effectors in leaves of Low- and High-Pi rice leaves. Expression of BAS1 (MGG_04795), BAS3 (MGG_11610), BAS4 (MGG_10914), and PWL2 (MGG_04301) at the indicated times after inoculation with *M. oryzae* spores is shown. Gene expression was measured by RT-qPCR and normalized with the Actin gene (MGG_03982). Values represent mean ± SEM of three biological replicates (three plants per replicate, three technical replicates each). At each time point, comparisons have been made between Pi treatment (t test, $^{**}p < 0.01$, $^{***}p < 0.001$, $^{****}p < 0.0001$).

Together, results here presented indicate that Pi content in rice leaves influences the two partners of the interaction, the rice plant and the fungus. On the plant side, Pi accumulation negatively influences the accumulation of Pathogenesis-Related (PR) proteins. On the pathogen

side, Pi accumulation stimulates the expression of fungal effectors. These findings are consistent with the observation that plants accumulating Pi in their leaves are more susceptible to infection by *M. oryzae*. To further investigate into the effect of Pi in the rice-*M. oryzae* interaction, we approached the characterization of the apoplastic proteome of rice leaves grown under different Pi conditions **(Section 2).**

Section 2 – Proteomic analysis of the leaf apoplast in rice plants grown under different Pi supply conditions

2. Proteomic analysis of the leaf apoplast in rice plants grown under different Pi supply conditions

The apoplast is the space external to the plasma membrane that includes cell walls, middle lamella, and intercellular spaces. The fluid that moves freely within the walls and intercellular spaces is known as the extracellular fluid or apoplastic fluid (AF). In the apoplast, the first communication between the plant and the pathogen takes place. In response to pathogen infection, plants secrete different types of defense proteins into the apoplastic region, including PR proteins, whereas pathogens secrete effectors proteins that can manipulate plant cellular responses to its own benefit. The apoplast also provides the environment for translocation of nutrients in the plant. Therefore, the protein composition of the apoplast may be important for the establishment and progression of the infection. To gain further insights into the effect of Pi content on blast disease, a comparative proteomic analysis of leaf apoplasts of High-Pi and Low-Pi plants was carried out.

2.1 Isolation of apoplastic proteins

The surface of rice leaves is highly hydrophobic. In this work, the vacuum infiltration method was used for isolation of the apoplastic fluid of rice leaves (Kim SG *et al*., 2013). For this, the rice plants were grown under Low-Pi and High-Pi (as described in **Section 1**). SDS-PAGE of apoplastic proteins followed by silver staining confirmed the absence of RuBisCO, an indicator of chloroplastic contamination in the apoplastic fluid **(Figure 2.1A)**. To further assess the purity of extracted apoplastic

proteins, we used the Malate Dehydrogenase (MDH) assay. MDH is a cytoplasmic enzyme and measurement of its activity is widely used to identify degree of cell membrane integrity and level of cytosolic contamination in apoplast protein preparations. As shown in **Figure 2.1B**, MDH activity in apoplast preparations was minimal (less than 0,1% of the MDH activity detected in total protein extracts of rice leaves). The apoplast preparations were then used for proteome analyses.

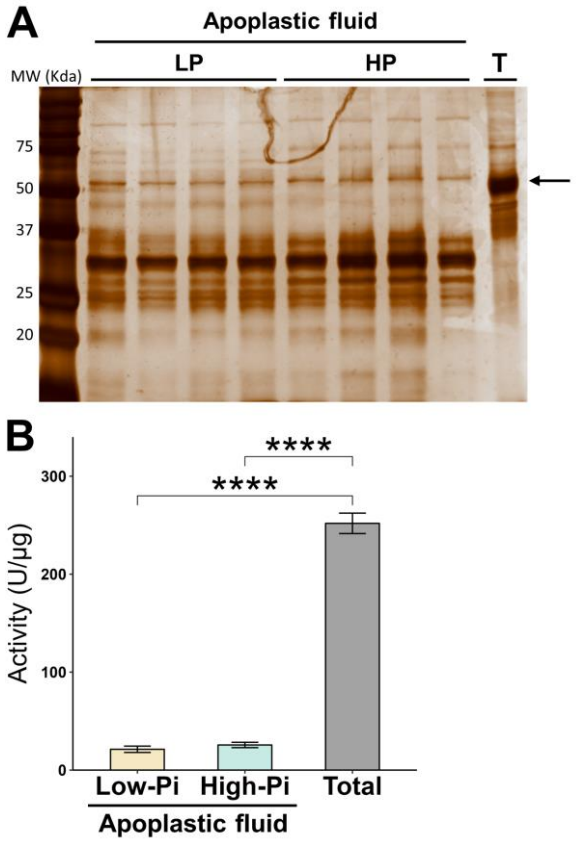

Figure 2.1. Apoplastic proteins isolated from Low-Pi (LP) and High-Pi (HP) rice leaves. A) Proteins were separated on 15% SDS-PAGE followed by silver staining. Representative analysis of total soluble proteins (T) from rice leaves. Four biological replicates for each condition were analyzed. The arrow on the right side indicates RuBisCO Large Subunit (LSU- RuBisCO). **B)** Purity assessment of apoplastic fluid based on malate dehydrogenase (MDH) assay. MDH activity was determined in the apoplastic fluid obtained leaves of Low-Pi and High-Pi rice plants (15 days of Pi treatment) or total soluble proteins from rice leaves (Total). Bars represent mean of four biological replicates (three pooled plants in each replicate) ± *SEM* (*t*-test, ****$p < 0.0001$).

2.2 Treatment of rice plants with high-Pi causes apoplast hydration.

Water hydration is an important factor during pathogen infection. Depending on the lifestyle of the pathogen, water can limit nutrient acquisition (Gentzel *et al*., 2022). Being a hemibiotrophic pathogen, *M. oryzae* acquires nutrients from the apoplast in the first stages of infection (biotrophic phase) (Cao *et al*., 2016).

We examined whether Pi treatment of rice plants has an effect on apoplastic hydration. For this, the apoplastic fluid was extracted from leaves of High-Pi and Low-Pi plants. The *apoplast dilution factor* was calculated by infiltrating the apoplast with a solution containing indigo carmine (O'Leary *et al*., 2014). Measurements of the apoplast dilution factor revealed a higher dilution factor in leaves of plants that have been grown under high-Pi supply than in low-Pi plants **(Figure 2.2)**. The volume of the apoplast solution obtained from leaves of High-Pi plants was found to be approx. four times higher than in Low Pi. Presumably, apoplast hydration in High-Pi plants might support *M. oryzae* growth more efficiently than in Low-Pi plants by facilitating uptake of water and nutrients from the apoplast. A similar result was previously described during biotrophic proliferation of a bacterial pathogen of maize (Gentzel *et al*., 2022). Here, the bacterial pathogen of maize causes apoplast hydration during biotrophy, and the hydrated apoplast was found to be enriched in metabolites usable by the bacteria (Gentzel *et al*., 2022).

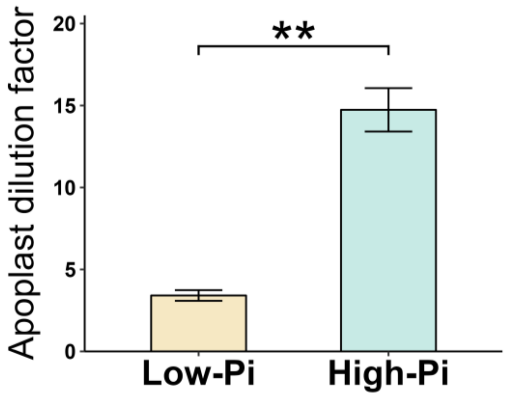

Figure 2.2. Apoplast dilution in leaves of plants grown under Low-Pi or High- Pi. Leaves from week-old plants (3-4 leaf stage) were harvested after 15 days of Pi treatment. Leaves (1g of fresh weight) were vacuum infiltrated with apoplast extraction buffer (CA buffer) with or without indigo carmine and centrifuged to extract the apoplastic fluid. The apoplast dilution factor was calculated from the corrected absorbance values as: Apoplast dilution factor = OD_{610} infiltrate / (OD_{610}infiltrate - OD_{610} apoplastic fluid). Bars represent mean of three biological replicates ± *SEM* (*t*-test, ***p* < 0.01).

2.3 Proteomic changes in the leaf apoplast in response to Pi supply conditions

A proteomic approach was used to get some insight into the dynamics of the leaf apoplastic proteome in rice plants in response to Pi treatment. Liquid chromatography-tandem mass spectrometry (LC-MS/MS) allowed the identification of apoplastic proteins in leaves of Low-Pi and High-Pi plants (3 biological replicates, each condition), and data sets were compared. Differences were observed in the total number of proteins identified in High-Pi and Low-Pi plants: 294 and 61 proteins in the apoplast of Low-Pi and High-Pi plants, respectively **(Figure 2.3A; Annex I)**. Of them, 52 proteins were present in the apoplast of both High-Pi and Low-Pi plants.

Gene Ontology (GO) analysis of apoplastic proteins in the category of Cellular Components revealed that an important number of

proteins categorized in the terms of “Extracellular region”, “Apoplast”, “Membrane” proteins and “Cell Wall” **(Figure 2.3B) (Annex I)**. In the category of Molecular Function, proteins in the terms of “Metal ion binding”, “Heme binding” and “Peroxidase activity” were highly represented in the apoplast of both Low-Pi and High-Pi rice plants **(Figure 2.3C)**. GO terms over-represented in the apoplast of Low-Pi compared to High-Pi plants were: “Hydrolase activity-Hydrolyzing O-glycosyl compounds”, “ATP binding“, “Chitinase activity and chitin binding”, “Lipid binding”, “Serine-type carboxypeptidase activity”, “Serine-type endopeptidase activity”, “Carbohydrate binding “, “Glucan endo-1,3-beta-D-glucosidase activity”, and “Oxidoreductase activity”. **(Figure 2.3C, Annex I)**.

GO terms in the category of Biological Processes were shared by both Pi conditions, but the relative number is greater in Low-Pi plants compared to High-Pi plants **(Figure 2.3D; Annex I)**. To note, the GO terms of “Response to Oxidative Stress”, “Proteolysis”, “Hydrogen Peroxide Catabolic Process”, “Chitin catabolic processes”, “Defense response” and “Defense response to fungus” were highly represented in the apoplast of Low-Pi plants **(Figure 2.3D, Annex I)**. Besides, GO terms in Biological Processes for “Lipid Transport”, “Chitin catabolic process”, “Polysaccharide Catabolic Process”, “Cell Wall Macromolecule Catabolic Process”, and “Regulation of root development” were more represented in Low-Pi plants than in High-Pi plants.

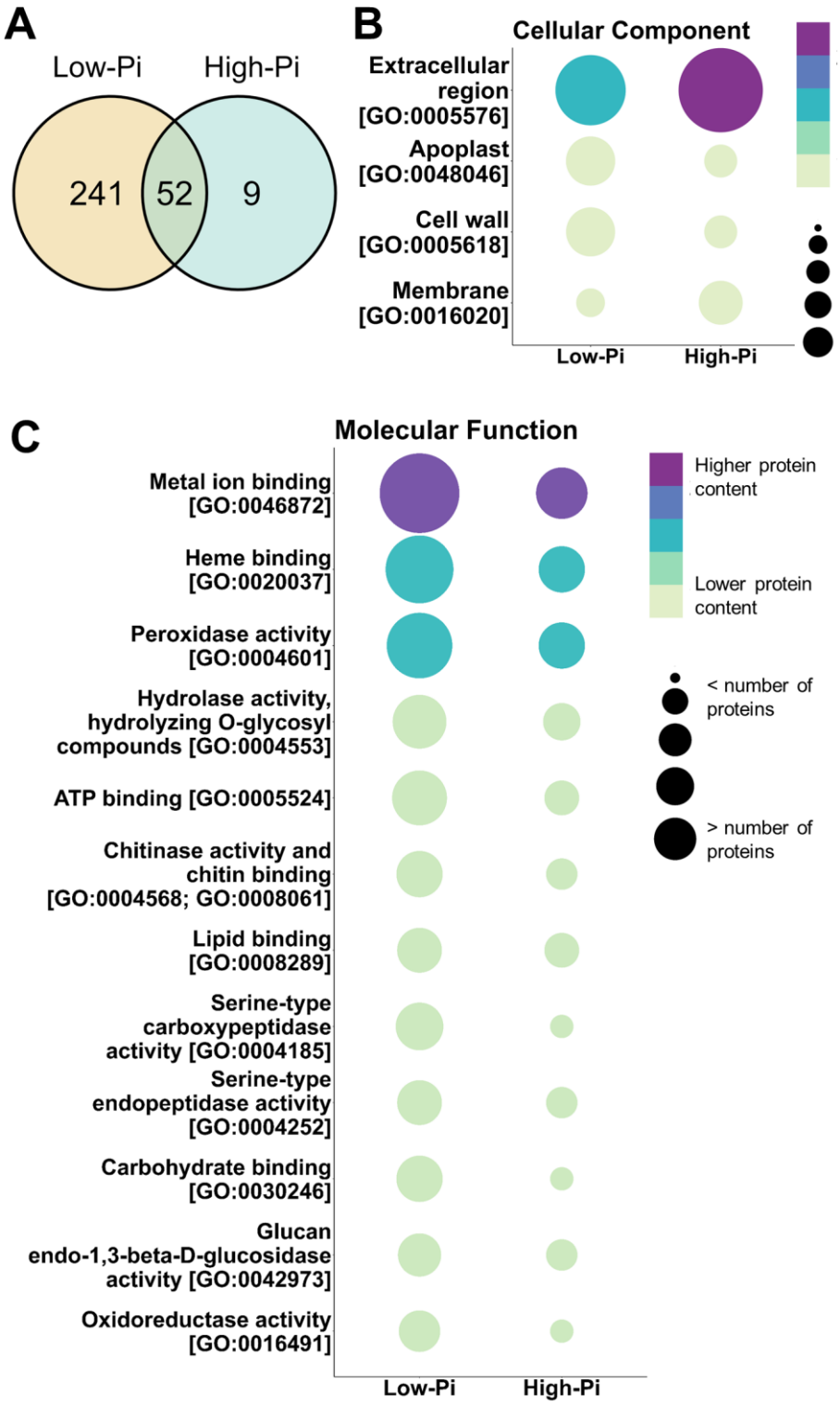
A
Low-Pi
High-Pi
241
52
9
B
Cellular Component
Extracellular region [GO:0005576]
Apoplast [GO:0048046]
Cell wall [GO:0005618]
Membrane [GO:0016020]
Low-Pi
High-Pi
C
Molecular Function
Metal ion binding [GO:0046872]
Heme binding [GO:0020037]
Peroxidase activity [GO:0004601]
Hydrolase activity, hydrolyzing O-glycosyl compounds [GO:0004553]
ATP binding [GO:0005524]
Chitinase activity and chitin binding [GO:0004568; GO:0008061]
Lipid binding [GO:0008289]
Serine-type carboxypeptidase activity [GO:0004185]
Serine-type endopeptidase activity [GO:0004252]
Carbohydrate binding [GO:0030246]
Glucan endo-1,3-beta-D-glucosidase activity [GO:0042973]
Oxidoreductase activity [GO:0016491]
Low-Pi
High-Pi
Higher protein content
Lower protein content
< number of proteins
> number of proteins

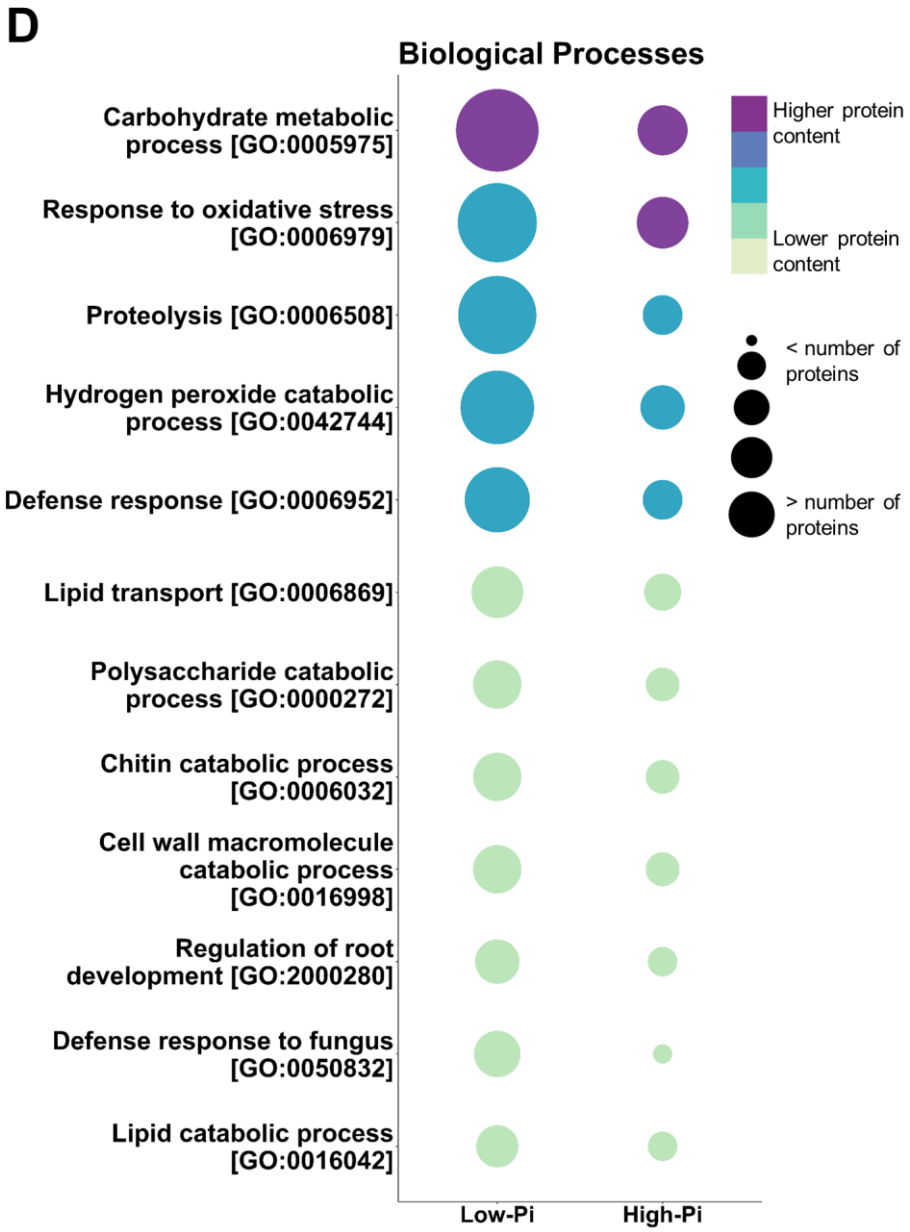

Figure 2.3 Analysis of the apoplastic proteome of leaves from rice plants grown under Low- and High Pi. A) Venn diagram for comparisons between all proteins identified in the apoplast of Low- and High-Pi rice plants. **B-D)** Bubble plots summarizing the annotation of detected proteins under each treatment for Cellular Component (**B**), Molecular Function (**C**) and Biological Processes (**D**) according to Gene Ontology (GO) terms. The relative number of GO terms was manually assessed (fraction of proteins in each term in each condition vs. total number of proteins). Circle size is indicative of the relative number of proteins of the GO terms. Circle color is indicative of the number of proteins in each condition of the GO terms.

We noticed that, in addition to well characterized apoplastic proteins, several cytoplasmic proteins or proteins that lack an N-terminal signal peptide were present in the apoplast of rice plants. Some examples are: Fructose-bisphosphate aldolase (B8B4J4), Thioredoxin-like_fold domain-containing protein (A2XPF9), Putative chaperonin 21 (Q69K73), and Purple acid phosphatase (Q84V55). Here, it should be mentioned that increasing evidence support that metabolism-related proteins, which are mainly cytosolic, are frequently identified in the leaf apoplast in different plant species, also during pathogen attack (Agrawal *et al*., 2010; Gupta *et al*., 2015). These proteins, known as leaderless secretory proteins (LSPs), do not have the typical N-terminal signal peptide for secretion. It has been proposed that LSPs are secreted to the apoplast via non classical protein secretion pathways (e.g., independent of the endoplasmic reticulum-Golgi secretory pathway), and might be essential for plant immune responses (Gupta *et al*., 2015).

However, the possibility that cytoplasmic proteins identified in the leaf apoplast have been released during preparation of the apoplastic fluid (a process in which leaves are cut and submitted to vacuum infiltration) should not be ruled out.

2.4 Defense related proteins accumulate in the leaf apoplast of Low-Pi rice plants

Analysis of proteins in the leaf apoplast of Low-Pi and High-Pi plants revealed the presence of proteins related to defense responses, such as PR proteins and peroxidases. These proteins were more frequently found in the apoplast of Low-Pi plants compared to High-Pi **(Figure 2.4)**. Detailed information about *Uniprot Accessions* of apoplastic proteins is available in **Table 2**.

Proteins involved in oxidative stress were represented in Low-Pi, including: peroxidases (and Class III peroxidases), Catalases, Thioredoxin-like superfamily, and glutathione-S-Transferases (GSTs) **(Figure 2.4)**. Regarding peroxidases, these enzymes participate in a broad range of processes in plant defense responses, such as ROS production, cross-linking of cell wall components, and phytoalexin biosynthesis (Almagro *et al.,* 2009). In total, 24 peroxidases proteins were detected in the apoplast of Low-Pi, but only 6 in the apoplast of High-Pi plants **(Table 2)**. Moreover, several members of the Class III peroxidase family were detected in the apoplast of Low-Pi plants (prx117, prx57, prx112, prx122, prx62, prx20, prx110). Class III peroxidases are known to be secreted into the apoplast for regulation of ROS homeostasis. They are also thought to trigger cell wall loosening or polymerization of cell wall components. Catalases typically respond to different stresses by upregulating their production, assisting plants in regulating ROS levels (Khan *et al*., 2020). Interestingly, the catalase enzymes A3REN3 and Q10S81 were exclusively detected in Low-Pi plants.

In the apoplast of Low-Pi plants, two proteins from the Thioredoxin-like superfamily, including one thioredoxin and one peroxiredoxin (B9FRZ1; A2XPF9), were identified, which were absent in the apoplast of High-Pi plants. Thioredoxins play a vital role in protecting cells from oxidative stress in a variety of cellular processes. (Ya Ma *et al*., 2023). Furthermore, two glutathione transferase (GST) enzymes (A3C154 and B9FKC8) were exclusively identified in the apoplast of Low-Pi plants. GSTs are responsible for catalyzing the conjugation of xenobiotics or their metabolites with glutathione, a crucial step in detoxification processes (McGoldrick *et al.,* 2005).

In the group of phosphatases, Metallophosphoesterase / Purple Acid Phosphatase proteins were highly represented in the apoplastic

proteome of Low-Pi plants. Purple acid phosphatases (PAPs, more represented in the apoplast of Low-Pi than in High-Pi), are known to be involved in phosphate acquisition and utilization as a strategy to cope with phosphate-limiting conditions (Bhadouria & Giri, 2022). Some PAPs have double subcellular localization. For instance, *OsPAP3b* was found to have a nuclear localization, this protein being also identified in the secretome of rice cell suspension cultures (Bhadouria *et al.,* 2023).

Proteome analysis also indicated that treatment with Pi results in alterations in the accumulation of glycosyl hydrolases, also more abundant in the apoplast of Low-Pi plants than in the apoplast of High-Pi plants **(Figure 2.4)**. Glycosyl hydrolases play diverse roles in cell wall metabolism, plant defense, signaling, and starch hydrolysis (Rafiei *et al*., 2021). As glycosyl hydrolases are important for maintenance of cell wall integrity, the presence of an important number of these enzymes in the leaf apoplast, is indicative of the important role that cell wall modifications might play in resistance against *M. oryzae*, particularly in Low-Pi plants. In our results, up to 27 families of glycosyl hydrolases were identified in Low-Pi plants, while only 5 families of glycosyl hydrolases were detected in the apoplast of High-Pi plants **(Figure 2.4, Table 2)**. Glycosyl hydrolases identified in this study belong to family 3 (O-Glycosyl hydrolases), family 5 (Cellulases A), family 20 (Beta-hexosaminidases), family 27 (Alpha-galactosidases), family 28 (Polygalacturonases), family 32 (Glycoside hydrolases), family 35 (Beta-galactosidases), family 38 (Alpha-mannosidases), family 51 (Non-reducing end alpha-L-arabinofuranosidases), and family 79 (Heparanases) **(Figure 2.4, Table 2)**.

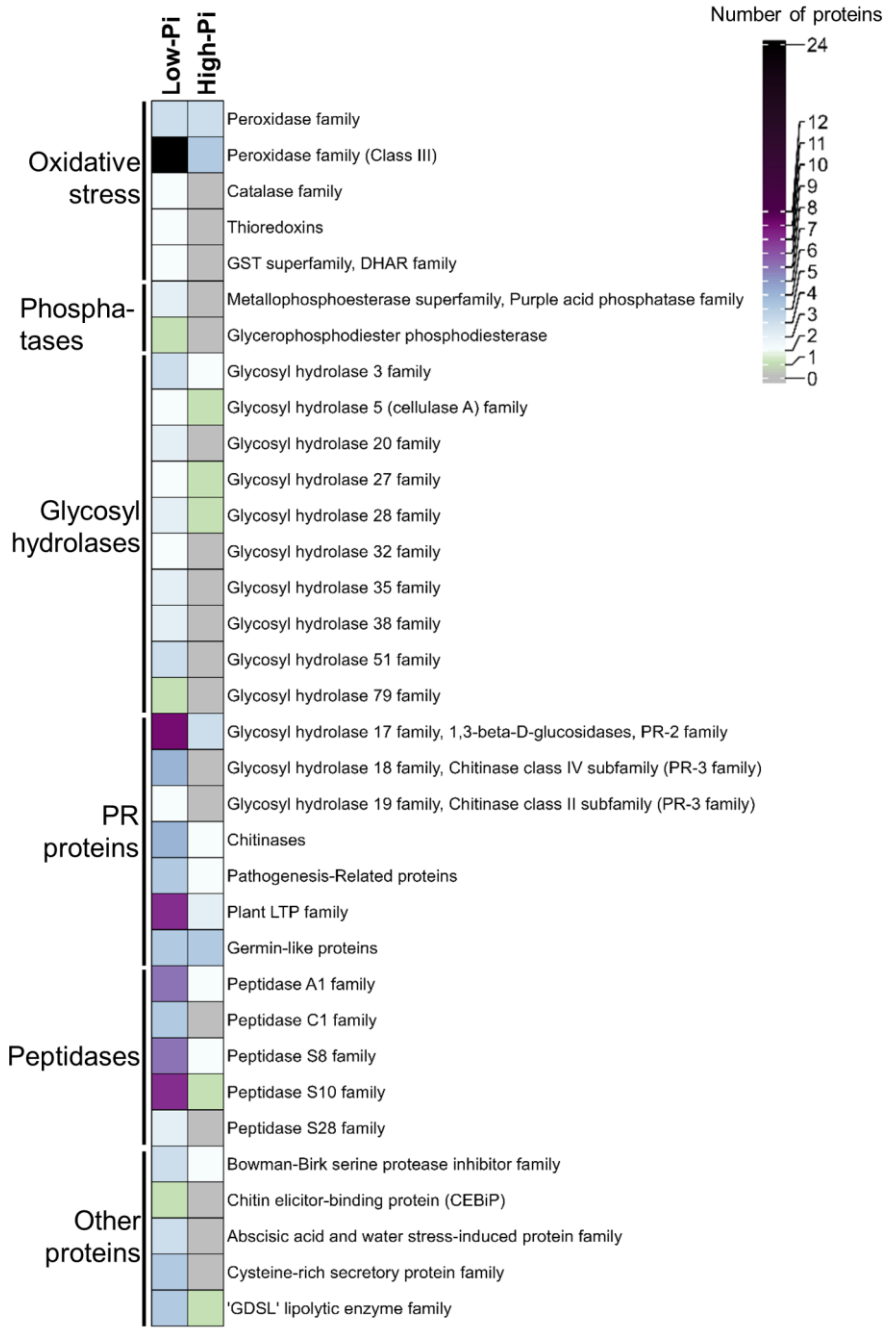

Figure 2.4. Heatmap illustrating the presence of defense-related proteins within the apoplast of leaves obtained from both Low- and High-Pi rice plants. The proteins have been clustered based on their respective protein families as detailed in **Table 2**. The color scale represents the abundance of proteins within each family: grey (no proteins detected), green (one protein identified), shades of blue to purple (ranging from two to twelve proteins identified), and black (twenty-four proteins).

Table 2. List of proteins detected within the apoplast of leaves obtained from both Low-Pi and High-Pi plants. The presence or absence of each protein in each respective Pi condition is indicated by "+" and "–" symbols, denoting detection, and non-detection, respectively.

Protein family	Protein name	Detected in Low Pi	Detected in High Pi	Accession
Oxidative stress				
Peroxidase family	Os05g0134400 protein	-	+	A0A0P0WHK7
	Peroxidase (EC 1.11.1.7)	+	-	A2WPA9
	Peroxidase (EC 1.11.1.7)	+	+	A2Y041
	Peroxidase (EC 1.11.1.7)	-	+	A3A4Y2
	Peroxidase (EC 1.11.1.7)	**+**	**+**	**A3A4Y3**
	Peroxidase (EC 1.11.1.7)	+	-	B9FUV7
Peroxidase family Classical plant (class III) peroxidase subfamily	Peroxidase (EC 1.11.1.7)	+	-	A0A0P0WHX2
	Peroxidase (EC 1.11.1.7)	+	-	A0A0P0XR31
	Peroxidase (EC 1.11.1.7)	+	-	A2X2T0
	Peroxidase (EC 1.11.1.7)	+	-	A2XEA4
	Peroxidase (EC 1.11.1.7)	+	-	A2XEA5
	Peroxidase (EC 1.11.1.7)	+	-	A2YBR3
	Peroxidase (EC 1.11.1.7)	+	-	A2YDW9
	Peroxidase 2 (EC 1.11.1.7)	+	-	A2YPX3
	Peroxidase (EC 1.11.1.7)	+	-	A3C1W9
	Peroxidase (EC 1.11.1.7)	+	-	B8A753
	Peroxidase (EC 1.11.1.7)	**+**	**+**	**B8B3L5**
	Peroxidase (EC 1.11.1.7)	+	-	B8B5W6
	Peroxidase (EC 1.11.1.7)	+	-	B9FV80
	Peroxidase (EC 1.11.1.7)	-	+	O22438
	Peroxidase (EC 1.11.1.7)	+	-	Q0IV54
	Peroxidase (EC 1.11.1.7)	+	-	Q5U1H6
	Peroxidase (EC 1.11.1.7)	+	-	Q5U1I3
	Peroxidase (EC 1.11.1.7)	+	-	Q5U1N1
	Peroxidase (EC 1.11.1.7)	+	-	Q5U1S3
	Peroxidase (EC 1.11.1.7)	+	-	Q5U1U2
	Peroxidase (EC 1.11.1.7)	**+**	**+**	**Q69WA0**
	Peroxidase (EC 1.11.1.7)	+	-	Q6K4J4
	Peroxidase (EC 1.11.1.7)	**+**	**+**	**Q7F1U0**
	Peroxidase (EC 1.11.1.7)	+	-	Q7XMP4
	Peroxidase (EC 1.11.1.7)	+	-	Q9ST80
	Peroxidase (EC 1.11.1.7)	-	+	Q9ST82
Catalase family	Catalase (EC 1.11.1.6)	+	-	A3REN3
	Catalase-1, putative, expressed	+	-	Q10S81
Thioredoxin-like superfamily	Thioredoxin-like_fold domain-containing protein	+	-	A2XPF9
	Thioredoxin-dependent peroxiredoxin (EC 1.11.1.24)	+	-	B9FRZ1
GST superfamily, DHAR family	Glutathione transferase (EC 2.5.1.18)	+	-	A3C154
	Glutathione transferase (EC 2.5.1.18)	+	-	B9FKC8
Phosphatases				
Metallophosphoesterase superfamily Purple acid phosphatase family	Purple acid phosphatase (EC 3.1.3.2)	+	-	A2WVM5
	Purple acid phosphatase (EC 3.1.3.2)	+	-	Q0J6R1
	Purple acid phosphatase (EC 3.1.3.2)	+	-	Q84V55
Glycerophosphodiester phosphodiesterase	Glycerophosphodiester phosphodiesterase (EC 3.1.4.46)	+	-	A3AK86
Glycosyl hydrolases				
Glycosyl hydrolase 3 family	Uncharacterized protein	+	-	A2XM08
	Fn3_like domain-containing protein	**+**	**+**	**B8AIS2**
	Fn3_like domain-containing protein	**+**	**+**	**B8AV76**
	Os03g0749500 protein	+	-	Q0DNJ7
Glycosyl hydrolase 5 (cellulase A) family	**Mannan endo-1,4-beta-mannosidase (EC 3.2.1.78)**	**+**	**+**	**A2Z6I9**
	Mannan endo-1,4-beta-mannosidase (EC 3.2.1.78)	+	-	B8AVH9
Glycosyl hydrolase 20 family	Beta-N-acetylhexosaminidase (EC 3.2.1.52)	+	-	A0A0N7KK17
	Beta-hexosaminidase (EC 3.2.1.52)	+	-	B8AYA3
	Beta-hexosaminidase (EC 3.2.1.52)	+	-	B9FM55
Glycosyl hydrolase 27 family	**Alpha-galactosidase (EC 3.2.1.22) (Melibiase)**	**+**	**+**	**A0A0P0XVT5**
	Alpha-galactosidase (EC 3.2.1.22) (Melibiase)	+	-	Q7XIV4
Glycosyl hydrolase 28 family	**Os06g0106800 protein**	**+**	**+**	**Q5VS63**
	Glycoside hydrolase family 28 protein, putative, expressed	+	-	Q10B12
	Os07g0245200 protein	+	-	Q6ZLN7
Glycosyl hydrolase 32 family	Uncharacterized protein	+	-	B9F0D3
	CIN1	+	-	D5L622
Glycosyl hydrolase 35 family	Beta-galactosidase (EC 3.2.1.23)	+	-	B8AYI0
	Beta-galactosidase 15 (Lactase 15) (EC 3.2.1.23)	+	-	Q0INM3
	Beta-galactosidase 6 (Lactase 6) (EC 3.2.1.23)	+	-	Q10NX8
Glycosyl hydrolase 38 family	Alpha-mannosidase (EC 3.2.1.-)	+	-	A0A0P0Y2R8
	Alpha-mannosidase (EC 3.2.1.-)	+	-	Q10A54
	Alpha-mannosidase (EC 3.2.1.-)	+	-	Q10A55

Glycosyl hydrolase 51 family		Non-reducing end alpha-L-arabinofuranosidase (EC 3.2.1.55)	+	-	B8B657
		Non-reducing end alpha-L-arabinofuranosidase (EC 3.2.1.55)	+	-	B8BLU8
		Non-reducing end alpha-L-arabinofuranosidase (EC 3.2.1.55)	+	-	Q10M79
		Non-reducing end alpha-L-arabinofuranosidase (EC 3.2.1.55)	+	-	Q8LIG5
Glycosyl hydrolase 79 family		Heparanase (EC 3.2.1.31)	+	-	A2Y9Y7
PR proteins					
Glycosyl hydrolase 17 family,1,3-beta-D-glucosidase	PR-2 family	Uncharacterized protein	+	-	A0A0N7KTE6
		Glucanase I	+	-	A2WYX5
		Glucan endo-1,3-beta-D-glucosidase (EC 3.2.1.39)	+	+	**A2WYX6**
		Glucan endo-1,3-beta-D-glucosidase (EC 3.2.1.39)	+	-	A2Y402
		Uncharacterized protein	+	-	A2YIJ5
		Uncharacterized protein	+	+	**B0EVM5**
		Glucan endo-1,3-beta-D-glucosidase (EC 3.2.1.39)	+	-	B8B6Z9
		Glucan endo-1,3-beta-D-glucosidase (EC 3.2.1.39)	+	-	B9FXP8
		Glucan endo-1,3-beta-D-glucosidase (EC 3.2.1.39)	+	+	**B9FXQ1**
		Glucan endo-1,3-beta-D-glucosidase (EC 3.2.1.39)	+	-	Q6YVU7
		Glucan endo-1,3-beta-D-glucosidase (EC 3.2.1.39)	-	+	Q84S76
		Beta-1,3-glucanase (EC 3.2.1.39)	+	-	Q9SXY8
Glycosyl hydrolase 18 family, Chitinase class IV subfamily	PR-3 family	GH18 domain-containing protein	+	-	A2WX14
		GH18 domain-containing protein	+	-	A2WX72
		GH18 domain-containing protein	+	-	A2WX73
		GH18 domain-containing protein	+	-	A2Z7A7
		Chitinase	+	-	Q7XXQ0
		Chitinase	+	-	Q8GZT6
Glycosyl hydrolase 19 family, Chitinase class II subfamily		Chitinase 11 (EC 3.2.1.14) (Pathogenesis related (PR)-3 chitinase 11)	+	-	Q10S66
		Chitinase 6 (EC 3.2.1.14) (Pathogenesis related (PR)-3 chitinase 6)	+	-	Q6K8R2
Chitinases		Chitinase (EC 3.2.1.14)	+	-	A2YH54
		Chitinase (EC 3.2.1.14)	+	-	A2YH55
		Chitinase (EC 3.2.1.14)	+	-	A2Z9V6
		Chitinase (EC 3.2.1.14)	+	+	**Q7GC32**
		Chitinase (EC 3.2.1.14)	+	-	O24007
		Chitinase (EC 3.2.1.14)	+	+	**Q6U5G8**
Pathogenesis-Related proteins	PR-1 family	**Pathogenesis related protein 1**	+	+	**A0A0D3QSW1**
		Pathogenesis-related protein PR1b	+	-	A0N0C2
	PR-5	**Osmotin (14b)**	+	-	Q40630
		Thaumatin-like protein	+	+	**P31110**
	PR-12 family	Defensin-like protein CAL1 (OsCPT1) (Pathogen-related protein 12) (OsPR12) (Protein CADMIUM ACCUMULATION IN LEAF 1)	+	-	Q6K209
Plant LTP family	PR-14 family	**Non-specific lipid-transfer protein**	+	+	**A0A0P0WNP9**
		Non-specific lipid-transfer protein 3 (LTP 3)	+	-	A2ZAS9
		Non-specific lipid-transfer protein	+	+	**A2ZAT1**
		Non-specific lipid-transfer protein	+	-	A2ZAT2
		Non-specific lipid-transfer protein	+	-	Q0IQK7
		Non-specific lipid-transfer protein 2B (LTP 2B) (LTP B1)	+	-	Q2QYL2
		Non-specific lipid transfer protein-like 1 (OsLTPL1)	+	-	Q6ASY2
		Non-specific lipid-transfer protein 2A (LTP 2A)	+	+	**Q7XJ39**
		AAI domain-containing protein	+	-	A2Y766
		Os10g0505700 protein	+	-	Q0IWJ3
Germin family	PR-16 family	**Germin-like protein 5 (OsGER5)**	+	+	**Q6ZBZ2**
		Germin-like protein	+	-	A2X5N7
		Germin-like protein	+	-	A2XN31
		Germin-like protein 5-1	+	-	Q6I544
		Germin-like protein 1-1 (Germin-like protein 4) (OsGER4)	+	-	Q7F731
Peptidases					
Peptidase A1 family		**Nucellin-like aspartic protease (Os11g0183900 protein)**	+	+	**A0A0P0XZY8**
		Os11g0183900 protein	+	-	A0A0P0Y0G8
		Peptidase A1 domain-containing protein	+	-	A2Z2G2
		Peptidase A1 domain-containing protein	+	-	A2Z9R9
		Peptidase A1 domain-containing protein	+	-	A2ZM43
		Peptidase A1 domain-containing protein	+	+	**A3CIV7**
		Putative nucleoid DNA binding protein	+	-	Q0IW25
		Os06g0119600 protein	+	-	Q5VPQ6
Peptidase C1 family		Uncharacterized protein	+	-	A2WSK3
		Uncharacterized protein	+	-	A2XQH0
		Cysteine proteinase rd21a	+	-	A6N1K8
		Oryzain beta chain (EC 3.4.22.-)	+	-	P25777
		Os04g0208200 protein	+	-	Q0JES7

Peptidase S8 family	Os01g0868900 protein	-	+	A0A0P0VAU9
	Os09g0482660 protein	+	-	A0A0P0XNY9
	Uncharacterized protein	+	-	B8A8Z9
	Uncharacterized protein	+	-	B8ATZ3
	Os04g0127200 protein	+	-	Q0JF92
	Os04g0121100 protein	+	-	Q0JFA2
	Os05g0435800 protein	+	+	**Q6I5K9**
	Cucumisin-like serine protease	+	-	Q75I27
	OSJNBa0084A10.2 protein	+	-	Q7XQQ3
Peptidase S10 family	Carboxypeptidase (EC 3.4.16.-)	+	-	A0A0P0VMA7
	Carboxypeptidase (EC 3.4.16.-)	+	-	A0A0P0X9L2
	Carboxypeptidase (EC 3.4.16.-)	+	-	B8AAJ3
	Carboxypeptidase (EC 3.4.16.-)	+	-	B8AFT0
	Carboxypeptidase (EC 3.4.16.-)	+	-	B8B5L7
	Carboxypeptidase (EC 3.4.16.-)	+	+	**B8BP32**
	Carboxypeptidase (EC 3.4.16.-)	+	-	Q0ITV6
	Carboxypeptidase (EC 3.4.16.-)	+	-	Q10K78
	Carboxypeptidase (EC 3.4.16.-)	+	-	Q6H7I6
	Carboxypeptidase (EC 3.4.16.-)	+	-	Q84QY7
Peptidase S28 family	Uncharacterized protein	+	-	B9FQ77
	Os10g0511400 protein	+	-	Q0IWG2
	Putative serine peptidase	+	-	Q94GW4
Other proteins				
Bowman-Birk serine protease inhibitor family	Bowman-Birk type bran trypsin inhibitor (OSE727A) (Protein RBBI3-3) (RBTI)	+	-	A2WK50
	BOWMAN_BIRK domain-containing protein	+	+	**A2WKA8**
	Bowman-Birk type bran trypsin inhibitor	+	-	A6MZH2
	BOWMAN_BIRK domain-containing protein	+	+	**B8AD05**
Chitin elicitor-binding protein (CEBiP)	(OsCEBiP) (Lysin motif-containing protein 1) (Os-LYP1)	+	-	Q8H8C7
Abscisic acid and water stress-induced protein family	Filaggrin-2	+	-	A0A6G9KGR1
	Abscisic stress ripening protein 2	+	-	A6N0H8
	Uncharacterized protein	+	-	B8ATR4
	OSIGBa0076I14.3 protein	+	-	Q01L89
Cysteine-rich secretory protein family	SCP domain-containing protein	+	-	A2YHS1
	SCP domain-containing protein	+	-	A2YHS4
	SCP domain-containing protein	+	-	A2YHS8
	SCP domain-containing protein	+	-	B8B754
	SCP domain-containing protein	+	-	L7IP43
GDSL' lipolytic enzyme family	Putative proline-rich protein APG	+	-	A0A0N7KG26
	Os07g0586200 protein	+	-	A0A0P0X8E6
	Uncharacterized protein	+	-	A2WPE0
	Putative esterase	+	+	**B8B307**
	cDNA clone:J023118N06, full insert sequence	+	-	Q9LHX6

Regarding PR proteins, this is a heterogeneous group of proteins related with plant defense responses. Previous studies have shown that some PR proteins have antimicrobial activity, but they have a distinct mode of action (Kaur *et al*., 2022). In the PR2 family (ß-1,3-glucanases, classified as glycosyl hydrolases family 17), we detected 12 proteins which were highly represented in the apoplast of Low-Pi plants (11 and 4 proteins were detected in Low-Pi and High-Pi, respectively). Among glycosyl hydrolases, families 18 and 19 consist of bifunctional chitinase/lysozyme activity (PR3 family), these proteins exhibiting lytic activity against components of fungal and bacterial cell walls, respectively (Fukamizo, 2000). In Low-Pi plants, 8 chitinases were identified, six of them belonging to the glycosyl hydrolase family 18 and the other two belonging to the glycosyl hydrolase family 19 **(Figure 2.4, Table 2)**. Also, we detected 6 chitinases (EC 3.2.1.14) in the apoplast of Low-Pi plants, but only 2 in High-Pi plants **(Figure 2.4, Table 2)**.

Plus, in our analyses, we detected two PR1 family members (PR1b, PR1). Whereas PR1 was found in Low- and High-Pi regime, PR1b was specifically found in Low-Pi plants **(Figure 2.4, Table 2)**. Members of the PR1 family have been reported to inhibit pathogen growth. However, despite the widespread use of PR1 family as defense marker, its specific biochemical function remains elusive. The presence of the PR1 consistently appears in situations in which the induction of programmed cell death (and its potential to cause cellular damage) is dependent on sterol sequestration (Gamir *et al*., 2017; Bakare *et al*., 2021).

Other PR proteins identified in the proteomic analysis of rice apoplast were defensins (PR12 family of PRs) and lipid transfer proteins (LTPs, PR14 family of PR proteins). In the apoplast of Low-Pi plants, up to 10 LTP proteins were identified, including LTP2A, LTP2B and LTP3 **(Figure 2.4)**. These PR proteins exhibit antimicrobial activity and play

an important role in plant defense against pathogenic microbes (Megeressa *et al*., 2020).

Peptidases are also used as markers of resistance in infection (Ali *et al.*, 2018). Particularly, we detect 9 peptidases from S8 family and 8 peptidases from A1 family, which are subtilases and aspartic proteases respectively, both related with defense responses (Darino *et al.,* 2022). From S10 family (carboxypeptidases), 10 proteins were detected in the apoplast of Low-Pi plants, but only one in High-Pi plants.

Remarkably, in the apoplast of Low-Pi plants we detected the rice chitin elicitor binding protein (CEBiP). This protein is known to bind chitin, a component of the cell wall in many pathogenic fungi, and functions as a receptor for chitin elicitors. This recognition triggers the activation of multiple signaling events involved in rice immunity, including Ca^{2+} influx, oxidative burst, and Mitogen-activated protein kinase (MPK) cascades (Shimizu *et al*., 2010).

Notably, four Abscisic acid (ABA) stress-inducible proteins were exclusively present in Low-Pi plant apoplast. ABA is recognized for its role in responding to abiotic stress, including drought and salinity, but it also contributes to biotic stress defense, particularly against pathogens (Bharath *et al*., 2021). Research has clarified the multifaceted role of ABA in the context of the rice-*Magnaporthe* interaction. It has been demonstrated that altering ABA signaling can lead to complex outcomes in this interaction: reducing ABA signaling enhances resistance to blast disease, whereas the introduction of exogenous ABA renders rice more susceptible to *M. oryzae* (Yazawa *et al*., 2012; Jiang *et al*., 2017). Consequently, the exclusive presence of ABA stress-inducible proteins in the apoplast of Low-Pi rice plants hints at a potential function for ABA

in fine-tuning defense mechanisms under conditions of limited phosphate availability.

Taken together, this study demonstrated that the leaf apoplast of Low-Pi plants is highly enriched in proteins involved in defense reactions in plants. The presence of these proteins in the apoplast of Low-Pi rice plants would then correlate with the phenotype of resistance that is observed in these plants **(see Figure 1.3)**. To further investigate the effect of Pi in resistance/susceptibility to *M. oryzae* infection at the protein level, we characterized the phosphorylation pattern of proteins in leaves of rice plants. For this, we analyzed the phosphoproteome of total soluble proteins from leaves of rice plants that had been grown under Low-Pi or High-Pi conditions, inoculated with *M. oryzae* or mock-inoculated in each case **(Section 3).**

Section 3 – Protein phosphorylation in leaves of rice plants grown under different phosphate supply and in the presence/absence of infection

3. Protein phosphorylation in leaves of rice plants grown under different phosphate supply and in the presence/absence of infection

Phosphorylation is a key mechanism for regulation of protein activity that affects many essential processes, including metabolism, cell signaling and cell cycle, cytoskeletal dynamics, and hormone responses. Protein phosphorylation events in plants can also regulate plant responses to abiotic and biotic stresses (Saini *et al*., 2023). It causes conformational changes in the phosphorylated protein that might affect protein activity and protein-protein interactions. However, most studies to determine the effects of environmental stress on protein phosphorylation have been performed on plants exposed to an individual stress. So far, there is limited research to determine how protein phosphorylation is associated with combined abiotic and biotic stress in plants. In this study, we conducted phosphoproteomic studies to identify changes in protein phosphorylation in rice leaves with a twofold objective: i) protein phosphorylation associated with Pi treatment, and ii) protein phosphorylation in the response of rice plants to pathogen infection.

3.1 Depletion of abundant Ribulose-1.5-bisphosphate carboxylase/oxygenase (RuBisCO) from leaf protein extracts

In this work, a phosphoproteomic approach was carried out to identify changes in protein phosphorylation in rice leaves. For this, the rice plants (cv. Tainung 67) were grown under Low- or High-Pi conditions for 15 days, and then spray-inoculated with a suspension of *M. oryzae* spores, or mock-inoculated (as in **Section 1**). Leaf samples for phosphoproteomic analysis were collected at 40-hpi. Total soluble

proteins were obtained for each condition: mock-inoculated Low-Pi, *M. oryzae*-infected Low-Pi, mock-inoculated High-Pi, and *M. oryzae*-inoculated High-Pi.

Depletion of abundant proteins is an effective way to improve detection and identification of low-abundance proteins. In particular, protamine sulfate precipitation has been shown to be effective to deplete abundant RuBisCO from leaf protein extracts (Kim ST *et al*., 2013). Protamine sulfate is a positive charged protein that binds to RuBisCO. To avoid RuBisCO hampering phosphoproteomic analysis, a protamine sulfate precipitation step was carried out prior phosphoproteomic analysis of rice leaves.

Total protein extracts were then incubated with protamine sulfate. Following centrifugation, RuBisCO depletion in the supernatant fraction was verified by SDS-PAGE and Coomassie brilliant blue staining **(Figure 3.1)**.

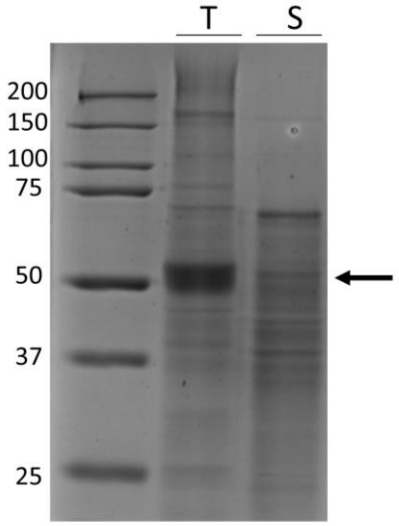

Figure 3.1. Depletion of RuBisCO using Protamine sulfate. Protein extracts before (T) and after (S) protamine sulfate precipitation were resolved on 10% SDS-PAGE followed by staining with colloidal coomassie brilliant blue (CBB). The RuBisCO Large Subunit (LSU- RuBisCO) protein is marked by an arrow. Representative gel image of four biological replicates for each condition (Pi treatment, infection) is shown.

3.2 Phosphoproteomic analysis of rice leaves

RuBisCO-depleted leaf extracts were subjected to phosphoproteome analysis. Tryptic peptides were enriched in phosphopeptides using Ti-immobilized metal affinity chromatography followed by LC-MS/MS. The name assigned to each plant material and condition was as follows: LPM (Low-Pi, mock-inoculated), LPI (Low-Pi, infected), HPM (High-Pi, mock-inoculated), and HPI (High-Pi, infected). In each case, three independent biological replicates were analyzed. Pair-wise comparisons were made to declare differentially phosphorylated proteins in response to: i) Pi treatment (Low-Pi mock *vs.* High-Pi mock), and ii) *M. oryzae* infection in each Pi condition (Low-Pi mock *vs*. Low-Pi infected; High-Pi mock *vs*. High-Pi infected) **(Figure 3.2A)**.

Rigorous criteria were employed for confident identification at both protein and peptide spectrum match levels, including a stringent false discovery rate (FDR) threshold of 1% **(see Annex II for details)**. In this way, a total of 1,011 phosphorylation sites mapping to 839 unique phosphopeptides were identified. These phosphopeptides showed 1 or more phosphorylated residues (e.g., 1 to 3). The predominant phosphorylation events were associated with serine residues, constituting 85.9% of the total, followed by threonine residues at 13%, and tyrosine residues at 1.1% **(Figure 3.2B, left panel)**. Remarkably, 80.6% of the phosphopeptides featured a solitary phosphorylation site, while 18.4% exhibited two phosphorylation sites, and only 1.1% manifested three phosphorylation sites **(Figure 3.2B, right panel)**. Each phosphopeptide corresponded to a unique phosphorylated protein, exemplifying a one-to-one relationship between phosphopeptides and proteins. Thus, our phosphoproteomic analysis revealed 839 unique phosphoproteins in rice leaves.

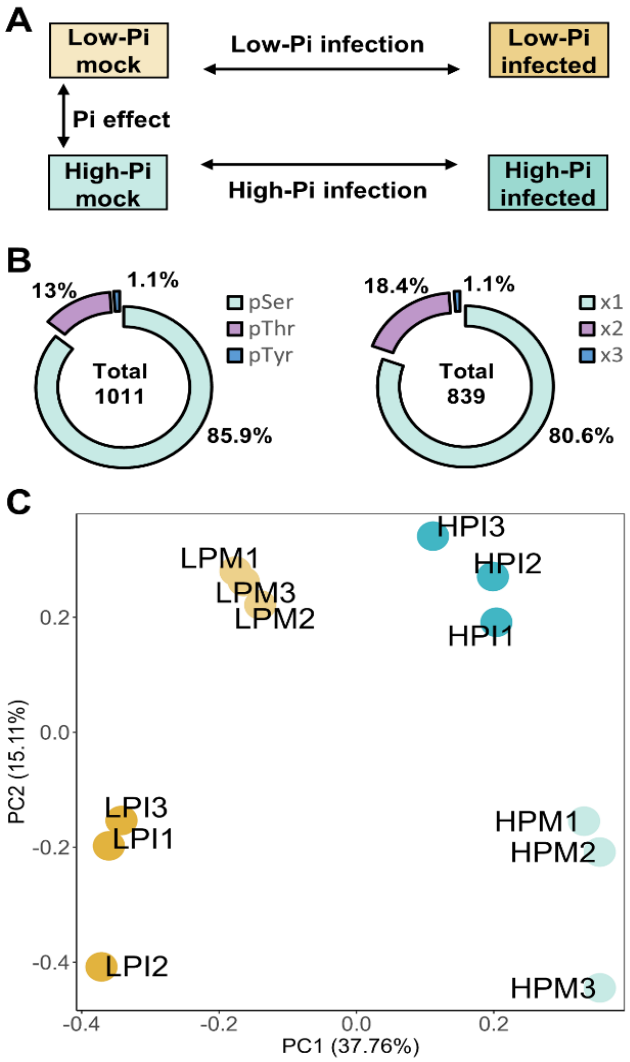

Figure 3.2. Phosphoproteomic analysis in rice leaves. Rice plants were grown under Low or High-Pi condition for 15 days (low-Pi, 0.025 mM; high-Pi, 2,5 mM) and then mock-inoculated or *M. oryzae*-inoculated (5x10^5 spores/ml). Leaves were harvested at 40 hours post-inoculation. Three independent biological replicates were analyzed for each condition. **A)** Overview of comparisons made for identification of differentially phosphorylated proteins to assess the effect of Pi (LPM *vs.* HPM), the effect of *M. oryzae* infection in Low-Pi plants (LPI *vs.* LPM), and the effect of *M. oryzae* infection in High-Pi plants (HPI *vs.* HPM). **B)** Percentage of pSerine (pSer), pThreonine (pThr) and pTyrosine (pTyr) sites (left panel) and distribution of phosphopeptides containing 1, 2 or 3 phosphorylation sites (right panel). **C)** Principal Component Analysis (PCA) of Pi treatment and *M. oryzae* infection (n = 3). The first two components explained 15.11% and 37.76% of the variances, respectively. Abbreviations: LPM, Low-Pi, non-infected (mock); LPI, Low-Pi, infected; HPM, High-Pi, non-infected; and HPI, High-Pi, infected.

Principal Component Analysis (PCA) revealed a clear separation between High-Pi and Low-Pi plants, supporting that Pi treatment has a strong impact on the leaf phosphoproteome. Equally, clear differences occurred between mock-inoculated and *M. oryzae*-inoculated plants in each Pi condition **(Figure 3.2C)**. Collectively, the PC1 and PC2 components account for 52.87% of the total observed variability. Criteria used for assignment of differentially accumulated phosphopeptides across the various comparisons were: fold change > 0.5, and p-value < 0.05. In this way, phosphopeptides that are over-accumulated or under-accumulated in each comparison were identified.

3.2.a Pi-responsive phosphoproteome in rice leaves

Up to 292 phosphoproteins were found to be regulated by Pi treatment in rice leaves (LPM *vs.* HPM comparison) (Annex III). A Volcano plot exhibiting over- and under-accumulated phosphoproteins in the LPM *vs.* HPM comparison was constructed to better illustrate changes in phosphorylation levels in response to Pi treatment **(Figure 3.3)**. Of the 292 phosphoproteins regulated by Pi, 97 and 195 phosphoproteins were found to under-accumulate and over-accumulate in Low-Pi plants, respectively (LPM *vs* HPM). Over-accumulating phosphoproteins in Low-Pi plants included two Respiratory burst oxidase proteins (RBOHB, Q2R351; and RBOHD; Q5ZAJ0) and Synaptosomal-associated protein of 32 kDa (SNAP32, Q5EEP3) **(Figure 3.3)**. RBOH proteins play a significant role in the generation of ROS in response to pathogen infection (Kadota *et al*., 2015), while SNAP32 contributes to resistance to rice blast throught the interaction with a syntaxin (Cao *et al*., 2019).

Several other proteins associated with the plant defense response to pathogen infection were also found to overaccumulate in

leaves of Low-Pi plants, including Mitogen-activated protein kinase kinase kinase 27 (MAPKKK27, M1SX00), Leucine-rich repeat transmembrane protein kinase (LRR-RLKs, Q84VG3), GTP binding protein (Q6ATJ0), and Serine/threonine-protein phosphatase (PPP, B9FTT3) **(Figure 3.3)**. Additionally, Acyl-CoA-binding domain-containing protein (ACBP2, Q5VRM0), known for its involvement in plant defense responses (Du *et al*., 2016), was also found to overaccumulate in Low-Pi plants. Another protein accumulating in Low Pi plants was Indoleacetic acid-induced protein 17 (IAA17, Q75GB1), which is associated with auxin responses. Furthermore, we detected two proteins associated with transcriptional regulation of gene expression phosphorylated in Low-Pi plants, namely Basic helix-loop-helix protein 9 (MYC2/BHLH9, Q336P5) and Transcription initiation factor IIF subunit alpha (TFIIF-alpha, A2Z5M1).

Among the proteins under-accumulating in Low-Pi conditions (e.g., over-accumulating in High-Pi plants), we identified chloroplastic Peroxiredoxin Q (PrxQ, P0C5D5) **(Figure 3.3)**. Peroxiredoxins are components of the plant antioxidant defense and redox signaling network, and their activity can be regulated through phosphorylation (Ya Ma *et al*., 2023). Defense-related proteins that are regulated by Pi treatment or *M. oryzae* infection are further discussed in **Section 3.3**.

Additional proteins under-accumulating in Low-Pi condition were Late embryogenesis abundant protein 1 (LEA1, A2XG55), Pyruvate Phosphate DiKinase (PPDK1), Ferredoxin-NADP reductase, chloroplastic leaf isozyme 2 (LFNR2, Q6ZFJ3), and DegP2 protease (DegP2, Q6Z806; homologue of the prokaryotic Deg/Htr family of serine endopeptidases), and a peptidase.

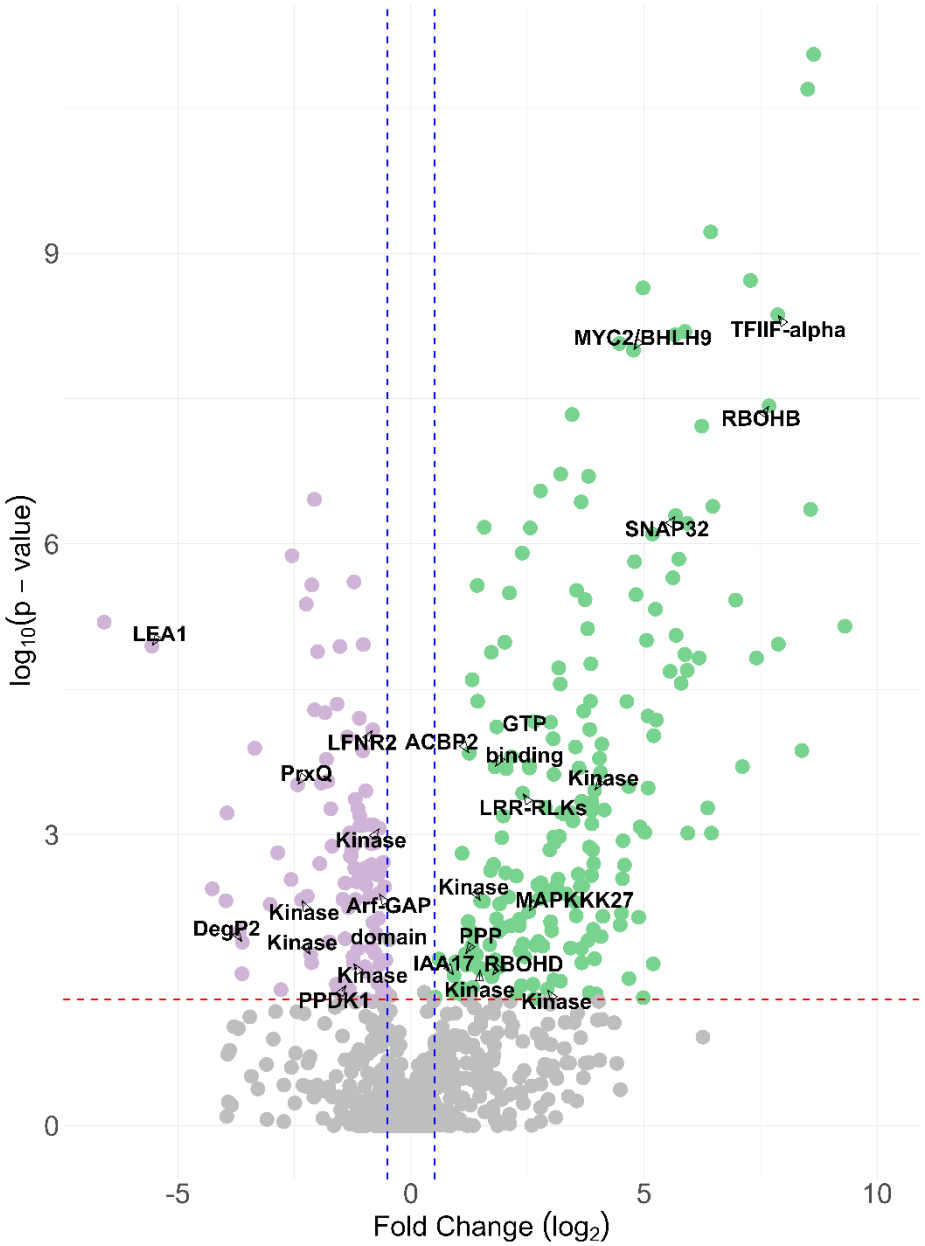

Figure 3.3. Analysis of differentially regulated phosphoproteins attending to the effect of Pi (LPM *vs.* HPM). Volcano plot. Purple and green filled points represent significantly over-accumulated and under-accumulated phosphoproteins, respectively. Red and blue dash lines indicated the confidence threshold of $p<0.05$ and fold-change >0.5, respectively. Number of differentially phosphorylated proteins are indicated above. The full list of proteins depicted in the Volcano plot is presented in **Annex II, Table S2**. Abbreviations: LPM, Low-Pi, non-infected (mock); HPM, High-Pi, non-infected (mock).

Furthermore, the Arf-GAP domain-containing protein (Arf-GAP domain, A2YMN9) involved in auxin signaling overaccumulated in High-Pi plants **(Figure 3.3)**. It is worth noting that proteins belonging to the protein kinase superfamily were identified in the set of phosphoproteins that either under-accumulated or over-accumulated in leaves of Low-Pi plants **(Figure 3.3)**.

Gene Ontology (GO terms) of rice phosphoproteins regulated by Pi treatment (Low-Pi vs High-Pi plants) is presented in **Figure 3.4 (for details, see Annex III, Table S3 and S4**). Differentially regulated phosphoproteins were identified using a fold change cutoff of > 0.5 and *p-value* < 0.05. In the category of **Biological Processes**, terms such as "Regulation of transcription DNA-templated," "Phosphorylation", and "Protein phosphorylation" were enriched in the set of phosphoproteins identified both in Low- and High-Pi plants. The GO terms of “Proteolysis” and “Protein transport” were prevalent among the over-accumulated proteins in High-Pi plants, whereas “mRNA processing”, "rRNA processing" and “mRNA splicing, via spliceosome” were specific to Low-Pi plants **(Figure 3.4 and Table S3)**. Some examples are Synaptosomal-associated protein of 32 kDa (SP32, Q5EEP3) for “Protein transport” (GO:0015031) and DegP2 protease (Q6Z806) for “Proteolysis” (GO:0006508). In the context of "mRNA processing" (GO:0006397), we identified the RRM domain-containing protein (A2Z2C1), for “mRNA splicing, via spliceosome” (GO:0000398) Small ribonucleoprotein (A3C5X6), and DEAD-box ATP-dependent RNA helicase 28 (B8BPM9) for “rRNA processing” (GO:0006364).

On the other hand, the GO terms "Abscisic acid-activated signaling pathway" and "Response to abscisic acid" were predominant in High-Pi plants, indicating phosphorylation regulation in hormone signaling pathways in the rice response to High Pi treatment.

Specifically, we detected two proteins from Ninja-family protein (Q6YVY6 and A2XDX5) and UspA domain-containing protein (A2Y3M2) **(Figure 3.4 and Annex III, Table S3)**.

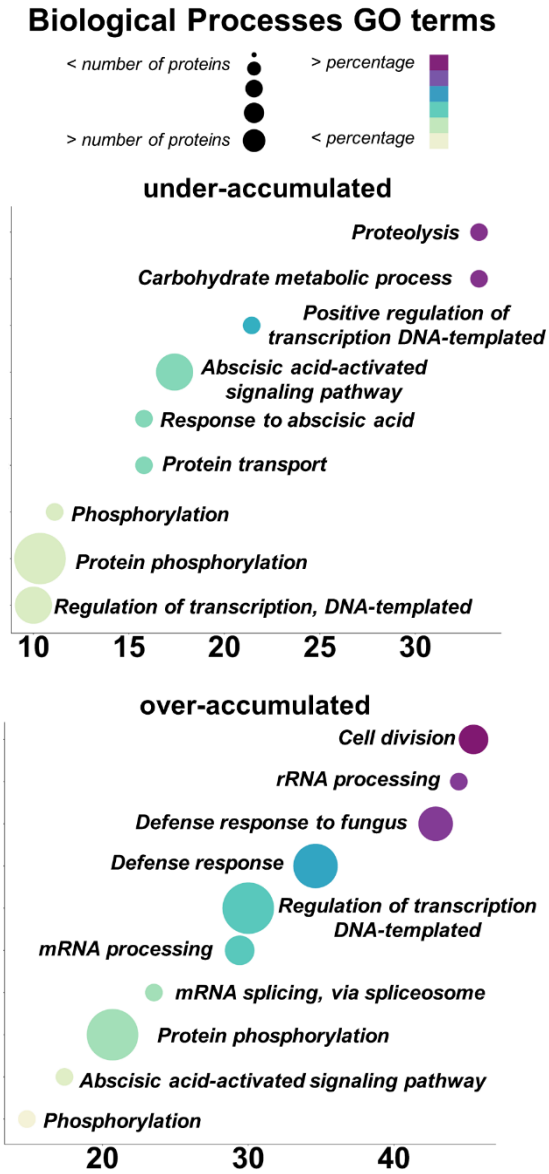

Figure 3.4. Bubble plots summarizing the Gene Ontology (GO) terms detected in leaves of rice plants grown under Low-Pi or High-Pi conditions in the category of Biological Processes (Low-Pi vs High-Pi). The relative number of GO terms was manually assessed (fraction of proteins in each term in each condition *vs.* total number of proteins). Circle size is indicative of the number of phosphoproteins in each condition. Circle color represents the proportion of phosphoproteins for each GO term.

To note, terms related to defense response, such as "Defense response to fungus" and "Defense response" were overrepresented in the set of differentially phosphorylated proteins in response to Pi treatment (overaccumulated in LPM vs HPM) **(Figure 3.4)**. The defense-related proteins included the above mentioned Respiratory burst oxidase proteins (involved in regulation of cell death and ROS production) and SNAP32 (protein transport). Other defense-related proteins regulated by phosphorylation in Low-Pi plants are involved in responses to ABA, ethylene signaling or cell wall organization **(Annex III, Table S4)**. These observations reinforce the notion that protein phosphorylation plays a role in the defense response *to M. oryzae* infection.

Gene Ontology (GO) terms related to **Molecular Function** in proteins differentially phosphorylated in the LPM *vs.* HPM comparison (FC > 0.5, *p-value* < 0.05) are presented in **Figure 3.5 (detailed in Annex III, Table S5)**. Phosphoproteins responsive to Pi treatment were enriched in GO terms related to “DNA-binding transcription factor activity”, “mRNA binding”, DNA binding” and “RNA binding” in both Low-Pi and High-Pi plants **(Figure 3.5)**. Some examples are: BZIP domain-containing protein (A3C9S2), Transcription factor MYC2/Basic helix-loop-helix protein 9 (Q336P5), Transcription initiation factor IIF subunit alpha (Q33AE7), PB1 domain-containing protein (A2YYR3) and DEAD-box ATP-dependent RNA helicase 28 (B8BPM9). This observation was also indicative of the relevance of protein phosphorylation events in controlling gene expression (and post-transcriptional regulation of gene expression) in the response of rice plants to Pi treatment **(Figure 3.5)**.

Equally, the terms of “Protein serine/threonine kinase activity” and “ATP binding” were highly represented among differentially regulated proteins in response to Pi treatment, being more represented

in Low-Pi plants than in High-Pi plants. Among them, we identified seven Protein kinase domain-containing proteins in Low-Pi plants (B8AIF3, B9FNI9, Q10RH1, B8A9P2, A0A0P0WT68, Q10NI9, Q5W6B4) and three in High-Pi plants (B8B5N5, B8B0Q9, A2ZX29). Given that Pi is a crucial factor for both ATP binding proteins and protein kinases, it is reasonable to expect that variations in the plant's Pi status might influence the extent of proteins within these GO terms.

To note, GO terms associated with "Calcium ion binding" and "Hydrolase activity" were within the pool of proteins over-accumulating in Low-Pi plants **(as depicted in Figure 3.5)**. Respiratory burst oxidase homolog protein B and D (Q5ZAJ0; Q2R351) and Calcium-binding EF hand protein-like (A3BFL8) correspond to “Calcium ion binding” (GO:0005509) GO term. Related to “Calcium ion binding”, it is well known that Ca^{2+} acts as an important second messenger in plant defense signaling pathways. The “Hydrolase activity” (GO:0016787) GO term includes DEAD-box ATP-dependent RNA helicase 28 (B8BPM9), HAD-superfamily hydrolase, subfamily IA–(Q10ME8), and DEAD-box ATP-dependent RNA helicase 24 (B9F826). Enrichment in “Hydrolase activity” is likely attributed to the plant's adaptive response to phosphate deficiency. Under low-phosphate conditions, plants may intensify hydrolytic processes as a mechanism to efficiently scavenge and utilize the limited phosphate resources at their disposal. The degree of enrichment of these GO terms would then be tied to the plant's phosphate status.

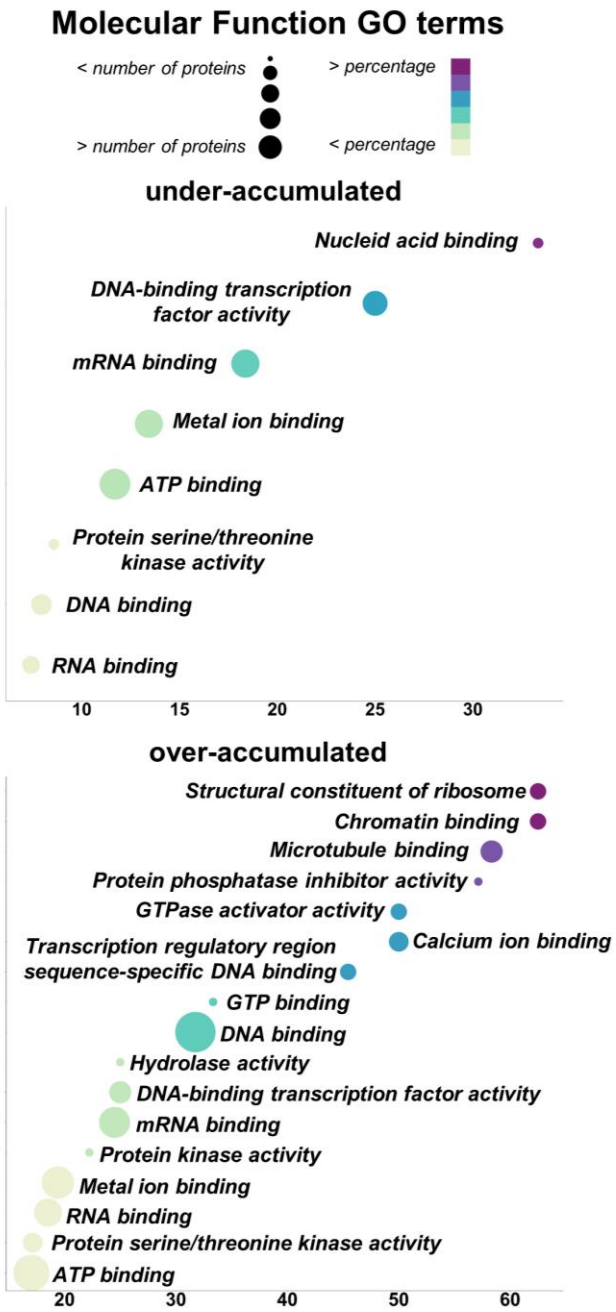

Figure 3.5. Bubble plots summarizing the Gene Ontology (GO) terms detected in leaves of rice plants grown under Low-Pi or High-Pi conditions in the category of Molecular Function. The relative number of GO terms was manually assessed (fraction of proteins in each term in each condition *vs.* total number of proteins). Circle size is indicative of the number of phosphoproteins in each condition of the GO terms. Circle color represents the proportion of phosphoproteins for each GO term.

3.2.b Phosphoproteome changes in leaves of Low- and High-Pi rice plants in response to M. oryzae infection

To investigate whether Pi content in rice leaves influences the status of protein phosphorylation during *M. oryzae* infection, we performed pair-wise comparisons: Low-Pi infected *vs* Low-Pi mock (LPI/LPM), and in High-Pi infected vs *High-Pi* mock (HPI/HPM) conditions. Volcano plots depicting phosphoproteomic changes in response to *M. oryzae* infection in leaves of Low-Pi and High-Pi rice plants are shown in **Figure 3.6**. The list of phosphoproteins that either over-accumulate or under-accumulate during pathogen infection in each Pi condition is shown in **Annex IV (Table S6, LPI_LPM)** and **Annex V (Table S10, HPI_HPM)**.

Using a FC > 0.5 and p-value < 0.05 cutoff, a total of 70 proteins were identified as being differentially regulated by phosphorylation in leaves Low-Pi plants during *M. oryzae* infection. Of them, 52 and 18 phosphoproteins over-accumulated and under-accumulated in low-Pi *M. oryzae*-inoculated plants relative to mock inoculated plants (LPI *vs.* LPM) **(Figure 3.6A and Annex IV, Table S6)**. In High-Pi plants, a total of 175 phosphoproteins were regulated by phosphorylation, of which 152 and 23 over-accumulated and under-accumulated, respectively **(Figure 3.6B and Annex V, Table S10)**. These observations highlight the relevance of protein phosphorylation in the rice response to *M. oryzae* infection, with a greater impact in High-Pi plants compared to Low-Pi plants.

The set of phosphoproteins overaccumulating in Low-Pi plants in response to infection (52 proteins in total) included: PTEN phosphatase protein (PTEN , Q2QT4); Squamosa promoter-binding-like protein 15 (SPL15, Q6Z8M8); UDP-glucose 6-dehydrogenase 5 (UGD5, Q2QS13); Root specific pathogenesis-related protein 10 (RSOsPR10,

Q75T45); Serine/threonine-protein kinase (Nek6, Q6YY75); and Eukaryotic translation initiation factor 4G (eIF4G, B9FXV5) **(Figure 3.6A and Annex III, Table S7)**. Proteins that exhibited under-accumulation in Low-Pi plants during infection (18 proteins in total) included: Ribulose bisphosphate carboxylase large chain (rbcL, A0A8G0G6R8); Thioredoxin-dependent peroxiredoxin (TPx-Q, Q69QW0); Pyrophosphate phospho-hydrolase (IPP, Q0DYB1); CHCH domain-containing protein (B9F7A0); and Reticulon-like protein (Q0DN13) **(Figure 3.6A and Annex IV, Table S7)**.

In High-Pi plants, 152 phosphoproteins were found to overaccumulate during by *M. oryzae* infection. Among them, there were Protein kinase (B8AIF3), DegP2 protease (Q67VP5), WRKY transcription factor (Q2R432), Filaggrin-2 (A0A6G9KGR1), Respiratory burst oxidase protein (RBOHD, Q2R351), Respiratory burst oxidase homolog protein B (RBOHB, Q5ZAJ0), Synaptosomal-associated protein of 32 kDa (SP32, Q5EEP3), Mitogen-activated protein kinase kinase kinase 27 (MAPKKK27, M1SX00), PTEN phosphatase protein (PTEN, Q2QT4), Plasma membrane ATPase (OSA2, Q43002), Root-specific pathogenesis-related protein 10 (RSOsPR10, Q75T45), Eukaryotic translation initiation factor 5B (IF2_eIF5B, A2Y845), Transcription factor MYC2/Basic helix-loop-helix protein 9 (MYC2/BHLH9, Q336P5), and C3H1-type domain-containing protein (A0A8J8XWW6), and Auxin response factor 4 (ARF4, Q5JK20) **(Figure 3.6B and Annex V, Table S11)**. For some of these proteins, a function in the plant response to biotic stress has been described (i.e., RBOHD, RBOHB, SP32) that will be discussed below.

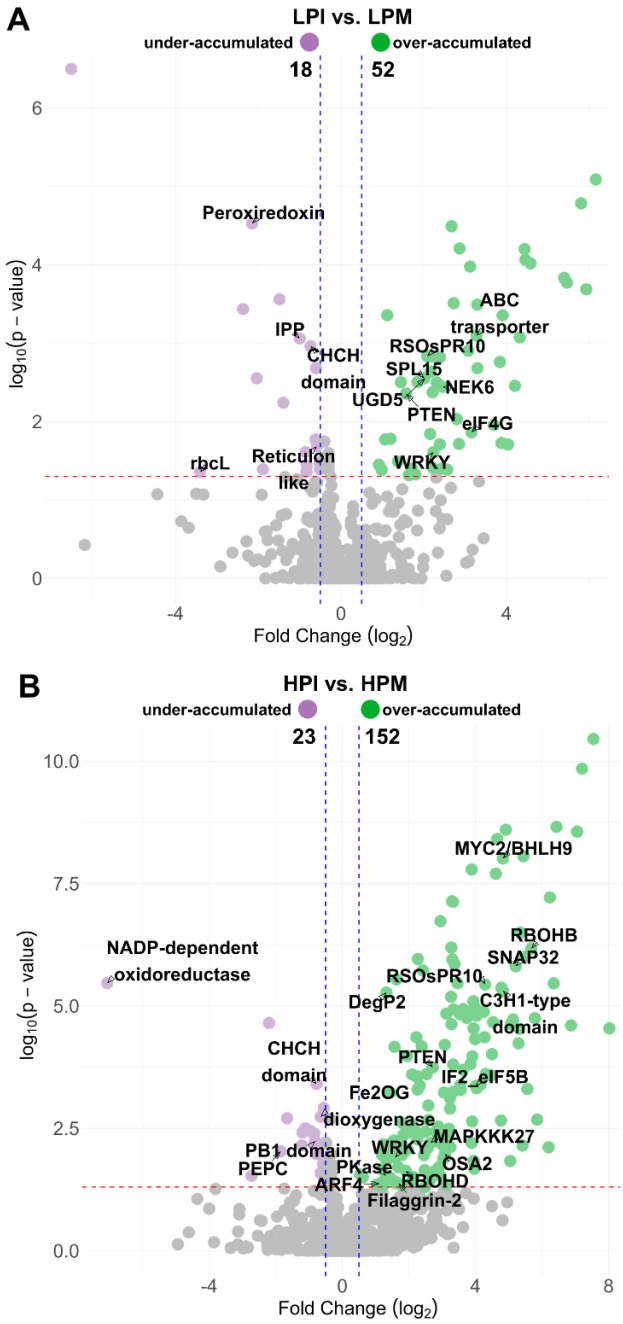

Figure 3.6. Volcano plots of the differentially regulated phophoproteins in leaves from rice plants grown under Low- or High Pi supply and inoculated, or not, with *M. oryzae*. Purple and green filled points represent significantly over-accumulated and under-accumulated phosphoproteins, respectively. Red and blue dash lines indicated the confidence threshold of $p<0.05$ and fold-change >0.5, respectively. Number of differentially phosphorylated proteins is indicated in the upper part.

As previously mentioned, Respiratory burst oxidase proteins play a crucial role in generating reactive oxygen species against pathogens (Kadota *et al*., 2015), and SP32 may contribute to host resistance to rice blast disease (Cao *et al*., 2019). It is important to note that, in the absence of pathogen infection, these proteins over-accumulated in Low-Pi plants compared to High-Pi plants. Whereas no differences were observed in the phosphorylation status of these proteins during infection of Low-Pi plants (LPI *vs.* LPM), they overaccumulated during infection of High-Pi plants **(Figure 3.6 and Annex V, Table S11)**.

Proteins related to oxidative stress responses were found to under-accumulate in *M. oryzae*-inoculated High-Pi plant relative to mock-inoculated High-Pi plants (HPI *vs.* HPM). They were: NADP-dependent oxidoreductase (B9FVG3) and Fe2OG dioxygenase (B8AP95) **(Annex V, Table S11)**. Other proteins that exhibited significant under-accumulation were Phosphoenolpyruvate carboxylase (PEPC, A2YUJ4), PB1 domain-containing protein (A2YYR3) and CHCH domain-containing protein (B9F7A0) **(Annex V, Table S11)**.

Details regarding GO terms comparing LPI *vs.* LPM can be found in **Annex IV** (**Table S8** for Biological Processes and **Table S9** for Molecular Functions). Similarly, information about HPI *vs.* HPM is provided in **Annex V** (Biological Process in **Table S12** and Molecular Function details in **Table S13**).

Next, an UpSet plot was created to examine differences and/or similarities in protein phosphorylation associated with both Pi treatment and infection (FC > 0.5; P value < 0.05) **(Figure 3.7)**. The UpSet plot shows the overlap between the LPI *vs.* LPM and HPI *vs.* HPM comparisons. The plot generalizes a Venn diagram by indicating the

overlapping sets with dots on the bottom and the size of the overlaps with the bar graph. This analysis revealed distinct regulation patterns in phosphoproteins depending on the Pi and infection conditions. In the HPI/HPM comparison, 141 phosphoproteins were found to over-accumulate under infection conditions while 20 phosphoproteins under-accumulated. However, these proteins remained unchanged in the LPI/LPM comparison. On the other hand, 43 phosphoproteins were found to over-accumulate in the LPI/LPM comparison, while 13 phosphoproteins under-accumulated. None of these phosphoproteins were regulated by infection in High-Pi plants **(Figure 3.7)**.

When comparing pathogen-regulated phosphoproteins in one or another Pi condition (LPI *vs.* LPM compared to HPI *vs.* HPM comparison), 9 proteins over-accumulated in both comparisons, while 3 proteins under-accumulated **(Table 3)**. Overaccumulated proteins included: RNA polymerase II degradation factor 1 (A0A4P7NM30); two uncharacterized proteins (A2WV12 and A2XQZ9) related with defense response and protein phosphorylation (GO:0006952 and GO:0006468), respectively; BSD domain-containing protein (A2X959); C2 domain-containing protein (A3BLL8); Nascent polypeptide-associated complex subunit beta (D9J2J5); PTEN phosphatase protein family (Q2QT46); WRKY transcription factor (Q2R432); Root specific pathogenesis-related protein 10 (RSOsPR10, Q75T45) **(Table 3)**. Under accumulated proteins included: FYVE/PHD zinc finger; PH domain-like protein (B8A981); Fe2OG dioxygenase domain-containing protein (B8AP95) and CHCH domain-containing protein (B9F7A0). Remarkably, two proteins exhibited discernible regulatory responses to the infection, Thioredoxin-dependent peroxiredoxin (TPx-Q, Q69QW0), related with oxidoreductase activity [GO:0016491] and Os04g0465000 protein (Q7X7Y6), related with methyltransferase activity [GO:0008168] **(Table 3)**. These two proteins manifested under-accumulation in Low Pi

conditions, but over-accumulation in High Pi plants. For additional information on proteins regulated by *M. oryzae* infection in leaves of rice plants grown under Low-Pi or High-Pi supply, see **Table 3.2**. These observations underscore a nuanced and intricate response of these proteins as part of the dynamic interplay between Pi signaling and immune signaling in rice plants.

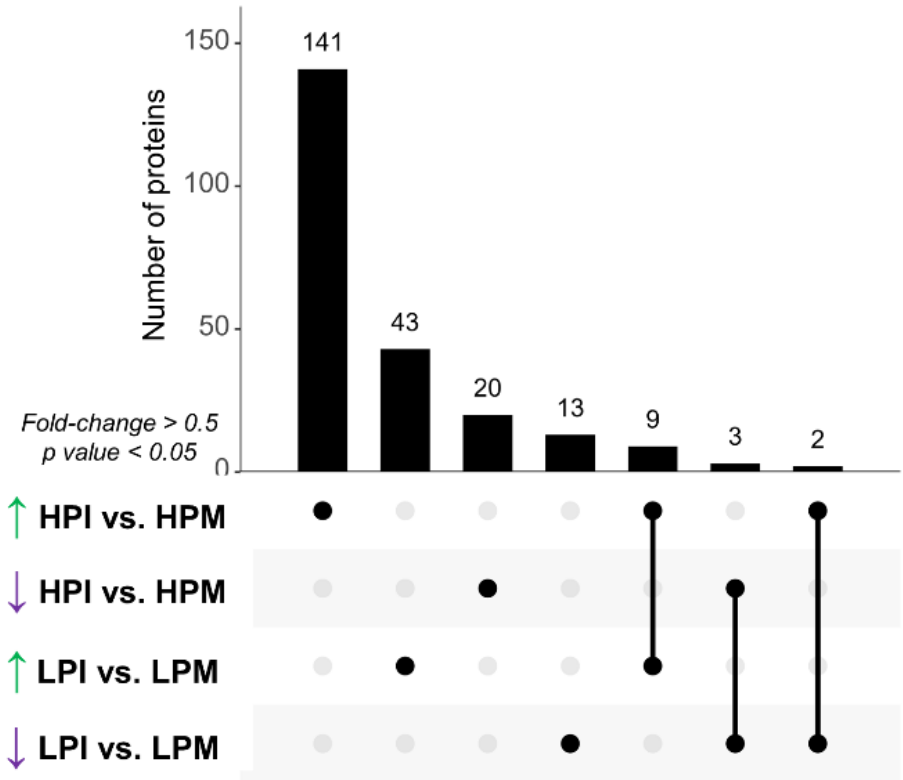

Figure 3.7. Upset plot illustrating differential protein phosphorylation among conditions (Low-Pi and High-Pi, infected and non-infected). Bars in the upper graph represent the number of proteins. Points in the lower part indicate regulation in the different comparisons. Joined black circles indicate that the same differentially regulated proteins were common to the pairwise comparison shown at the left side. In each comparison, green and purple arrows indicate proteins that over-accumulate and under-accumulate Abbreviations: LPM, Low-Pi, non-infected (mock); LPI, Low-Pi, infected; HPM, High-Pi, non-infected; and HPI, High-Pi, infected.

Table 3. List of phosphorylated proteins regulated by *M. oryzae* infection in leaves of rice plants grown under Low- and High Pi supply. Proteins over-accumulating (green) and under-accumulating (purple) in LPI *vs.* LPM and HPI *vs.* HPM comparisons (log2 abundance ratio > 0.5; P-value < 0.05) are shown.

Uniprot Accession	Protein name	Protein family	GO term: Biological process	GO term: Molecular function	log2 abundance ratio: LPI vs. LPM	log2 abundance ratio: HPI vs. HPM
A3BLL8	C2 domain-containing protein	C2 domain (Calcium/lipid-binding domain, CaLB)	mRNA transport [GO:0051028]; defense response [GO:0006952]	phospholipid binding [GO:0005543]	4,58	2,49
A0A4P7NM30	RNA polymerase II degradation factor 1	DEF1 family	regulation of gene expression [GO:0010468]	ubiquitin binding [GO:0043130]	4,32	3,55
D9J2J5	Nascent polypeptide-associated complex subunit beta	NAC-beta family		mRNA binding [GO:0003729]	2,45	1,82
A2WV12	Uncharacterized protein		defense response [GO:0006952]		2,39	1,61
Q2R432	WRKY transcription factor	WRKY DNA-binding domain	response to stimulus [GO:0050896]	DNA-binding transcription factor activity [GO:0003700]; sequence-specific DNA binding [GO:0043565]	2,23	1,58
Q75T45	Root specific pathogenesis-related protein 10	Pathogenesis-related protein	abscisic acid-activated signaling pathway [GO:0009738]; regulation of protein serine/threonine phosphatase activity [GO:0080163]	abscisic acid binding [GO:0010427]; protein phosphatase inhibitor activity [GO:0004864]; signaling receptor activity [GO:0038023]	2,09	4,29
Q2QT46	PTEN	PTEN phosphatase protein family	dephosphorylation [GO:0016311]; lipid metabolic process [GO:0006629]	phosphatidylinositol-3,4,5-trisphosphate 3-phosphatase activity [GO:0016314]	1,58	2,72
A2X959	BSD domain-containing protein	BSD domain-like			1,20	3,37
A2XQZ9	Uncharacterized protein		protein phosphorylation [GO:0006468]	protein serine/threonine kinase activity [GO:0004674]	0,92	1,45
B8AP95	Fe2OG dioxygenase domain-containing protein	Clavaminate synthase-like		oxidoreductase activity [GO:0016491]	-0,52	-0,65
B9F7A0	CHCH domain-containing protein	Cysteine alpha-hairpin motif		transferase activity [GO:0016740]	-0,73	-0,78
B8A981	Uncharacterized protein	FYVE/PHD zinc finger; PH domain-like; RCC1/BLIP-II	abscisic acid-activated signaling pathway [GO:0009738]; DNA damage response [GO:0006974]	metal ion binding [GO:0046872]	-1,49	-2,20
Q69QW0	Thioredoxin-dependent peroxiredoxin (EC 1.11.1.24)	NHL repeat	protein phosphorylation [GO:0006468]	antioxidant activity [GO:0016209]; oxidoreductase activity [GO:0016491]	-2,15	3,27
Q7X7Y6	Os04g0465000 protein	SAM/Pointed domain	methylation [GO:0032259]	methyltransferase activity [GO:0008168]	-2,36	3,74

Taken together, phosphoproteomic studies indicated that both Pi and *M. oryzae* infection have an effect in the phosphorylation status of rice proteins. On the one hand, we show that leaf proteins are differentially phosphorylated in response to *M. oryzae* infection, thus, demonstrating the importance of protein phosphorylation in shaping the plant's defense response. On the other hand, our findings indicate that the Pi status in the host plant influences the phosphorylation status of rice proteins. Presumably, Pi-mediated regulation of protein phosphorylation might also have an impact on rice immunity. Protein phosphorylation can then be considered an important factor in determining the outcome of the interaction, resistance or susceptibility. The interplay between Pi signaling and immune signaling adds a layer of complexity to regulatory networks involved in blast resistance in rice. Further research into specific phosphorylation events and their functional consequences will be required to get a better grasp of the specific biological function of these proteins in the rice response to Pi supply and/or pathogen infection.

3.3 Defense related proteins are regulated by phosphorylation

The information gained in our phosphoproteomic analysis of rice leaf proteins prompted us to further investigate defense-related proteins that are regulated by phosphorylation in response to Pi treatment and/or infection in rice. *A priori*, each phosphorylation event may be involved in the plant response to one factor (Pi and infection, separately), or to the combination of the two factors (Pi and infection).

Peroxiredoxins function in the antioxidant defense and redox signaling network of the cell and have been previously linked to pathogen defense. Our phosphoproteomic analysis revealed

phosphorylation events in two distinct peroxiredoxins, namely a thioredoxin-dependent peroxiredoxin (TPx-Q, Q69QW0) and the chloroplastic Peroxiredoxin Q (PrxQ, P0C5D5) **(Figure 3.8A)**. The phosphorylation status of TPx-Q exhibited regulation in response to both Pi treatment and infection. In the absence of pathogen infection, the level of TPx-Q phosphorylation in Low-Pi plants was higher than that in High-Pi plants **(Figure 3.8A; LPM *vs.* HPM)**. Intriguingly, during infection, a contrasting pattern of phosphorylation emerged for TPx-Q. Thus, TPx-Q phosphorylation level decreased during infection in Low-Pi plants (LPI vs LPM), while increasing in High-Pi plants (HPI vs HPM) **(Figure 3.8A)**. Opposite to what was observed from TPxQ, phosphorylation of PrxQ was higher in High-Pi plants (LPM *vs.* HPM). During infection, its level increased or decreased depending on the Pi condition (LPI *vs.* LPM, HPI *vs.* HPM).

Among the set of differentially phosphorylated proteins was MAP kinase phosphatase 1 (MKP1, A2V7M8). Although the MKP1 phosphorylation level did not fulfill the requirement of having a FC > 0.5, its phosphorylation status appeared to be severely affected by Pi treatment in the absence of pathogen infection (reduced level of phosphorylation In Low-Pi plants relative to High-Pi plants, LPM vs HPM) **(Figure 3.8B)**. In the presence of *M. oryzae* infection, the phosphorylated MKP1 levels declined in Low--Pi plants (LPI *vs.* LPM), whereas an increase was observed in High-Pi plants (both LPM *vs.* HPM and HPI *vs.* HPM).

Regarding MAP kinase phosphatases, it is well known that these enzymes play an important role in pathogen-induced signal transduction pathways (MAPK signaling cascades). Phosphoproteomic analysis revealed that phosphorylation of the Serine/threonine-protein kinase Nek6 (Q6YY75) substantially increased during infection of Low-Pi plants

(LPI *vs.* LPM) **(Figure 3.8B)**. This particular protein kinase has been previously associated with a positive regulation of drought resistance (Ning *et al*., 2011). Its function during pathogen infection remains to be investigated.

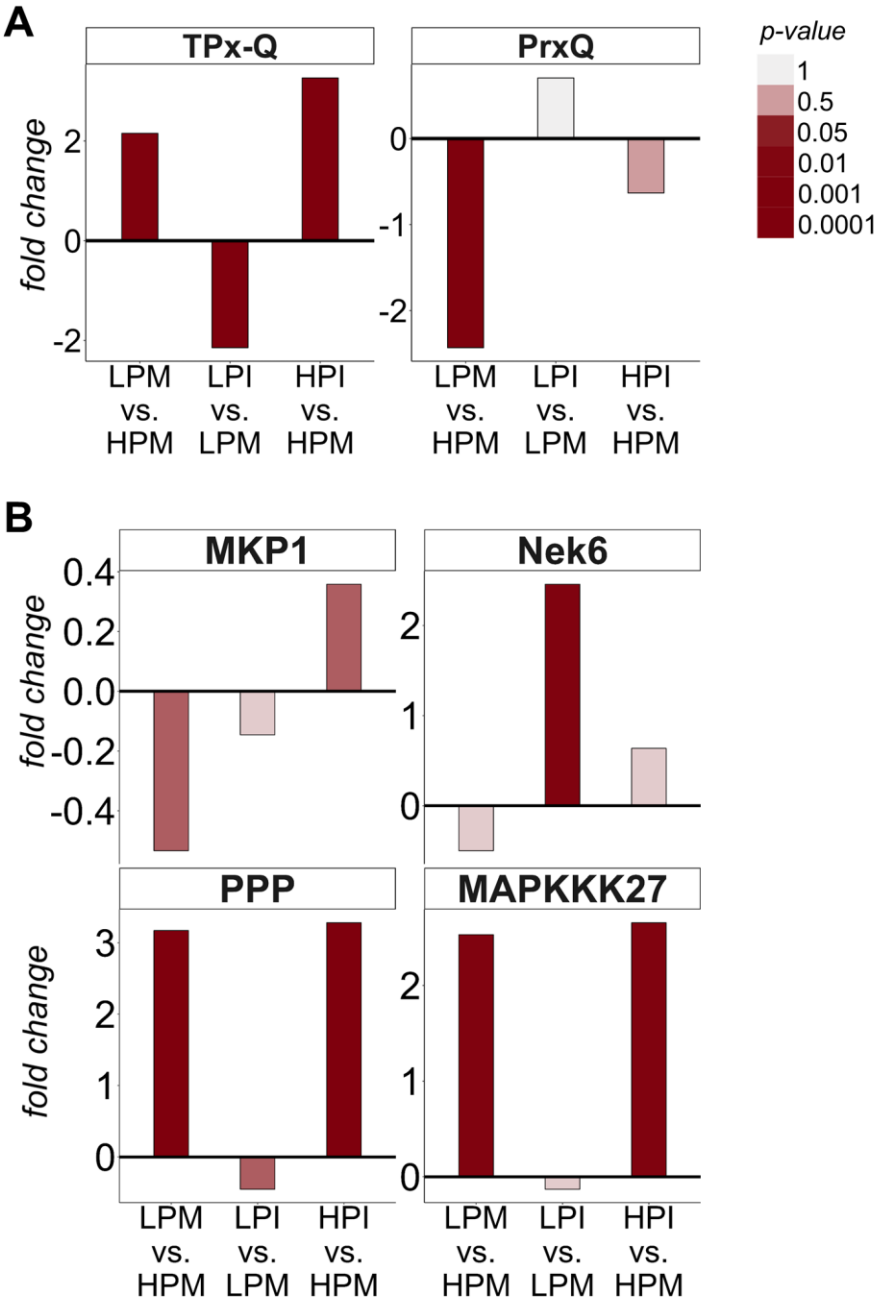

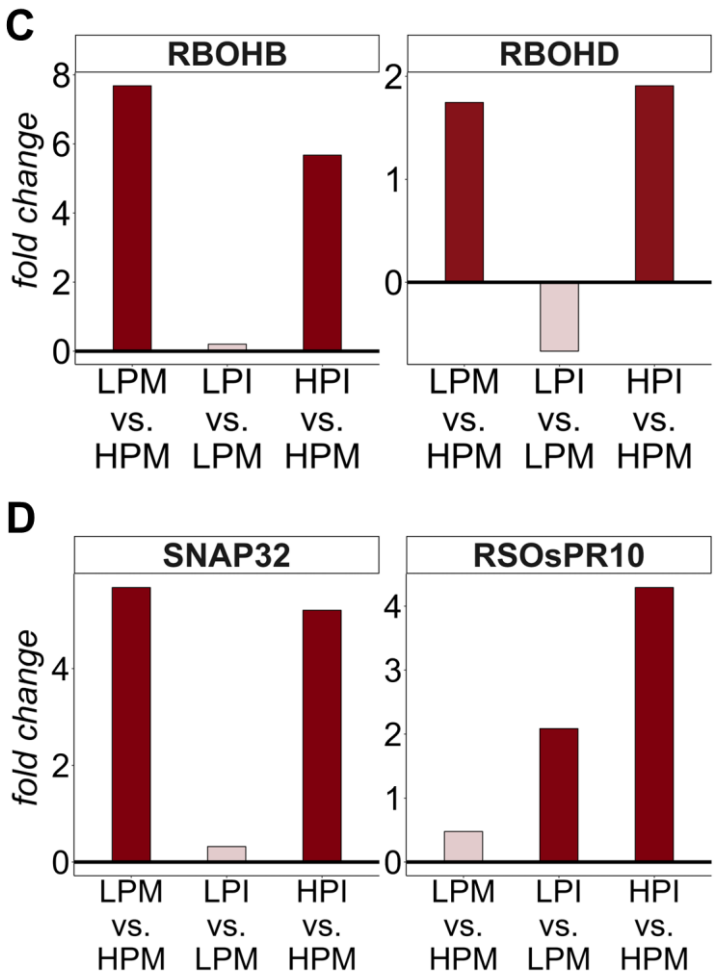

Figure 3.8. Defense related protein that are differentially phosphorylated in response to Pi and pathogen infection as revealed by phosphoproteomic analysis. Bars represent the fold change (log2 average abundance ratio) for each comparison: Pi (LPM *vs.* HPM); Low-Pi infection (LPI *vs.* LPM); High-Pi infection (HPI *vs.* HPM). Bar color represents the p-value for each comparison, with red indicating greater significance and white indicating lower significance. Abbreviations: Low-Pi, non-infected (mock) (LPM), Low-Pi, infected (LPI), High-Pi, non-infected (HPM), High-Pi, infected (HPI). Protein description: **A)** TPx-Q (Thioredoxin-dependent peroxiredoxin, Q69QW0); PrxQ (Peroxiredoxin Q, chloroplastic, P0C5D5); **B)** MKP1 (MAP kinase phosphatase, A2V7M8); Nek6(Serine/threonine-protein kinase Nek6, Q6YY75); PPP (Serine/threonine protein kinase, B8A9P2); MAPKKK27 (Mitogen activated protein kinase kinase kinase 27, M1SX00); **C)** RBOHB (Respiratory burst oxidase homolog protein B, Q5ZAJ0); RBOHD (Respiratory burst oxidase protein D, Q2R351); **D)** SNAP32 (Synaptosomal-associated protein of 32 kDa, Q5EEP3) and RSOsPR10 (Root specific pathogenesis-related protein 10, Q75T45).

In the absence of infection, the Serine/threonine-protein kinase (PPP, B8A9P2) and Mitogen activated protein kinase kinase kinase 27 (MAPKKK27, M1SX00) were found to be phosphorylated at a higher level in Low-Pi plants compared to High-Pi plants (LPM *vs.* HPM) **(Figure 3.8B)**. During *M. oryzae* infection, however, no significant changes were observed in Low-Pi plants (LPI *vs.* LPM), while its phosphorylation level increased by *M. oryzae* infection in High-Pi plants (HPI *vs.* HPM) **(Figure 3.8B)**.

Of interest, the phosphorylation status of RBOH proteins (RBOHB, Q5ZAJ0; RBOHD, Q2R351) was notably affected by the plant's Pi status. Specifically, phosphorylated RBOHB significantly increased under Low-Pi conditions (non-infection conditions) **(Figure 3.8C)**. The same trend was found for RBOHD. During *M. oryzae* infection, RBOH phosphorylation was important in High-Pi plants, both RBOHB and RBOHD (HPI *vs.* HPM) **(Figure 3.8C)**. As previously mentioned, the SNAP32 protein (Synaptosomal-associated protein of 32 kDa, Q5EEP3) has been recognized as a positive regulator of defense against blast disease (Cao *et al*., 2019). In our analysis, we observed overaccumulation of phosphorylated SNAP32 in Low-Pi plants relative to High-Pi plants (in the absence of infection) (LPM *vs.* HPM). When infected by *M. oryzae*, SNAP32 phosphorylation significantly increased in High-Pi plants (HPI *vs.* HPM) **(Figure 3.8D)**.

Finally, phosphoproteomic analysis revealed alterations in the phosphorylation status of a member of the PR10 family of PR proteins, the so called Root-specific pathogenesis-related protein 10 (RSOsPR10, Q75T45). Pi content had a small impact on the phosphorylation status of RSOsPR10 (with a small increase in LPM vs HPM). However, significant alterations could be observed in the phosphorylation status of RSOsPR10 during infection in both Low-Pi and High-Pi plants. Thus, accumulation of phosphorylated RSOsPR10

significantly increased during infection **(Figure 3.8D)**. The relevance of phosphorylation in PR10 family members (and phosphopeptides identified in RSOsPR10) is discussed below.

3.3.a Phosphorylation of rice PR10 proteins

The rice genome contains five *PR10* genes organized in tandem on chromosome 12: *RSOsPR10*, a *PR10 pseudogene*, *OsPR10b*, *OsPR10e*, and *OsPBZ1* (further discussed in **Section 4** of this Thesis). As previously mentioned, PR10 expression has been shown to respond to diverse biotic and abiotic stresses in different plant species (Sinha *et al*., 2020). In particular, *OsPBZ1* is known to be induced by pathogen infection and its overexpression has been linked to enhanced pathogen resistance. However, the specific mechanisms by which *OsPBZ1* confers pathogen resistance remain unclear (Huang *et al*., 2016). In the present thesis, we approached the functional characterization of *OsPBZ1*, the most highly expressed *OsPR10* gene of this family (see **Section 4**).

RSOsPR10 (root-specific pathogenesis-related 10 protein) was first described to be specifically induced in roots by biotic and abiotic stresses (Hashimoto *et al*., 2004). Phosphoproteomic analysis showed an increase in RSOsPR10 phosphorylation in response to *M. oryzae* infection in both Low-Pi plants and High-Pi plants, with a greater increase in plants grown under High-Pi conditions **(Figure 3.8D and Figure 3.9A)**. Two phosphopeptides originating from the RSOsPR10 protein were identified by phosphoproteome analysis of rice leaves **(Figure 3.9B)**. Comparison of the RSOsPR10 and PBZ1 amino acid sequences revealed 83.13% similarity (68.75% identity) between these proteins. Here, it is worth mentioning that phosphopeptides identified in our phosphoproteomic analysis of rice leaves were automatically assigned to RSOsPR10. However, examination of the amino acid

sequences surrounding the phosphosites in RSOsPR10 and PBZ1 revealed conservation of these sequences between the two PR10 family members.

A

Accession	Protein name	Gene Names	Gene Symbol	log2 abundance ratio: LPM vs. HPM	log2 abundance ratio: LPI vs. LPM	log2 abundance ratio: HPI vs. HPM
Q75T45	Root specific pathogenesis-related protein 10	LOC_Os12g36830	RSOsPR10	0,477	2,086	4,291

B

```
RSOsPR10      1 ·MAPVSISDERAVSVSAERVWKVFSDAPAMPKVCAGFIDAIEVEGDGGAGT·  50
PBZ1          1 ·MAPACVSDEHAVAVSAERLWKAFMDASTLPKACAGLVDDIAVEGNGGPGT·  50

RSOsPR10     51 ·VTTMKLNPAVDDGGSFKTRVVARDNAAHIIKSEVLDVPAGSKVGKLKSHV· 100
PBZ1         51 ·IYTMKLNPAAGVGSTYKTRVAVCDAASHVLKSDVLE--AESKVGKLKSHS· 100

RSOsPR10    101 ·TETKIEAAGAGSCLAKINVEYELEDGGSLSPEKEKLILDGYFGMLKMIED· 151
PBZ1        101 ·TETKLEATGDGSCVAKLKVEYELEDGSSLSPEKEKDIVDGYYGMLKMIED· 151

RSOsPR10    152 ·YLVAHPTEYA· 160
PBZ1        152 ·YLVAHPAEYA· 158
```

C

PHOSFER

Protein	Peptide	Serine position	Score
RSOsPR10	PAVDDGGSFKTRVVA	65	52
PBZ1	NPAAGVGSTYKTRVA	64	337

Protein	Peptide	Serine position	Score
RSOsPR10	YELEDGGSLSPEKEK	128	787
RSOsPR10	LEDGGSLSPEKEKLI	130	737
PBZ1	EYELEDGSSLSPEKE	125	613
PBZ1	YELEDGSSLSPEKEK	126	793
PBZ1	LEDGSSLSPEKEKDI	128	793

Netphos-3.1b

Protein	Peptide	Serine position	Score
RSOsPR10	DDGGSFKTR	65	0.693
PBZ1	AGVGSTYKT	64	0.759

Protein	Peptide	Serine position	Score
RSOsPR10	EDGGSLSPE	128	0.510
RSOsPR10	GGSLSPEKE	130	0.994
PBZ1	EDGSSLSPE	126	0.510
PBZ1	GSSLSPEKE	128	0.996

Figure 3.9. Phosphopeptides identified in RSOsPR10 and prediction of phosphosites in the RSOsPR10 and PBZ1 proteins. A) Data obtained in the phosphoproteomic analysis of rice leaves indicating the log2 abundance ratio in the various pair-wise comparisons. **B)** Alignment of RSOsPR10 and PBZ1 amino acid sequences. Mismatches are indicated in gray and identities in bold. Phosphopeptides identified in the RSOsPR10 amino acid sequence by LC/MS-MS are highlighted in blue and yellow. Potential serine phosphorylation sites (S, Ser) are shown in red. Dashes indicate deletions. **C)** Prediction of phosphorylation sites in RSOsPR10 and PBZ1 using PHOSFER and Netphos-3.1.b softwares.

When using prediction software tools designed to identify phosphopeptides (e.g., PHOSFER, Trost & Kusalik, 2013; Netphos-3.1.b, Blom *et al*., 2004), a high reliability was found for serine residues within the phosphopeptides predicted not only in RSOsPR10 but also in PBZ1 **(Figure 3.9C)**. It is then reasonable to assume that PBZ1 might be regulated by phosphorylation, as it is the case for RSOsPR10.

3.3.b Phosphorylation sites in the tridimensional structure of PrxQ, RBOH and PR10 proteins

We examined the tridimensional (3D) structure of proteins of interest identified by phosphoproteomic analysis of rice leaves, namely PrxQ, RBOHs (RBOHB, RBOHD) and PR10 (RSOsPR10 and PBZ1) proteins. The 3D structure of the RBOHB protein was previously documented by crystallization and X-ray data collection (Oda *et al*., 2010). The 3D structure of PBZ1 (determined by X-ray crystallography) was obtained from the Tridimensional Structure database (https://www.rcsb.org/structure/1llt; PDB accession code 1LLT). The PyMOL tool was employed for visualization of the 3D structure of these proteins. Alphafold was utilized to predict the structures of Peroxiredoxin Q protein, RBOHD, and RSOsPR10. Subsequently, the phosphopeptides identified in our analysis were mapped onto these structures **(Figure 3.10)**. As anticipated, the phosphopeptides were located in external positions that were highly accessible to kinases for phosphorylation **(Figure 3.10)**. In the Peroxiredoxin Q protein, a cytoplasmatic protein, the putative phosphorylated residue (S75) located in a fully exposed region of the protein **(Figure 3.10A)**.

RBOH (Respiratory burst oxidase homolog) proteins are transmembrane proteins located in the plasma membrane. The presence of phosphopeptides originating from RBOH proteins in total soluble protein extracts would then reflect proteolytic processing of

these proteins, either during preparation of protein extracts or *in vivo*. Mapping the phosphopeptides into the RBOH proteins (S32 in RBOHB and S131 in RBOHD) revealed that the phosphorylated peptides identified in this study located in the cytoplasmic regions of these proteins **(Figure 3.10B)**.

Lastly, we examined both RSOsPR10 and PBZ1 due to the likelihood of both members being phosphorylated. In this case, three putative phosphorylated residues were identified (RSOsPR10: S64, S128 and S130; PBZ1: S64, S126 and S128). All these residues were found in external positions of the proteins, providing further confirmation of their potential for phosphorylation **(Figure 3.10C)**.

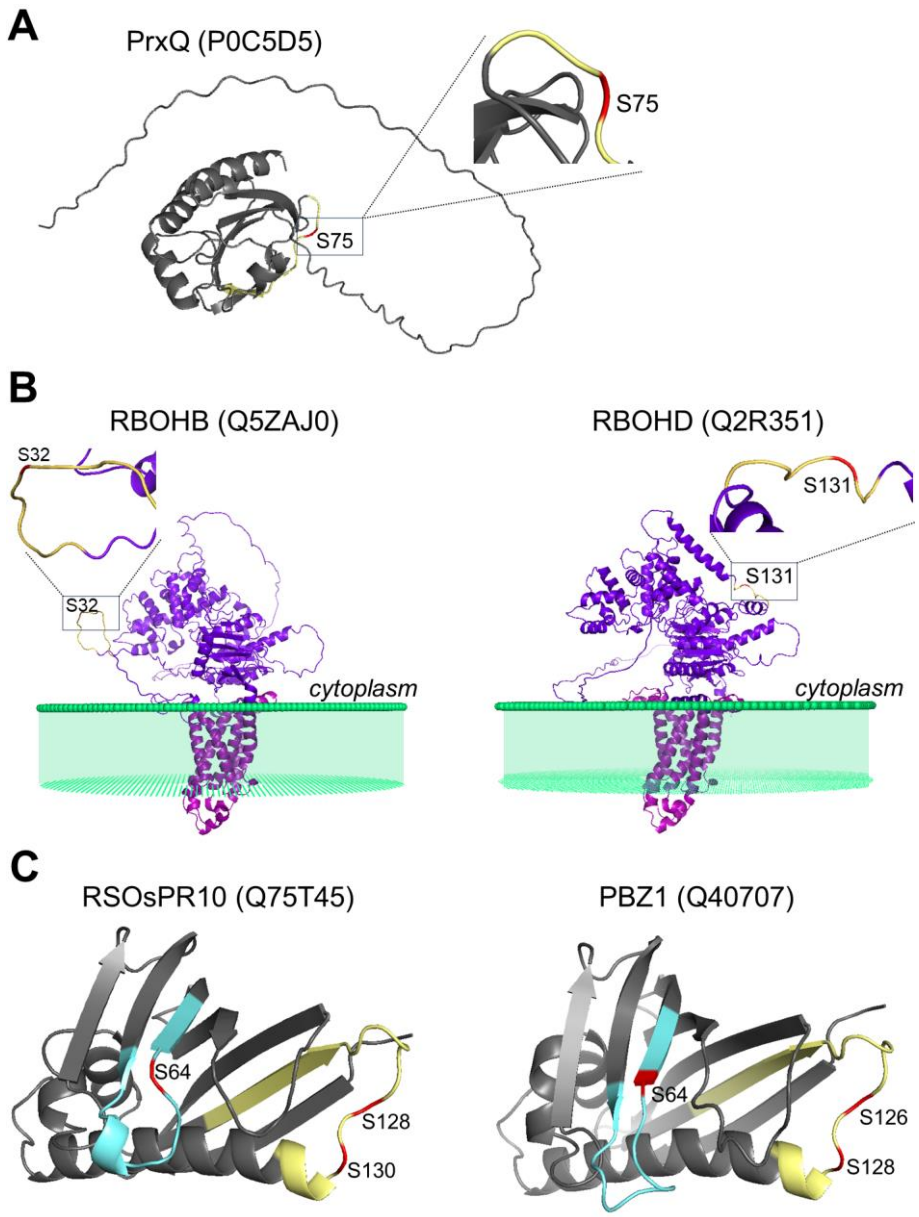

Figure 3.10. Tertiary structures of selected proteins. A) PrxQ (Peroxiredoxin Q, chloroplastic, P0C5D5) **B)** RBOHB (Respiratory burst oxidase homolog protein B, Q5ZAJ0) and RBOHD (Respiratory burst oxidase protein D, Q2R351); **C)** RSOsPR10 (Root specific pathogenesis-related protein 10, Q75T45); and PBZ1 (Q40707). Phosphorylation peptides are shown in yellow, phosphorylation residues are shown in red for all proteins. For transmembrane Respiratory burst oxidase protein, transmembrane motifs are shown in pink, cytoplasmatic motifs in purple and the phospholipid bilayer of plasma membrane in green. The phosphorylated residues (serine) are signal with the position number in the protein.

Collectively, results obtained in the phosphoproteomic analysis supported the involvement of phosphorylation events during *M. oryzae* infection. Moreover, the phosphorylation status of proteins, crucial for both the activation and deactivation of proteins, is maintained in Low-Pi plants, irrespective of whether they are subjected to mock conditions or infection. In contrast, High-Pi plants experience notable modifications in protein phosphorylation when confronted with *M. oryzae* infection. In particular, rice PR10 proteins appear to be under regulation by phosphorylation, at least the RSOsPR10 and possibly also PBZ1. This regulation might well be associated with the function of these proteins in the rice response to environmental stress, in particular to Pi conditions and/or pathogen infection. The functional characterization of *OsPBZ1* in the context of blast resistance in rice plants grown under different Pi conditions is discussed in detail in **Section 4**.

Section 4 – Role of the *OsPBZ1* gene in blast disease and Pi homeostasis

4. Role of the *OsPBZ1* gene in disease resistance in rice

The PR10 family of PR proteins consists of small acidic proteins whose amino acid sequence show high similarity to Bet v1, the major allergen of birch pollen (Fernandes *et al*., 2013; Agarwal & Agarwal, 2014). The rice genome contains five *PR10*-like genes, one of which is a pseudogene. The remaining four genes are known to be responsive to different types of biotic stresses, including pathogen infection, and treatment with the defense-related hormones SA and JA (McGee *et al*. 2001; Sinha *et al*., 2020). *PR10* genes are also induced by abiotic stresses (e.g., drought, salt and cold stress) (Lopes *et al*., 2023). The first identified gene in this *PR* family was *OsPR10a*, also known as *OsPBZ1* (Midoh & Iwata, 1996). It is also known that *OsPBZ1* overexpression confers resistance to pathogen infection (Huang *et al*., 2016). Although it is generally assumed that PR10 proteins play a role in plant defense against pathogen infection, the mechanism of action of these proteins remains poorly understood. It has been reported that rice, maize and potato PR10 proteins exhibit antifungal activity by yet unknown mechanisms (Kim *et al.,* 2011; Hanafy *et al*., 2013; Zandvakili *et al*., 2017).

OsPBZ1 is considered a marker for the induction of defense responses in rice, also during infection with the rice blast fungus *M. oryzae* (McGee *et al*., 2001; Kim *et al*., 2008). However, its role during infection of rice plants with *M. oryzae* remains elusive, and the biochemical function of *OsPBZ1/OsPR10a* is still under investigation. It was described that rice PBZ1 exhibit ribonuclease activity *in vitro* (Huang *et al*., 2016). This observation led the authors to hypothesize that PBZ1 may function in degradation of RNAs when the plant is under Pi limiting conditions (as a source of Pi for plant metabolic processes),

a function that has not been demonstrated. As the fungus needs to acquire Pi from the host plant, an increased RNase activity in the host plant (e.g., caused by PBZ1 activity) might also represent a source of Pi to the fungus.

In this study, we approached the functional characterization of *OsPBZ1/OsPR10a* (from now on *OsPBZ1*) during combined stress conditions: Pi stress and pathogen infection. The contribution of *OsPBZ1* to blast resistance was determined by generating CRISPR/Cas9-edited rice plants. We also examined whether Pi treatment influences blast resistance in PBZ1-edited rice plants.

4.1 *OsPBZ1* expression is up-regulated in Low-Pi rice plants.

Rice *PR10* genes are arranged in tandem in chromosome 12 of the rice genome spanning a region of approx. 21,200 bp. They are: *RSOsPR10* (LOC_Os12g36830), *PR10b* (LOC_Os12g36850), *OsPR10e* (LOC_Os12g36860), *OsPBZ1* (LOC_ Os12g36880) **(Figure 4.1A)**. The PR10-pseudogene also locates in this chromosomal region **(Figure 4.1A)**.

To investigate the effect of Pi supply on *PR10* gene expression, rice plants were grown for 15 days (three to four leaf stage) under low Pi (0.025mM) or high Pi (2.5mM). *OsPBZ1*, *RSOsPR10*, *PR10b* and *OsPR10e* expression was examined in the youngest rice leaf by RT-qPCR. *OsPBZ1* was found to be expressed at a much higher level than *RSOsPR10*, *PR10b* and *OsPR10e* **(Figure 4.1B)**. Stronger expression of *OsPBZ1* occurs in Low-Pi plants compared to High-Pi plants. (differences in *RSOsPR10*, *PR10b* and *OsPR10e* expression between Low-Pi and High-Pi plants were not statistically significant).

From these results it can be concluded that *OsPBZ1* is highly expressed in rice plants that have been grown under a low Pi regime, and *vice versa*, growing rice under high Pi conditions represses *OsPBZ1* expression.

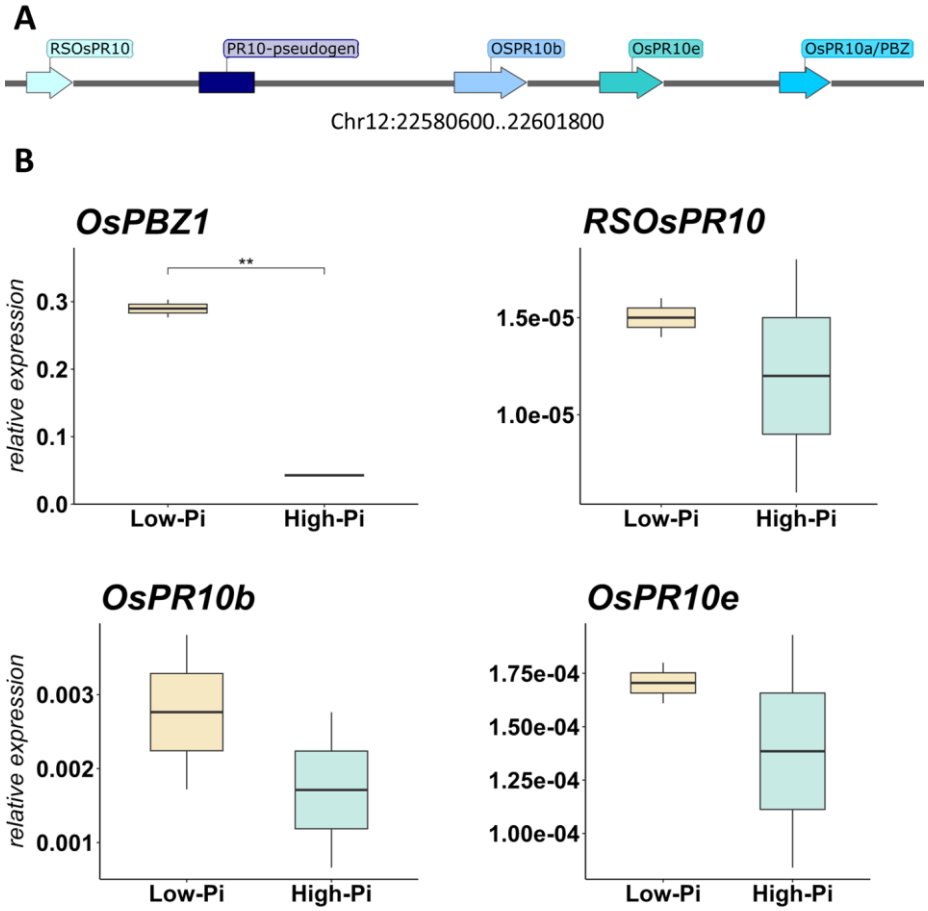

Figure 4.1. Expression of *OsPBZ1* is regulated by Pi treatment in rice leaves. A) Schematic representation of *PR10* genes in chromosome 12 of the rice genome, *RSOsPR10* (LOC_Os12g36830), *OsPR10*-pseudogen (LOC_Os12g36840 *PR10b* (LOC_Os12g36850), *OsPR10e* (LOC_Os12g36860), *OsPR10a/OsPBZ1* (LOC_Os12g36880). **B)** Expression of *OsPR10* genes in rice leaves grown under Low- or High-Pi for 15 days (three- to four-leaf stage). Boxes represent four biological replicates (three pooled plants in each replicate). The horizontal line within the box represents the median value (t test, **p < 0.01, Low-Pi *vs* High-Pi).

4.2 *OsPBZ1* expression is induced by *M. oryzae* infection

Next, we examined *PR10* expression in leaves of Low-Pi and High-Pi rice plants during infection with *M. oryzae*. Rice plants were grown under one or another Pi condition for 15 days and then inoculated with *M. oryzae* spores. The expression of *OsPR10* genes was determined at 48- and 72- hours post-inoculation (hpi).

OsPBZ1 was induced by *M. oryzae* infection independently of the Pi condition (Low-Pi and High-Pi plants) **(Figure 4.2)**. Upon pathogen challenge, however, stronger induction of *OsPBZ1* expression occurs in Low-Pi plants compared with High Pi plants. Although expressed at a lower level than *OsPBZ1,* expression of the other *PR10* family members (*OsPR10b*, *OsPR10e, RSOsPR10*) was also induced by *M. oryzae* infection in both Low-P and High-Pi plants **(Figure 4.2)**. Overall, this study revealed that treatment with high-Pi is associated with weaker induction of *OsPR10* expression compared to Low-Pi plants.

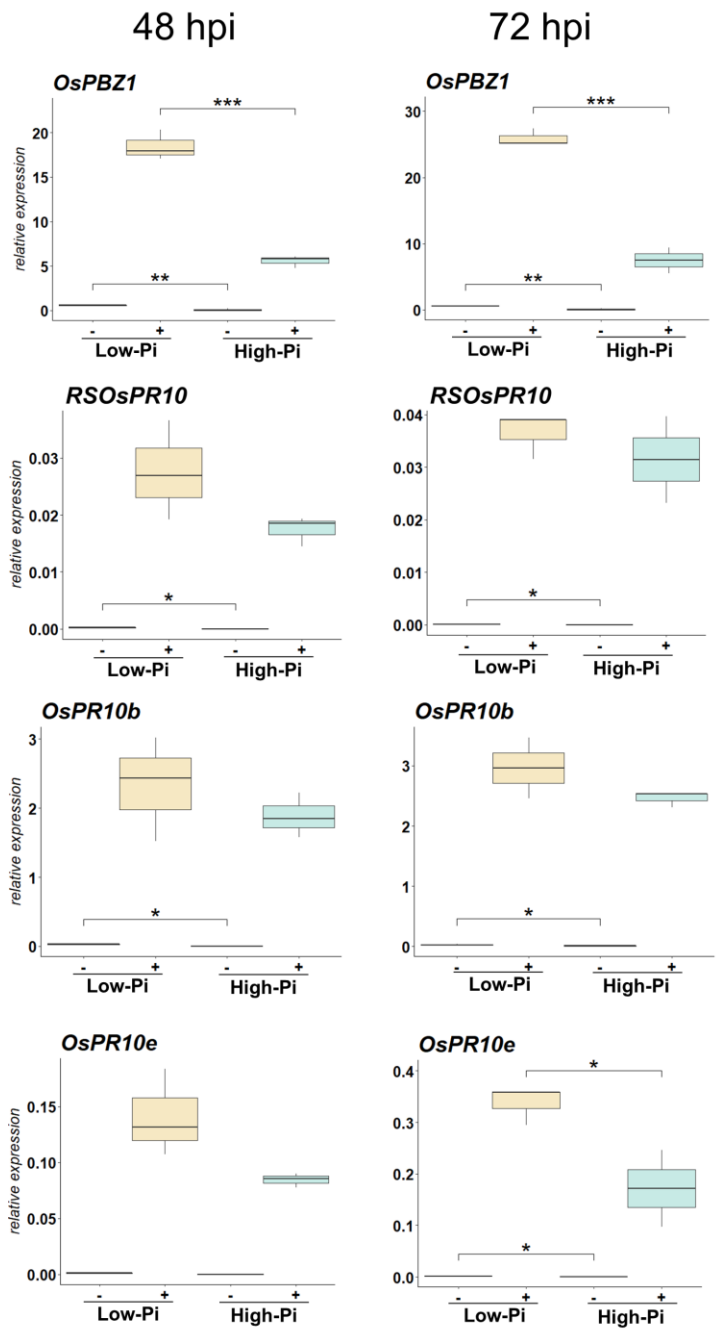

Figure 4.2. Expression of *OsPR10* genes in leaves of rice plants that have been grown under Low or High-Pi conditions and then inoculated with *M. oryzae.* RT-qPCR analyses were carried out at 48 hpi and 72 hpi (left and right panels respectively). Three biological replicates (three pooled plants each replicate) were analyzed. The horizontal line within the box represents the median value (t test, *p ≤ 0.05, **p ≤ 0.01, ***p < 0.001, Low-Pi *vs* High-Pi in non- and infected conditions at each time point.

4.3 CRISPR/Cas9-mediated mutagenesis of *OsPBZ1*

To investigate the contribution of *OsPBZ1* to blast resistance, we used the CRISPR/Cas9 technology using the vectors described by Miao *et al*. (2013) for CRISPR/Cas9 mutagenesis in rice **(Figure 4.3)**. A sgRNA was designed for targeting the *OsPBZ1* gene using the CRISPRP v2.0 tool. The *OsPBZ1* contains a Protospacer Adjacent Motif (PAM) sequence (TGG) within its coding sequence **(Figure 4.4A)**. Transgenic rice (*O. sativa* cv. Nipponbare) was produced by *Agrobacterium*-mediated transformation of embryogenic callus derived from mature embryos. PCR analysis of genomic DNA followed by DNA sequencing using gene-specific primers flanking the target site allowed us to identify CRISPR/Cas9-induced mutations. In this way, two mutant alleles were identified in hygromycin-resistant T0 plants containing a deletion of 4 nucleotides that results in a truncated protein **(Figure 4.4B)**. Homozygous lines for these mutations (from now on CRISPR*PBZ1* lines) were obtained at the T2 (line #9.4) and T3 (line #10.3.7) generations.

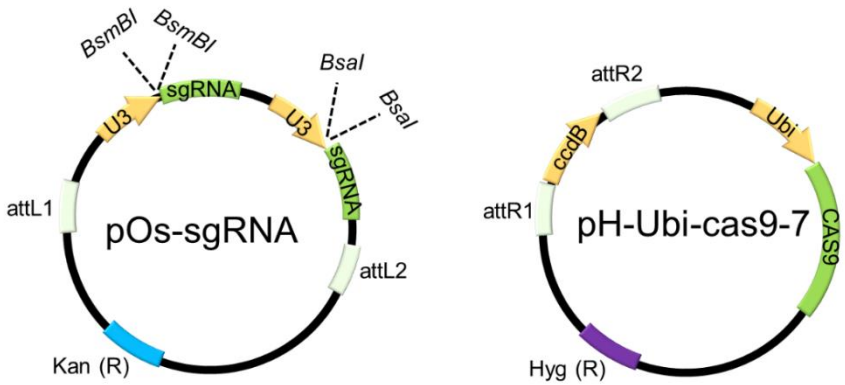

Figure 4.3. Schematic representation of plasmids pOs-sgRNA and pH-Ubi-cas9-7 used in this study for CRISPR/Cas9 mutagenesis of *OsPBZ1* (Miao *et al*., 2013). Abbreviatures: attachment sites (att), single guide RNA (sgRNA), Controller of Cell death or division B (ccdB), kanamycin (Kan), hygromycin (Hyg).

Hypothetical off-targets for the sgRNA used to generate the CRISPR*PBZ1* lines were predicted using the CRISPRP v2.0 tool. A potential off-target was identified in another PR10 family member, *OsPR10e* (LOC_Os12g36860), while other 5 possible off-target sites located in intergenic regions **(Figure 4.4B)**. DNA sequencing of PCR products for all 6 predicted off-target sites indicated that none of them had mutations in the corresponding loci in any of the CRISPR*PBZ1* lines generated in this work. Finally, RT-qPCR analysis confirmed *OsPBZ1* expression in *M. oryzae*-infected azygous plants, but not in *M. oryzae*-infected CRISPRPBZ1 mutant plants **(Figure 4.4C, left panel)**.

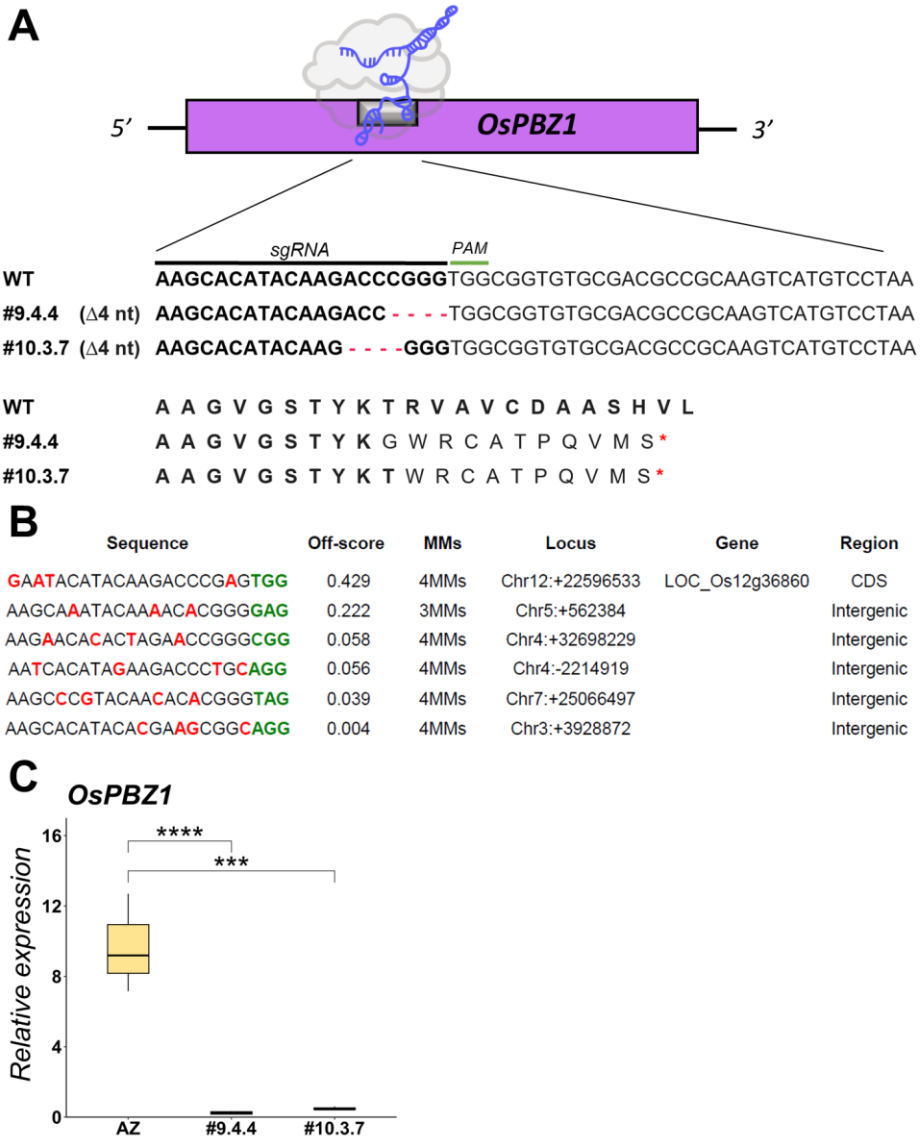

Figure 4.4. Mutations generated by CRISPR/Cas9 editing and expression of *PR10* genes. **A)** Two *OsPBZ1* alleles were identified, each one containing a deletion of 4 nucleotides. Dashes indicate deletions. The translated protein for each allele is shown in the lower part. CRISPR*OsPBZ1* lines assayed in this work were 9.4.4 and 10.3.7. **B)** Potential off-targets loci in the rice genome as predicted by the CRISPRP v2.0 tool. Mismatches of the sgRNA target sequence are indicated in red and the PAM sequence downstream in green. **C)** Expression of *OsPBZ1.* Plants (3-4 leaf stage) that have been grown in sufficient Pi condition were inoculated with *M. oryzae* spores (5x10^5 spores/ml). *OsPBZ1* expression was analyzed at 7 days-post-inoculation. Bars represent mean ± SEM of four biological replicates with three plants per replicate (t test, ***$p < 0.001$, ****$p < 0.0001$). AZ, azygous.

4.4 Resistance against rice blast in CRISPRPBZ1 mutant plants.

OsPBZ1 is widely used as a molecular marker of the induction of rice to pathogen infection. In line with this, *OsPBZ1* expression was found to be induced by *M. oryzae* infection in wild-type plants **(see Figure 4.2)**. Knowing this, we sought to investigate resistance to infection by *M. oryzae* in CRISPR*PBZ1* lines.

Initially, we examined blast resistance in plants that have been grown under normal conditions, that is under sufficient Pi supply. Azygous and homozygous CRISPR*PBZ1* plants (lines #9.4.4 and #10.3.7, T3 generation) at the 3-4 leaf stage were inoculated with *M. oryzae* spores. The CRISPR*PBZ1* lines appeared to be more resistant to *M. oryzae* infection than azygous plants, as revealed by visual inspection and quantification of the leaf area with blast lesions **(Figure 4.5A and B)**. Leaf Pi content did not significantly vary between CRISPR*PBZ1* and azygous plants **(Figure 4.5C)**, thus, excluding the possibility of a blast disease phenotype caused by alterations in Pi content in the CRISPR*PBZ1* plants.

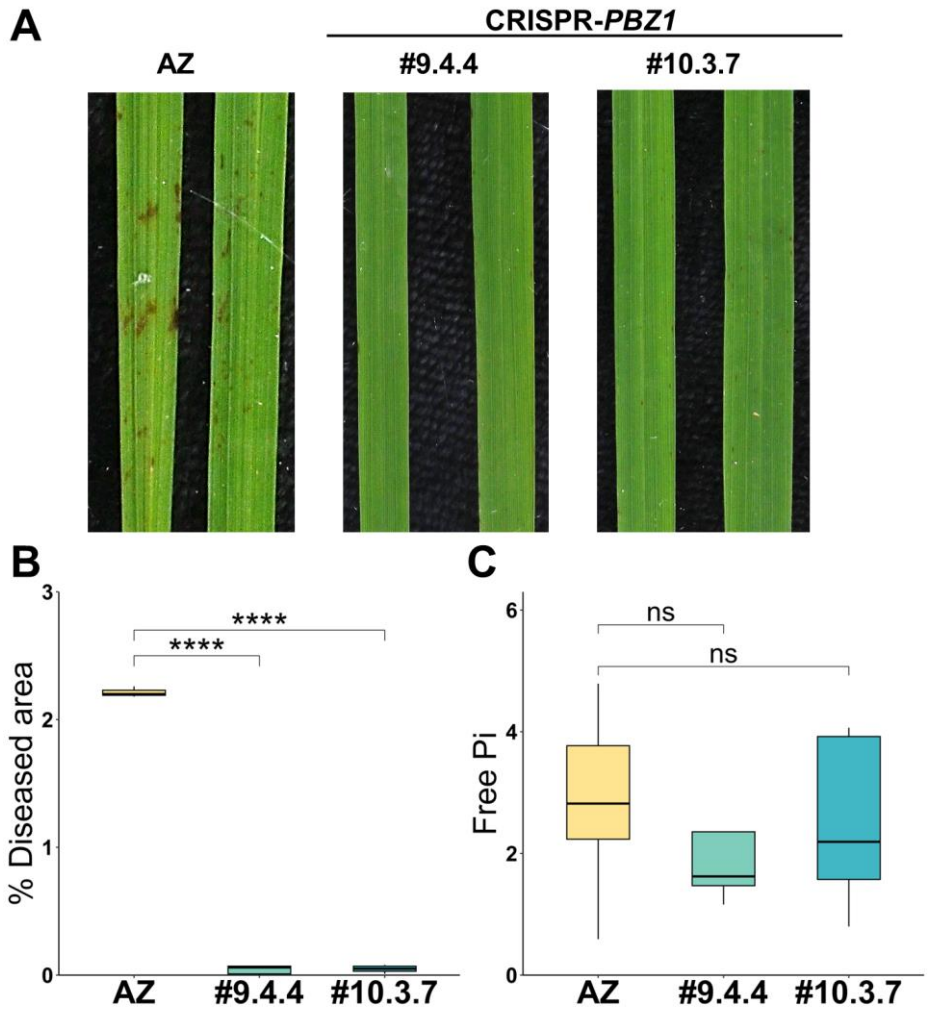

Figure 4.5. Blast resistance in CRISPR*PBZ1* lines. Plants were grown under sufficient Pi supply for 15 days (3-4 leaf stage) and then inoculated with *M. oryzae* spores ($5x10^5$ spores/ml). Azygous (AZ) and homozygous CRISPRPBZ1 lines were analyzed. **A)** Phenotype of azygous and CRISPR*PBZ1* mutant plants (lines 9.4.4 and 10.3.7) at 7 days post-inoculation with *M. oryzae* spores. **B)** Percentage of leaf area affected by blast lesions determined by image analysis (APS Assess 2.0). **C)** Pi content in azygous and CRISPR*PBZ1* plants. Three independent experiments were carried out with similar results (*t test* , ****p < 0.0001).

When assessing the expression of the defense-related genes *OsPR1a* and *OsChtIII* in *M. oryzae*-infected CRISPR*PBZ1* plants, a more robust induction of these genes could be observed in

CRISPR*PBZ1* plants compared to the azygous plants **(Figure 4.6)**. Regarding *OsMAPK5*, previous studies have reported induction of this gene early during *M. oryzae* infection (typically observed at 24 hours post-inoculation). In this work, pathogen-inducibility of *OsMAPK5* in CRISPR*PBZ1* plants was examined at 72 hours post-inoculation. These findings align with the observed phenotype of blast resistance that is observed in the CRISPR*PBZ1* lines.

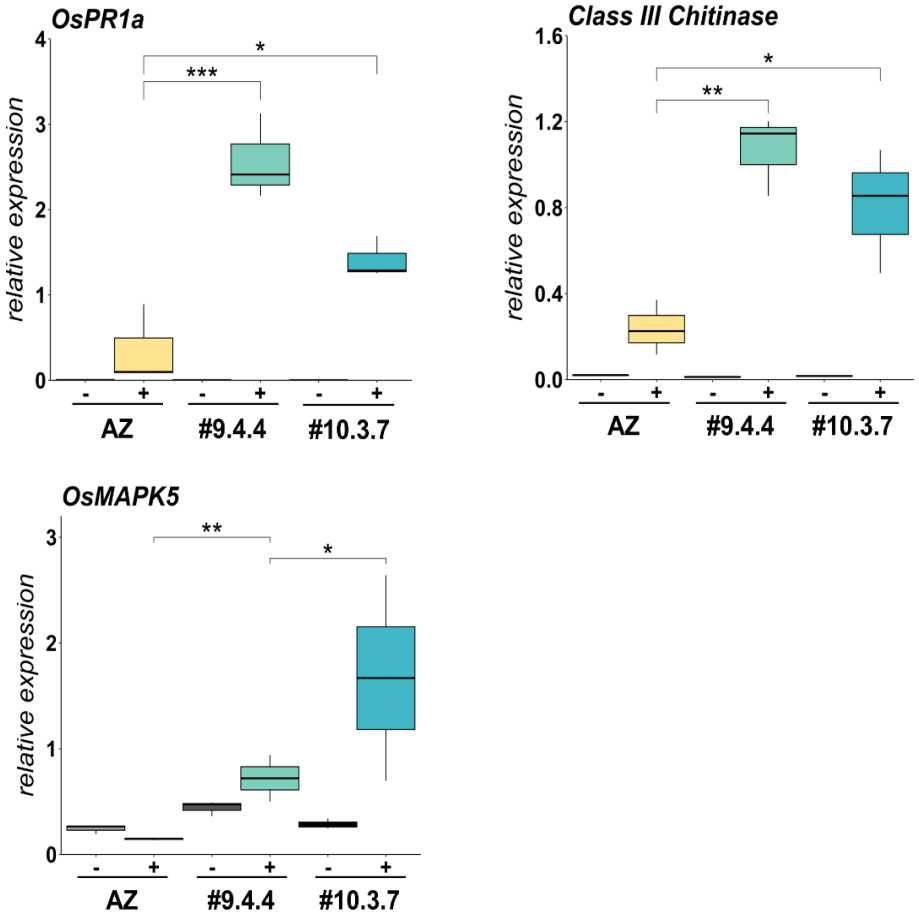

Figure 4.6. Expression of *OsPR1a, OsChtIII and OsMAPK5* in azygous (Az) and CRISPRPBZ1 rice plants. RT-qPCR analysis were carried out at 72-hours-post-inoculation (hpi) with *M. oryzae.* Bars represent four biological replicates (three pooled plants in each replicate) (t test, **p* ≤ 0.05, ***p* < 0.01, ****p* < 0.001).

As previously shown, CRISPR*PBZ1* lines, when grown under normal conditions (e.g., sufficient Pi supply), were found to be more resistant to *M. oryzae* infection than azygous plants **(see Figure 4.5)**. Next, we investigated whether the phenotype of resistance in CRISPR*PBZ1* plants is dependent on the Pi condition in which the rice plants are grown. Rice plants were grown under Low- or High-Pi conditions (0,025 mM and 2,5 mM, respectively) for 3 weeks (3-4 leaf stage) and then challenged with *M. oryzae*.

As shown in **Section 1 (Figure 1.3)**, growing wild-type rice plants under low-Pi conditions enhances blast resistance. Under these conditions (Low-Pi), no significant differences were observed in blast resistance between CRISPR*PBZ1* plants and azygous plants **(Figure 4.7A)**. Therefore, silencing of *OsPBZ1* had no significant effect on blast resistance when the plants are grown under low-Pi conditions.

We also knew that wild-type rice plants grown under High-Pi supply exhibit enhanced susceptibility to *M. oryzae* infection **(see Section 1, Figure 1.3)**. To note, infection assays revealed that *OsPBZ1* silencing further increased blast susceptibility in High-Pi plants. Thus, the CRISPR*PBZ1* lines showed more blast symptoms than azygous plants **(Figure 4.7B, upper panel)**. Quantification of lesion area and fungal biomass confirmed enhanced susceptibility to infection by the rice blast fungus in *CRISPRPBZ1* plants compared with azygous plants **(Figure 4.7B, lower panels)**. From these results, it can be concluded that *OsPBZ1* silencing promotes Pi-induced susceptibility to the blast fungus in rice. However, the role of *OsPBZ1* in blast resistance appears to be dependent on the Pi status in the host plant as no effect was observed in blast susceptibility in Low-Pi plants. Further studies are needed to determine the exact mechanisms by which *OsPBZ1* silencing fosters blast susceptibility in High-Pi rice. It will be also of interest to investigate possible connections between Pi signaling pathways and

immune signaling pathways leading to *OsPBZ1* induction during *M. oryzae* infection.

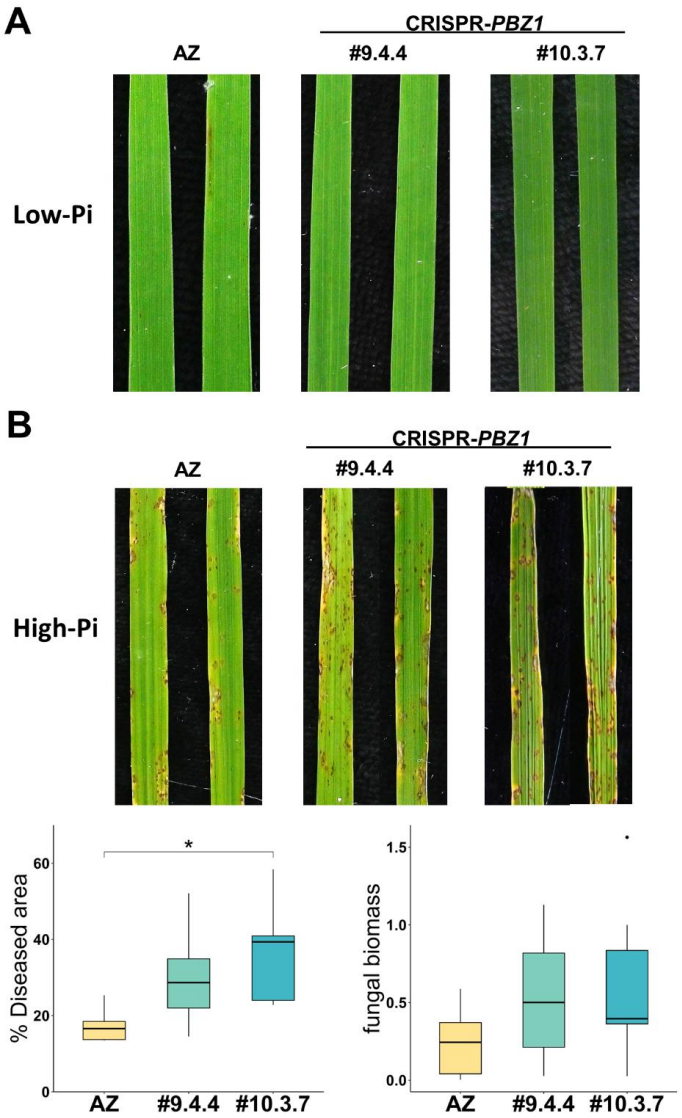

Figure 4.7. CRISPR*PBZ1* lines show different response to *M.oryzae* infection depending on Pi conditions. Plants were grown under Low-Pi (**A**) or High-Pi (**B**) condition for 15 days (3-4 leaf stage and inoculated with *M.oryzae* spores (5x10^5 spores/ml). Blast resistance was determined at 7 days post-inoculation with *M. oryzae* spores. The percentage of leaf area affected by blast lesions was determined by image analysis using the APS Assess 2.0 software (left panel) and fungal biomass was quantified at 7 dpi by RT-qPCR using specific primers of *M. oryzae* Mo28S and normalized to rice Ubiquitin 1 gene (right panel) (n = 10; *t test*, *p ≤ 0.05, **p < 0.01, ***p < 0.001).

4.5 Subcellular localization of rice PBZ1

Previous studies hypothesized that interactions with other proteins might determine the subcellular localization of PBZ1 and that these interactions might determine resistance or susceptibility to pathogen infection (Lopes *et al*., 2023). On the other hand, *in silico* prediction of the subcellular localization of rice PBZ1 by *InterPro* (*Uniprot*: Q40707) assigns a nuclear localization to PBZ1, albeit the amino acid sequence of this protein lacks a nuclear signal sequence. The subcellular localization of PBZ1 is still under debate.

To get experimental evidence on the subcellular localization of the rice PBZ1 protein, transient expression assays were carried out in *Nicotiana benthamiana* leaves using fluorescently-labeled PBZ1. For this, the *PBZ1* coding sequence was fused to the Green Florescent Protein (GPF) gene, either at its N-terminal or C-terminal (named as *PBZ1:GFP* and *GFP:PBZ1*, respectively) **(Figure 4.8A)**. As control, we used the *GFP* gene alone. *Agrobacterium*-mediated transformation of *N. benthamiana* leaves was then carried out. Western blot analysis confirmed accumulation of PBZ1 in the agroinfiltrated leaf tissues **(Figure 4.8B)**. Immunoreactive proteins with an apparent molecular weight of approximately 45 kDa were observed in leaves that have been agroinfiltrated with either PBZ1:GFP or GFP:PBZ, when protein extracts were probed with anti-PR10 or anti-GFP antisera. This molecular weight corresponds to the expected size of the PBZ1-GFP/GFP-PBZ1 fusion proteins (theorical molecular weight: PBZ1 19kDa, GFP 27kDa). Moreover, the PBZ1-GFP fusion protein accumulated at a higher level than the GFP-PBZ1 protein in *N. benthamiana* leaves **(Figure 4.8B)**. Western blotting using the anti-PR10 antibody also detected serological reaction with proteins of around 30 kDa. Whether these proteins correspond to the endogenous PR10 proteins in *N. benthamiana* leaves remains to be determined, as the theorical molecular weight of PR10

proteins is in the range of 16-19 KDa. The discrepancy between the theoretical and apparent molecular weights of PBZ1 suggests that either this protein might form oligomers or can bind to other proteins in the plant cell. In this respect, it is worth noting that other studies have demonstrated that PR10 proteins typically exist as monomers, although exceptions have been observed, where some form dimers and higher-order oligomers with differing functional implications (Fernandes *et al.,* 2013). Further experiments are required to elucidate this matter.

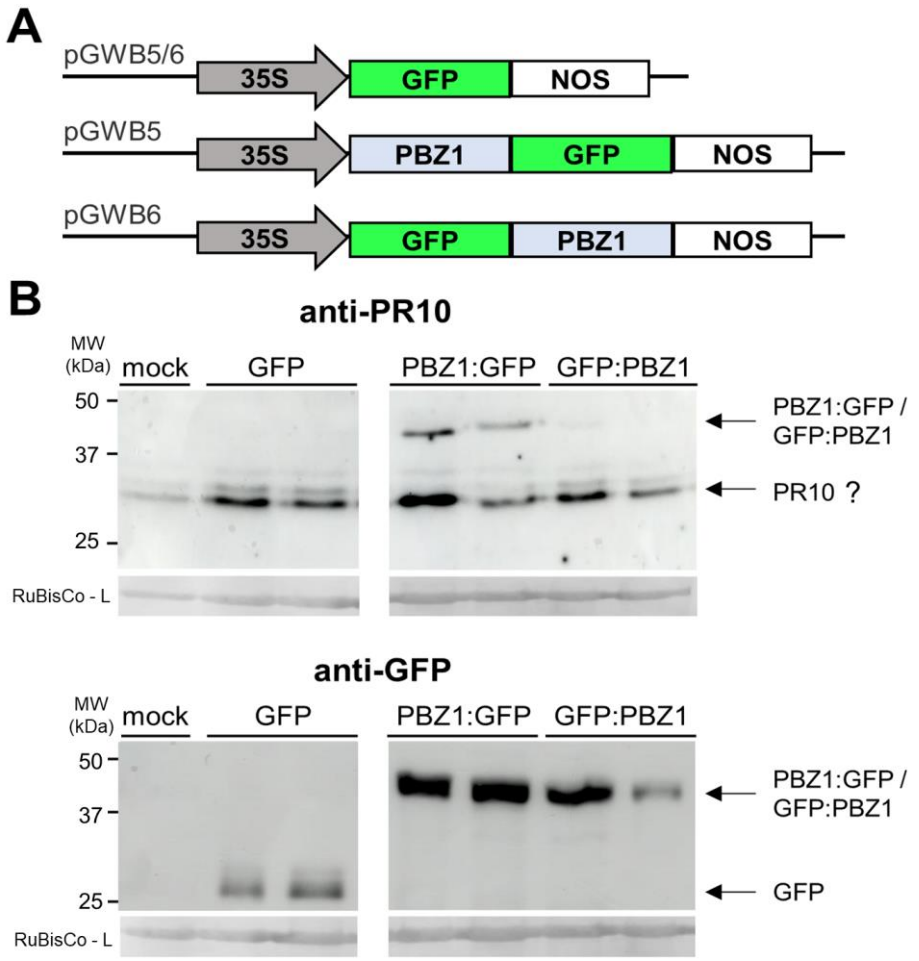

Figure 4.8. Accumulation of PBZ1-GFP fusion proteins in agroinfiltrated *Nicotiana benthamiana* leaves. **A)** Schematic representation of plasmids used for transient expression of *PBZ1-GFP* fusion genes. The *OsPBZ1* cDNA was fused to the N-terminal or C-terminal end of GFP. The fusion genes were transiently expressed in *N. benthamiana* leaves under the control of the constitutive *Cauliflower mosaic virus 35S promoter* (*35S*). As control, leaves were agroinfiltrated with the plasmid containing the *GFP* gene alone. **B)** Detection of PBZ1-GFP and GFP in proteins extracts obtained from *N. benthamiana* leaves that have been agroinfiltrated with the *GFP* construct (GFP, left panel) or with the *PBZ1:GFP* or *GFP:PBZ1* construct (right panel). Protein extracts (5 µg) were separated on 10% SDS-PAGE and probed with anti-PR10 (upper panel) or anti-GFP antibodies (lower panel). Detection of inmunological reactions was performed using horse rabbit peroxidase (HRP)-labelled donkey anti-Rabbit IgG (H+L) as the secondary antibody (Thermo Fisher Scientific) and visualized on an Amersham ImageQuant™ 800 CCD imaging system. The large subunit of RuBisCO-L (Ribulose-1,5-bisphosphate carboxylase-oxygenase) served as loading control after Ponceau Red staining. Serological reaction of the anti-PR10 antibody with aprox. 30 KDa proteins might correspond to endogenous PR10 from *N. benthamiana* (upper panel).

Next, the agroinfiltrated leaves were examined by fluorescence confocal microscopy. As expected, GFP (alone) accumulated in the cytoplasm of *N. benthamiana* leaf cells **(Figure 4.9A, left panels)**. The fusion protein PBZ1:GFP displayed a distribution very much resembling that of the GFP alone, that is, a cytosolic distribution **(Figure 4.9A, right panels)**.

To confirm cytoplasmic localization of PBZ1:GFP, co-transformation experiments of *N. benthamiana* cells were carried out with subcellular markers. The GFP-tagged *PBZ1* gene was co-expressed with either the cytoplasm marker monomeric red fluorescent protein mRFP (*Cyt:RFP*), or with the plasma membrane marker PIP2 from *Arabidopsis thaliana* fused to the red fluorescent protein mCherry (*AtPIP2:mCherry*). *AtPIP2* encodes a plasma membrane intrinsic protein (Alexandersson *et al.,* 2010). As shown in **Figure 4.9B**, PBZ1:GFP and Cyt:RFP proteins colocalized in the cytoplasm. As expected, the AtPIP2:mCherry protein, but not the PBZ1:GFP protein, localized at the plasma membrane **(Figure 4.9C)**. Thus, confocal microscopy demonstrated that PBZ1 accumulates in the cytoplasm in *N. benthamiana* leaf cells.

In conclusion, here we explored the pivotal role of the *OsPBZ1* gene in rice's defense against *M. oryzae*. *OsPBZ1* exhibited differential expression patterns under low-Pi conditions and during *M. oryzae* infection. CRISPR/Cas9-mediated mutagenesis of *OsPBZ1* resulted in altered blast resistance in rice plants, with mutants showing enhanced resistance under normal Pi conditions but increased susceptibility under high-Pi conditions. These findings suggest a complex interplay between *OsPBZ1*, Pi availability, and blast susceptibility. Additionally, the subcellular localization of OsPBZ1 was determined to be cytoplasmic. Further investigations are needed to elucidate the precise molecular

interactions and signaling pathways involving *OsPBZ1* in rice's defense against *M. oryzae*.

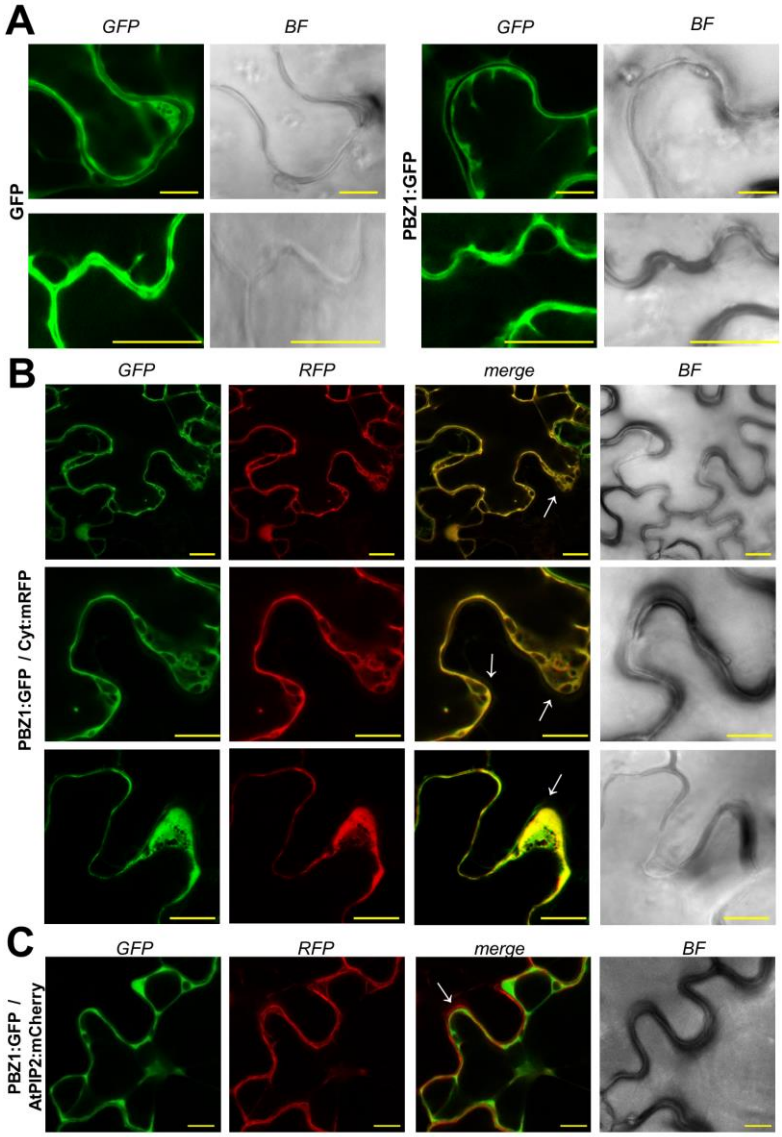

Figure 4.9. Subcellular localization of PBZ1 in *N. benthamiana* cells. Confocal images were taken at 72 h after agroinfiltration with the indicated plasmid constructs. **A)** Confocal fluorescence microscopy of *N. benthamiana* leaves transiently expressing either *GFP* (Green Fluorescent Protein) alone or *OsPBZ1-GFP*. GFP and bright-field (BF) channels are shown. **B)** Co-expression of *PBZ1:GFP* with the cytoplasm marker *Cyt:RFP*. White arrows show accumulation of the GFP-tagged PBZ1 in the cytoplasm. **C)** Co-expression of PBZ1-GFP with the plasma membrane marker *AtPIP2:mCherry*. The white arrow indicates the plasma membrane localization of *AtPIP2:mCherry* marker. Scale bar 10 µm.

Section 5 – Phosphate biosensors for detection of alterations in Pi content in rice plants

5. Phosphate biosensors for detection of alterations in Pi content in rice plants

Fluorescence resonance energy transfer (FRET) is a phenomenon in which nonradiative energy is transferred from an excited donor fluorophore to an acceptor molecule within close proximity. FRET-based Pi sensors can be used for live cell imaging, a process that helps when studying cellular processes at the organ level, either in plants or animals (Lalonde *et al.,* 2005; Okumoto *et al.,* 2012). Pi FRET-based sensors (named as Fluorescent Indicator Protein for inorganic Phosphate, FLIPPi), are genetically encoded fluorescent sensors consisting on chimeric genes formed by a cyan fluorescent protein (eCFP) fused to *Synechococcus* Pi binding protein (PiBP), and an enhanced yellow fluorescent protein (cpVenus) that act as FRET partner **(Figure 5.1A)**. In *Arabidopsis*, FLIPPi sensors have been successfully used to monitored cytosolic Pi dynamics in root cells in response to Pi deprivation and resupply (Mukherjee *et al.,* 2015; Assunção *et al.,* 2020). In this study, the authors also described differences in Pi content between developmental zones of the *Arabidopsis* root. Thus, changes in FRET ratio were better detected in the transition zone (TZ) of the Arabidopsis root (Banerjee *et al.,* 2016; Sahu *et al.,* 2020).

In this work, we evaluated the feasibility of using a FLIPPi sensor to monitor alterations in Pi content in rice plants. For this, transgenic rice plants expressing a FLIPPi sensor were generated, which were then used to assess the FRET response to Pi treatment or elicitor treatment in rice roots. Two different types of elicitors of the rice defense response were assayed: chitin (a general inducer of immune response) and elicitors obtained from the fungal pathogen *Fusarium fujikuroi,* a pathogen that infects the rice root.

5.1 cpFLIPPi transgenic rice plants respond to Pi treatment

Transgenic rice (Tainung 67) lines stably expressing either the cpFLIPPi sensor or a cpFLIPPi-null sensor (no FRET response) were generated. RT-qPCR analysis confirmed transgene expression in all lines, but not in azygous lines **(Figure 5.1B)**. To assess whether FLIPPi lines respond to Pi treatment, FLIPPi rice lines (homozygous lines), as well as azygous plants segregated from heterozygous lines, were grown for 15 days under different Pi regimes (Low-, Suff- and High-Pi). Pi content in rice roots was determined at 7- and 10-days of Pi treatment. Root Pi content increased when increasing the concentration of Pi supplied to the rice plant **(Figure 5.1C)**. As expected, differences between treatments (e.g., Low-Pi vs High-Pi) were higher at 10 days of treatment.

The FLIPPi lines were then used for live imaging of Pi in root epidermal cells. To avoid background fluorescence, the laser intensity was normalized using azygous lines. **Figure 5.1.D** shows a typical pattern of fluorescence in the cp-FLIPPi transgenic rice lines grown under normal conditions (e.g., sufficient Pi supply).

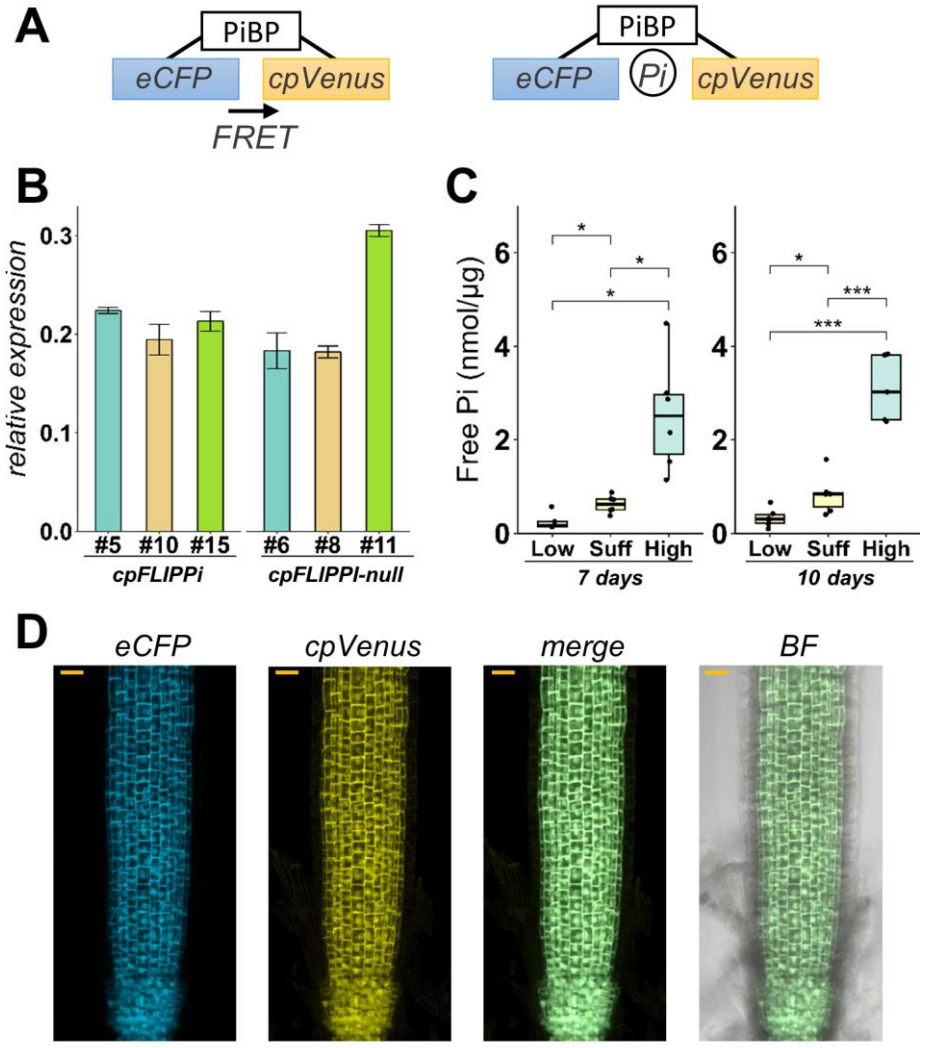

Figure 5.1. Live imaging of Pi in root epidermal cells of cpFLIPPi rice - plants. A) FLIPPi sensor scheme. When Pi binds to the Pi binding protein (PiBP), there is no energy transmission. **B)** Expression of the FLIPPi biosensor gene in cpFLIPPi and cpFLIPPi-null transgenic plants (T0 generation) determined by RT-qPCR. **C)** Pi content at 7 and 10 days of Pi treatment (left and right panels, respectively) in roots of rice plants that have been grown under Low-, Sufficient- or High-Pi conditions for 15 days. Three independent experiments were carried out. The mean ± *SEM* of two biological replicates with five plants per replicate is shown (*t* test, $*p \leq 0.05$, $***p < 0.001$). The horizontal line within the box represents the median value. **D)** Live imaging in root epidermal cells of cpFLIPPI rice plants. Representative images of roots from 10-day-old cpFLIPPI plants (line #10) that have been grown under Sufficient Pi conditions are shown. Scale bar: 20 µm.

5.2. Optimizing Microscope Settings for Specific Detection of eCFP and cpVenus

The absorption and emission spectra of the fluorescence proteins eCFP and cpVenus from the cpFLIPPi vector partially overlap. As shown in **Figure 5.2**, the fluorescence excitation spectra of eCFP and cpVenus overlap between 450 and 600 nm. Therefore, the excitation and emission wavelengths were adjusted to minimize fluorescence interference between the two proteins. We used a laser with a wavelength of 445 nm, that will only excite the eCFP protein and not the cpVenus protein. The emission spectrum of eCFP covers a range from 450 to 600 nm, while the emission spectrum of cpVenus covers a range from 500 to 650 nm. Therefore, the detection wavelength parameters used in these experiments were set to 481-534 nm for eCFP and 543-623 nm for cpVenus. These conditions allowed specific detection of each fluorescent protein and a more reliable analysis of the FRET response.

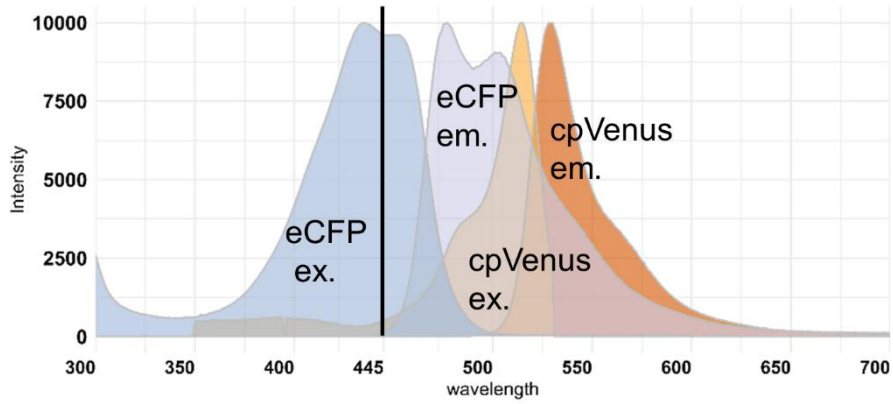

Figure 5.2. eCFP and cpVenus emission and excitation spectra. eCFP excitation (eCFP ex.): 350-500 nm; eCFP emission (eCFP em.): 450-600 nm); cpVenus excitation (cpVenus ex.): 450-550 nm;. cpVenus emission (cpVenus em.): (500-650 nm). Laser wavelength used for excitation is marked by a black line.

5.3 Live imaging of FRET response to Pi treatment in rice roots

Once the conditions were set, we measured FRET responses in roots of cpFLIPPi rice plants that have been grown under different Pi conditions, namely Low-Pi, Sufficient-Pi, or High-Pi conditions (0 mM, 0,25 mM, and 2,5 mM Pi respectively). The FRET ratio (eCFP/cpVenus intensities) was measured in roots of plants grown under each Pi condition. To ensure that changes in FRET ratio were due to changes in Pi concentration, the same measurements were performed in cpFLIPPi-null lines, these lines being unable to produce a FRET response. Two independent homozygous transgenic lines harbouring either the cpFLIPPi or the cpFLIPPi-NULL construct were analyzed. Measurements of eCFP and cpVenus fluorescence intensities were performed in the transition zone (TZ) and elongation zone (EZ) of rice roots **(Figure 5.3A)**.

Life imaging analysis revealed changes in the FRET ratio in roots of cpFLIPPi lines, but not in roots of cp-FLIPPi-null lines **(Figure 5.3B)**. No differences in FRET response were observed between the transition zone and the elongation zone, so average values of FRET ratio were recoded **(Figure 5.3B)**. The FRET (YFP/CFP) ratio decreased when increasing Pi concentration **(Figure 5.3B)**. A decrease in FRET ratio is consistent with increased Pi concentrations in rice roots when increasing Pi supply. No significant differences were, however, observed between Sufficient-Pi and High-Pi, indicating that above 0,25 mM Pi (corresponding to Sufficient-Pi) the system may be already saturated.

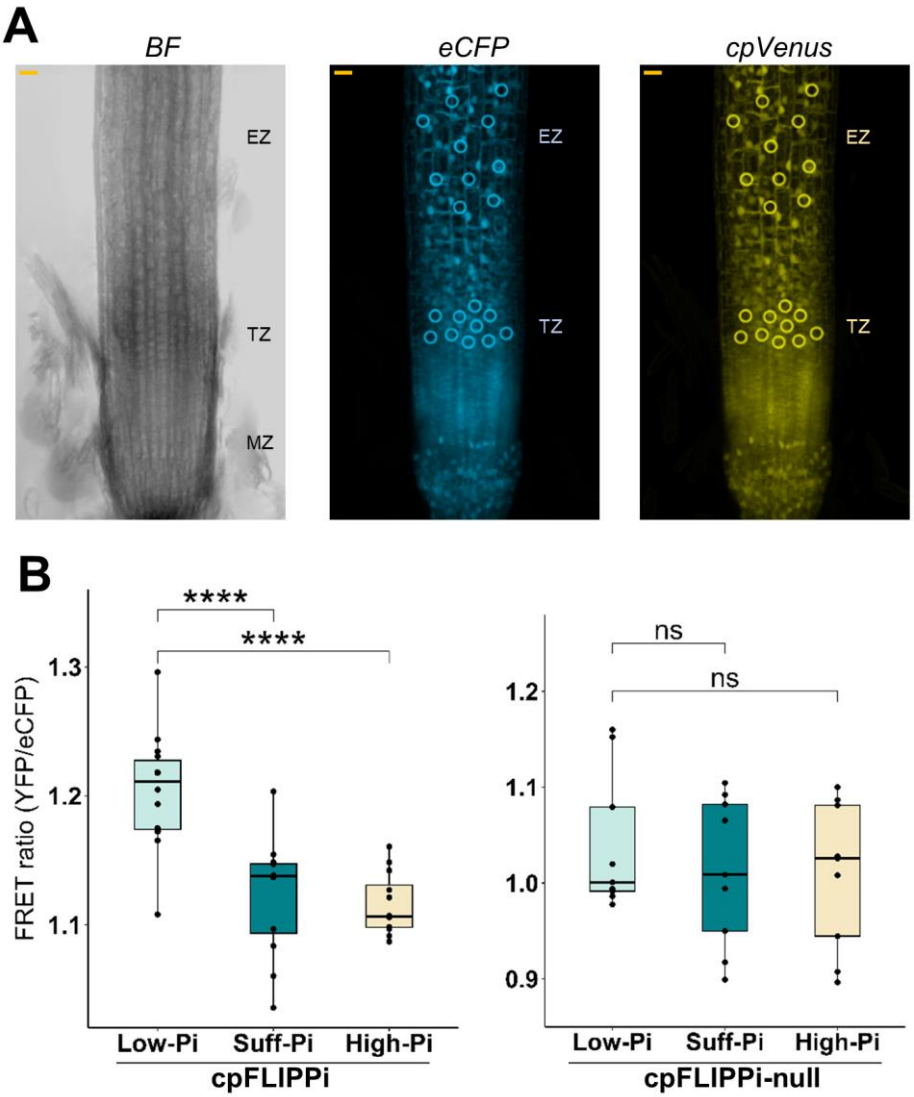

Figure 5.3. FRET response to Pi treatment in roots of rice FLIPPi sensor lines. A) Bright field microscopy image of the primary root from 10-days-old cpFLIPPi lines. Representative images of roots from plants that have been grown under Sufficient Pi conditions are shown. Root regions: EZ (elongation zone), TZ (transition zone), MZ (meristematic zone). Scale bar: 20 µm. **B)** Representative FRET ratios (cpVenus/eCFP) in roots from 10-days-old cpFLIPPi plants (line #10) that have been grown under Low-, Sufficient- or High-Pi conditions. Similar results were obtained with the cpFLIPPi line #15. Plotted FRET ratio values are means for ten seedlings ± *SEM* (*t* test, ****$p <$ 0.0001). The horizontal line within the box represents the median value. Mean of three independent experiments is shown.

Next, we assayed whether FRET ratios in Low-Pi plants could be reversed by treatment with high Pi. Seedlings of cpFLIPPi lines (lines 10 and 15) were grown for 10 days under Low-Pi or High-Pi supply, and FRET ratios were measured. Low-Pi plants were then changed to supplied with High-Pi. FRET ratios were monitored prior changing the Pi condition (time 0), and at different times following the change in the Pi condition (30 min, 1 hour and 3 hours). FRET responses were measured and compared with that of plants that were maintained under High-Pi condition. At 30 min of treatment with High-Pi, only a small decrease in FRET ratio could be detected **(Figure 5.4)**. FRET ratios further decreased with time of treatment with High-Pi. At 3 h of treatment with High Pi, FRET response showed significant decrease compared to FRET values at time 0 **(Figure 5.4)**. These findings suggest that Pi replenishment of plants that have been grown under Low-Pi occurs during the first hours of treatment with high Pi. These results also indicate that *in vivo* FRET responses are linked to the Pi status in the rice root, thus supporting the usefulness of the FLIPPI sensor to monitor alterations in Pi content in rice roots.

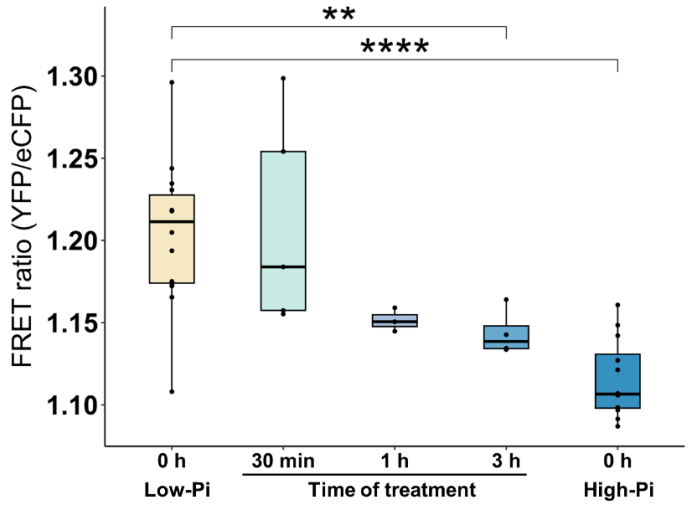

Figure 5.4. Replenishment of Pi content in roots of wild-type plants after Low-Pi treatment. cpFLIPPi plants were grown for 10 days under Low-Pi or High-Pi supply. Then, Low-Pi plants were supplied with High-Pi for 30 min, 1h or 3h. In parallel, a set of plants were allowed to continue growth under High-Pi conditions. FRET ratios were measured at the indicated time points (30 min, 1h and 3h). FRET values were monitored before Pi treatment (0 h) as reference values (Low- and High-Pi). Plotted FRET ratio values are means for six independent seedlings ± *SEM* (*t* test, $^{**}p < 0.01$, $^{****}p < 0.0001$). Two independent experiments were carried out with similar results.

5.4 Effect of elicitor treatment on Pi content in rice roots

Life imaging on FLIPPI rice plants was used to monitor Pi dynamics in root cells in response to treatment with elicitors of immune responses. In this study, two types of elicitors were assayed: i) chitin, a polysaccharide that is a major component of the cell walls of many fungal pathogens, and ii) crude elicitors obtained from the fungus *Fusarium fujikuroi,* a pathogen that infects the rice root. This study was carried out on cpFLIPPi plants that have been grown under Low-Pi or Sufficient-Pi conditions for 10 days. FRET ratio was measured before elicitor treatment (t = 0). Then, Low- and Suff-Pi treated plants were treated with a suspension of the elicitor under study (300 µg/mL *F. fujikuroi* elicitors; or 0,1 mg/mL of chitin). FRET response at 3 hours of

treatment (elicitors or chitin) was compared to that at t = 0. In roots of Low-Pi rice plants, elicitor treatment caused a reduction in FRET ratio (more pronounced in roots treated with chitin than in roots treated with *F. fujikuroi* elicitors) **(Figure 5.4)**. A reduction in FRET ratio would be consistent with an increase in Pi concentration in cells of elicitor-treated roots. In rice plants grown under sufficient Pi conditions, however, there were no significant variations in FRET ratio between elicitor-treated roots and untreated roots **(Figure 5.5)**. As mentioned above, saturation of sensor molecules might explain that elicitor treatment in sufficient-Pi plants does not result in important changes in FRET ratios.

Together, results obtained in this study support alterations in Pi content in the root response to elicitor treatment, and that this response is dependent on the Pi condition in which the rice plants have been grown. Treatment with elicitors of the rice immune response causes an increase in Pi content in roots of rice plants that have been grown under Low-Pi conditions.

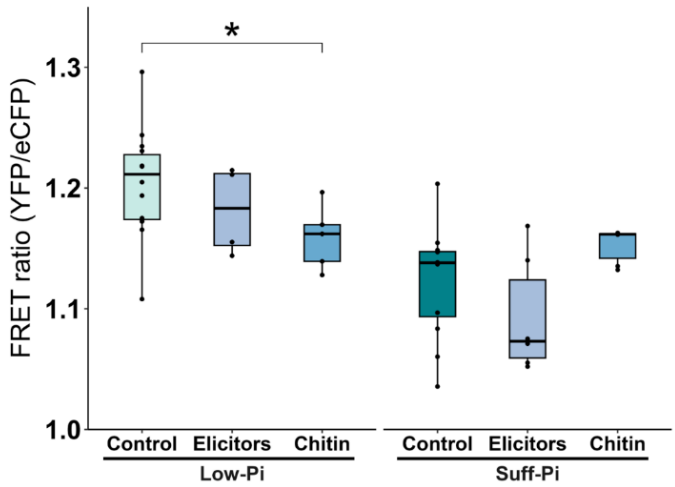

Figure 5.5. Chitin treatment increases Pi concentration in cells of rice roots. Plants were grown for 10 days under Low- or Sufficient (Suff-Pi) conditions. Then Low-Pi plants were treated for 3 hours with either *F. fujikuroi* elicitors or chitin. For each treatment, FRET ratios were measured before and after treatment. Plotted FRET ratio values are means for six independent seedlings ± *SEM* (*t* test, $*p \leq 0.05$). The horizontal line within the box represents the median value.

General Discussion

General Discussion

In recent years, significant advances have been made in our understanding of components and regulatory mechanisms involved in plant immunity. Integrated multi-omics approaches have revealed stress signaling components and networks of interactions in the plant response to environmental stresses. Understanding the various players driving the plant response to biotic and/or abiotic stress is essential for developing new strategies to improve crop resilience.

Current research in our group focuses on the effect of nutrient stress in disease resistance in rice, focusing on Pi nutrition and blast resistance. At present, fertilizers and pesticides are widely used to obtain optimal yield and to protect crops from diseases. Ironically, studies in our group revealed that Pi overfertilization renders the rice plant more susceptible to infection by the blast fungus *M. oryzae* (Campos-Soriano *et al.,* 2020). This fungus is one of the most important pathogens affecting rice production worldwide. It is then important to investigate the molecular mechanisms by which Pi fertilization influences the rice defense response to pathogen infection. In addition to its agricultural relevance, rice has been adopted as the model plant for functional genomics research in monocotyledoneous plant species.

In this PhD thesis, we investigated the effect of Pi on the proteomic response of rice plants to pathogen infection. We also examined the implication of *OsPBZ1,* a marker of the induction of rice defense responses, in the rice response to *M. oryzae* infection. These studies have been carried out in *japonica* rice cultivars (*O. sativa* cultivars Nipponbare and Tainung 67). The information gained in this PhD thesis demonstrated that Pi content in rice leaves significantly

affects the composition of the apoplastic proteome as well as the global phosphorylation pattern of rice proteins, ultimately impacting blast resistance.

Results obtained in **Section 1** indicated that treatment with high Pi of rice plants, and subsequent increase in Pi content in rice leaves, has an effect on the accumulation of Pathogenesis-Related proteins. Furthermore, Pi accumulation in rice leaves stimulates the expression of *M. oryzae* effectors during the biotrophic phase of the infection process. Reduced accumulation of PR proteins and stronger expression of fungal effectors during *M. oryzae* infection would be consistent with the enhanced blast susceptibility in rice plants that have been grown under a high Pi regime. To sum up, these results revealed that Pi accumulation in rice leaves has an effect on the two partners of the interaction, the rice plant and the fungus, while supporting the existence of links between Pi- and pathogen-induced signal transduction pathways in rice.

On the other hand, based on previous results from our group (Campos-Soriano *et al.,* 2020), treatment of rice plants with high Pi, not only represses pathogen-inducibility of rice defense responses, but also might provoke a stressful situation in the plant. This stress could affect diverse physiological processes contributing to blast susceptibility in rice plants accumulating Pi. In other studies, it was described that overexpression of the phosphate transporter *OsPT8* in rice is accompanied by suppression of PTI in rice plants (Dong *et al.,* 2019). However, in that study, the authors did not determine Pi content in *OsPT8* overexpressor plants.

Several studies in Arabidopsis have highlighted the interplay between the PSR and immune signaling (Castrillo *et al.*, 2017; Chan *et al.*, 2021). Notably, the transcription factor *PHR1,* a key regulatory

component of Pi starvation responses in Arabidopsis, has been shown to negatively regulate defense-related gene expression (Castrillo *et al*., 2017). This observation led the authors to propose that the plant prioritizes nutrition over defense. Furthermore, *phr1* mutant lines showed enhanced resistance to infection by the bacterial pathogen *P. syringae* DC3000 and the oomycete pathogen *Hyaloperonospora arabidopsidis* (Castrillo *et al.*, 2017). The introduction of a phytoplasma effector known as SAP11 into *Arabidopsis* plants results in activation of Pi starvation responses that rely on PHR1, leading to susceptibility to infection by *Pseudomonas syringae pv. tomato* (Lu *et al.*, 2014). Collectively, these findings provide substantial evidence supporting the cross-talk between Pi signaling and immune signaling in plants.

Regarding other macronutrients, nitrogen-induced susceptibility (NIS) to rice blast has long been associated with an increase in *M. oryzae* pathogenicity, and enhanced susceptibility to infection by M. oryzae (Huang *et al.,* 2017). Contrary to what is observed in rice, nitrogen fertilization reduces disease severity caused by *Verticillium spp* in *Solanum* species, indicating that no generic model can describe the role of N in each plant/pathogen interaction (Veresoglou *et al.,* 2013).

Other studies in our group indicated that exposure of rice plants to high iron enhances resistance to the fungus *M. oryzae* (Sánchez-Sanuy *et al.,* 2022). Iron plays a role in controlling the plant immune response to pathogen infection by regulating ROS production. On the other hand, *Arabidopsis* plants grown under iron-starvation conditions exhibited resistance to bacterial and fungal pathogens (*Dickeya dadantii* and *B. cinerea*, respectively) (Kieu *et al.,* 2012).

Globally, these results support that the nutrient status of the rice plant can influence its immune response, which can in turn affect its interactions with other organisms (e.g., resistance or susceptibility to

pathogen infection). However, the consequence of nutritional unbalances in a host plant during interaction with potential pathogenic microorganisms need to be studied on a case-by-case basis.

To get further insights into proteomic responses to Pi treatment, we examined the apoplastic proteome in rice plants that have been grown under different Pi regimes. Results obtained in this research are included in **Section 2**. It is known that hydration of the apoplast can be a factor contributing to disease against certain foliar pathogens. Accordingly, in this work we examined apoplast hydration in leaves of rice plants grown under different Pi supply conditions. This study demonstrated that water hydration in leaves of High-Pi plants is approximately four times higher than in Low Pi plants. It will then be of interest to further investigate whether water hydration in the apoplast of High-Pi plants determines fungal colonization. Another interesting aspect derived from this finding that deserves investigation would be to know whether the fungus can modify the host environment for its own benefit, thus, increasing blast susceptibility in High-Pi plants. In favor of this hypothesis, increasing evidence support that water availability in the apoplast might stimulate bacterial growth (Ekanayake *et al*., 2022). Pathogenic bacteria can also manipulate plant processes to establish a hydrated apoplast (Dixon *et al*., 2022).

Our analysis of apoplast proteins revealed proteomic changes in the apoplast of rice plants in response to Pi treatment. Notably, different types of defense proteins were identified in the apoplast of Low-Pi plants in the absence of pathogen infection, supporting a phenotype of blast resistance in these plants. PR proteins and proteins involved in oxidative stress were more frequently found in the apoplast of Low-Pi plants compared to High-Pi. Thus, changes in the apoplast proteome emphasize the dynamics of plant apoplast in response to Pi treatment

and shed some light on the mechanisms contributing to blast resistance/susceptibility in rice.

The analysis of the apoplast proteome revealed the presence of protein families that are worth highlighting, such those involved in ROS production and/or protection against oxidative stress (e.g., peroxidases, catalase, thioredoxins and GSTs). Plant peroxidases make the cell wall more resistant to enzymatic degradation by fungi through cross-linking of different cell wall components and polymerizing lignin monomers.

The relevance of ROS in plant immunity is well recognized. In addition to their function in the creation of interconnected plant cell wall polymers to form a protective barrier, ROS might also function as antimicrobial agents and signaling molecules in the plant. ROS signaling prompts the activation of signaling processes (e.g., kinase activation and Ca^{2+} influx into the plant cell) leading to the induction of *PR* genes. Additionally, ROS production in the early stages of infection plays a pivotal role in the orchestration of the HR and cell death. ROS production in the apoplast is mediated by NADPH oxidase activities encoded by the *Rboh* gene family, a central feature of the HR (Torres*,* 2010). The HR is a crucial defense strategy against biotrophic pathogens, leading to localized cell death that restricts pathogen replication during the initial stages of plant-pathogen interactions (Sachdev *et al*., 2023). However, this strategy is less effective against necrotrophic pathogens, which actively kill host tissues, underscoring the complexity of plant defense mechanisms against diverse pathogenic challenges (Dalio *et al.,* 2021). As excess of ROS production might be toxic for the host plant, the level of ROS should be tightly regulated to avoid cellular damage. In this process**,** thioredoxins play a vital role in protecting cells from oxidative stress (Ya Ma *et al*., 2023), while glutathione transferases are responsible for detoxification processes (McGoldrick *et al.,* 2005). Thus, the observed changes in apoplastic

proteins involved in ROS production and/or protection against oxidative stress in leaves in rice plants grown under a different Pi regime might determine the outcome of the interaction, resistance or susceptibility. In addition to PR proteins, apoplastic peroxidases, catalase, thioredoxins, and GSTs could potentially be linked to the enhanced blast resistance observed in low-Pi plants.

Additionally, numerous glycosil hydrolases were identified in the apoplast of Low-Pi plants. Glycosyl hydrolases play a role in remodeling the cell wall and generating ROS through chitin oligomer production, enhancing the plant's defense against fungal infection (Rafiei *et al*., 2021).

Regarding PR proteins, members of different PR families were identified in the apoplast of rice leave, some of them exhibiting direct or indirect antimicrobial activity. Among them, there were: PR1 proteins, ß-1,3-glucanases (PR2), chitinases (Classes IV and III; PR3 and PR8, respectively), defensins (PR12), and LTPs (Lipid Transfer Proteins (PR14). Notably, these proteins were found to be more abundant in the apoplast of Low-Pi plants compared to High-Pi plants, pointing to a basal defense operating in Low-Pi plants in the absence of pathogen infection. For instance, distinct members of the PR1 family were exclusively detected in the apoplast of Low-Pi plants (PR1b, A0N0C2) while others were present in both Low-P and High-Pi plants (A0A0D3QSW1). Although the precise biochemical function of PR1 in the immune response remains unclear, its defensive role appears to be linked to its capacity to inhibit cell death. Additionally, PR1 can potentially inflict cellular damage by sequestering sterols (Gamir *et al*., 2017; Bakare *et al*., 2021). Recent findings have unveiled that the PR1-like protein in *Ustilago maydis* possesses two discrete domains, allowing it not only to subdue plant defenses but also to bolster the infection process of fungal pathogens. These discoveries propose a mechanistic link, shedding

light on how fungal pathogens leverage a conserved domain to execute a function that contradicts the defensive role of PR1 (Lin *et al*., 2023).

Purple acid phosphatases were also identified in the leaf apoplastic proteome. These proteins exhibited high abundance in the apoplast of Low-Pi plants in the absence of infection. However, to understand how purple acid phosphatases might function in rice blast resistance, a better understanding of their substrates and the specific processes in which they are involved in plant immunity is required.

Remarkably, proteins from ABA and water stress-induced family were exclusively found in the apoplast of Low-Pi plants. ABA is primarily known for its role in responding to abiotic stresses like drought and salinity. However, it also has implications in biotic stress responses, particularly in defending plants against pathogen infection (Bharath *et al*., 2021). In concerted action with other defense-related hormones, ABA can play a positive or negative role in disease resistance depending on the pathogen and stage of the infection process. ABA triggers a signaling cascade involving receptors, protein kinases, and transcription factors, often leading to stomatal closure to reduce water loss, and modulation of gene expression to enhance stress tolerance. Numerous plant pathogens, including the rice blast fungus, can infect the rice leaf through stomata (Wang *et al*., 2020). As ABA mediates stomatal closure, a PI-mediated regulation of stomatal closure would also help in controlling infection. However, ABA's role varies, acting as both a positive and negative regulator in immune signaling during interactions with different pathogens (Nahar *et al., 2012;* Xu *et al.,* 2013; Jiang *et al*., 2017). In the context of rice's defense against *M. oryzae*, ABA has been shown to enhance susceptibility by suppressing defense genes and impairing pathogen recognition (Derksen *et al*., 2013). In other studies, Meng *et al*. (2019) described the accumulation of proteins in the ABA signaling pathway in rice leaves in response to treatment

with the *M. oryzae*-secreted protein MSP1 (a *M. oryzae* effector). Recent research has unveiled that the *M. oryzae* MSP1 induces alterations in the rice proteome and phosphoproteome levels (Lee *et al*., 2023). It will then be of interest to investigate whether ABA-related proteins in the apoplast of Low-Pi plants plays a role in blast resistance.

In our proteomic analysis of the leaf apoplast, we also detected the chitin elicitor binding protein (CEBiP) in Low-Pi plants. CEBiP is the major chitin oligomer-binding protein in rice and plays a major role in the perception of chitin elicitors for the activation of downstream signaling cascades, including Mitogen-activated protein kinase (MPK) signaling cascades.

To summarize, results obtained on the analysis of the leaf apoplast proteome suggest that the accumulation of defense-related proteins in Low-Pi rice plants might contribute to the resistance phenotype observed in these plants. In other words, a reduction in the accumulation of defense-related proteins in the apoplast of High-Pi plants could be responsible for increased susceptibility to blast disease.

In this Ph.D Thesis, we also approached global phosphoproteome analysis of leaves from rice plants that have been grown under different Pi conditions, in the presence or absence of pathogen infection. Results are presented in **Section 3**. This study unveiled the impact of stress imposed by Pi content on the rice phosphoproteome. Under low Pi conditions, we specifically observed an increase in the phosphorylation level of proteins related to defense responses, such as Respiratory burst oxidase proteins (RBOHB and RBOHD) and Synaptosomal-associated protein of 32 kDa (SNAP32, Q5EEP3). These proteins have been described to play a specific role in enhancing the host's ability to resist blast rice (Kadota *et al*., 2015; Cao *et al*., 2019). Specifically, RBOH proteins play a key role in generating

ROS, such as superoxide radicals, as part of plant defense responses (Kaur *et al*., 2016).

Moreover, we detected regulation by phosphorylation in proteins potentially involved in PTI signaling even in the absence of pathogen infection. Specifically, proteins such as mitogen-activated protein kinases (MAPKs) and calcium ion-binding proteins exhibit a heightened level of phosphorylation in Low-Pi plants. This observation aligns with a phenotype of disease resistance observed in Low-Pi plants. For instance, activation of MPK3 and MPK6 through phosphorylation has been associated with defense priming in *Arabidopsis*, thereby enabling more robust immune responses during pathogen infection (Beckers *et al*., 2009; Hönig *et al*., 2023). These MAPK-mediated signaling cascades have also been shown to be involved in ABA signaling pathways (Chen *et al*., 2021). Along with this, our phosphoproteomic analysis also identified proteins associated with ABA signaling in Low-Pi plants. Therefore, the phosphorylation status of these proteins can be associated with the phenotype of blast resistance in Low-Pi rice plants. This was further substantiated by the finding of more phosphorylation events in defense-related proteins in Low-Pi plants compared to High-Pi plants, along with noticeable changes in defense-related hormone signaling pathways, like ethylene and auxin signaling.

Regarding ethylene, a positive feedback loop of ethylene with CEBiP (receptor of chitin elicitors) has been proposed to mediate rice PTI against microbial infection (Helliwell, 2016). Phosphorylation of ethylene signaling components might well serve as a regulatory mechanism for the activation of defense-related genes during pathogen infection. As for auxin, the active form of auxin, Indole-3-acetic acid (IAA), has been reported to trigger the synthesis of expansins. Expansins facilitate cell wall loosening, thereby heightening rice susceptibility to pathogen attacks, notably by *M. oryzae*. Suppressing

auxin synthesis or signaling has been shown to reinforce resistance against blast (Fu *et al*., 2010). Consequently, rice might attenuate its own auxin response during *M. oryzae* infection, stalling growth and initiating a defense mechanism. To counteract this host hormonal response, *M. oryzae* could potentially generate IAA (Jiang *et al*., 2013). The observation of phosphorylation events in auxin-responsive proteins in non-infected Low-Pi plants (further intensified upon infection) might be associated with the resistance phenotype that is observed in Low-Pi plants.

To assess the effects of infection in rice plants grown under contrasting Pi conditions, we compared the phosphoproteome of non-infected and *M. oryzae*-infected leaves of Low-Pi and High-Pi plants **(Section 3)**. Initially, we observed that pathogen infection induces a greater degree of alterations in the phosphorylation status of proteins in the leaves of High-Pi plants as compared to Low-Pi plants. Nonetheless, the impact of protein phosphorylation on resistance or susceptibility would vary depending on the function of each particular phosphoprotein in disease resistance. For instance, no observable changes occurred in the phosphorylation status of RBOH proteins (RBOHB and RBOHD) and SNAP32 in Low-Pi plants that have been infected with *M. oryzae*. However, infection in High-Pi plants is accompanied by a significant increase in RBOH phosphorylation, these plants exhibiting enhanced blast susceptibility. These results support links between protein phosphorylation and ROS signaling in rice immunity.

Additional defense-related proteins that are regulated by phosphorylation, included peroxiredoxins, thioredoxins, phosphatases, kinases, among others **(Section 3.3)**. Peroxiredoxins and thioredoxins play crucial roles in antioxidant defense and redox signaling (Cejudo *et al*., 2021). In our study, we identified a Thioredoxin-dependent peroxiredoxin (Q69QW0) and Peroxiredoxin Q (P0C5D5) as being

regulated by phosphorylation. Phosphorylation-based control of peroxiredoxins in response to extracellular cues permits the localized accumulation of H_2O_2, thereby enabling its role as a signaling messenger (Woo *et al*., 2010; Rhe *et al*., 2012).

Among the set of proteins regulated by phosphorylation, MKP1 (MAP kinase phosphatase, A2V7M8) was found. MKP1 functions as a phosphatase, by dephosphorylating serine, threonine, and tyrosine residues on MAPKs (Jiang *et al*., 2018). MPK1 also acts as a negative regulator of MPK6, controlling innate immune signaling intensity and duration in *Arabidopsis* (Verma *et al*., 2021). Phosphorylation of MKP1 has been proposed to be essential for PAMP responses and resistance against bacterial infections, highlighting its critical role in plant defense mechanisms. Recognizing that the phosphorylation of protein kinases can influence both the extent and duration of their activity, as well as their subcellular localization and substrate selectivity, the observed modulation of the phosphorylation status in distinct MAP kinases in response to phosphorus (Pi) treatment and/or infection unveils novel avenues for prospective investigations. This prompts further exploration into the significance that this post-translational modification might hold in the regulation of rice immunity.

Overall, post-translational modifications might play a multifaceted role in governing plant immune responses by regulating protein stability, subcellular localization, activity, and interactions with target proteins. However, our understanding of post-translational modifications in the rice proteome, including protein phosphorylation, during the rice response to pathogen infection still remains limited.

In **Section 4**, we deve into *OsPBZ1* function in rice immunity. *OsPBZ1* is considered a marker for the induction of the rice defense response to pathogen infection, albeit its biological role is not clear.

Expression of the various PR10 family members was found to be down-regulated in High-Pi plants compared with Low-Pi plants (**Section 4**). Consistent with this, PR10 accumulates at a lower level in High-Pi plants (**Section 1**). Among PR10 family members, *OsPBZ1* showed the highest level of expression. *OsPBZ1* was also strongly induced by pathogen infection in Low-Pi plants compared to High-Pi plants. In line with this, the activity of the *OsPBZ1* promoter in transgenic rice plants expressing a *OsPBZ1 promoter:GUS* fusion gene under Pi starvation conditions, as well as during *Xanthomonas oryzae pv. oryzae (Xoo)* infection was previously described (Huang *et al.,* 2016; He *et al.*, 2018).

Regarding *RSOsPR10*, this gene was originally named as Root-specific rice PR10 because of its low level of expression in rice leaves, hence, it was primarily considered to be expressed in roots (Hashimoto *et al*., 2004; Yamamoto *et al*., 2018). Post-translational modifications of PBZ1 were previously proposed due to abnormal mobility of this protein in SDS-PAGE (Rakwal *et al.,* 1999; Kim *et al.,* 2003). Our phosphoproteomic study revealed a substantial impact of phosphorylation in RSOsPR10 in response to *M. oryzae* infection. Given the elevated expression of *OsPBZ1* and its significance as a defense marker, we generated CRISPRedited plants targeting *OsPBZ1*.

Analysis of CRISPR*PBZ1* rice plants, demonstrated that the phenotype of blast resistance/susceptibility to infection by *M.oryzae* infection in CRISPR*PBZ1* plants is dependent on the Pi content in rice leaves (**Section 4**). Under normal conditions (i.e., sufficient Pi supply), blast resistance in CRISPR*PBZ1* plants increased compared with WT (azygous) plants. Consistent with the phenotype of blast resistance that is observed in CRISPR*PBZ1* lines grown under sufficient Pi supply, stronger induction of *OsPR1a* and *OsChtIII* occurs during infection in CRISPR*PBZ1* plants than in azygous lines. There was then an apparent contradiction between the results obtained in CRISPRPBZ1 plants

(showing a slight increase in blast resistance under sufficient-Pi conditions) and results previously described on blast resistance in *OsPBZ1* overexpressor plants (Huang *et al*., 2016). However, this different behavior (present study; previous results in the literature) might be related to the experimental conditions used for growing the rice plants, as discussed below.

The experimental conditions used to grow the rice plants in this Ph.D. Thesis were: 0,025 mM for Low-Pi, 0,25 mM for Sufficient-Pi, and 2,5 mM for High-Pi supply). When grown under High-Pi conditions, the CRISPR*PBZ1* lines were found to be more susceptible to *M. oryzae* infection than wild-type (azygous) plants. Under sufficient Pi conditions, the CRISPR/PBZ1 plants become slightly more resistant to blast. Finally, there were no significant differences in blast resistance to *M. oryzae* infection between CRISPR*PBZ1* plants and azygous plants when the rice plants were grown under low-Pi conditions. These findings demonstrated that *OsPBZ1* silencing has different consequences in blast resistance depending on Pi content in rice leaves, also supporting a role of *OsPBZ1* in the rice response to both types of stress, phosphate stress and pathogen infection. Enhanced susceptibility in CRISPRPBZ1 plants grown under High-Pi conditions might be the consequence of the combination of stress caused by Pi excess and the lack of *OsPBZ1* function, whereas under Low-Pi conditions, silencing of *OsPBZ1* has no important consequences in resistance to *M. oryzae* infection. Maintenance of Pi homeostasis can then be associated with blast resistance in rice.

In the literature, it can be found that transgenic expression of *OsPR10* family members in different plant species confers resistance against pathogen infection (Huang *et al*., 2016; Wu *et al*., 2016). In particular, resistance to infection by the bacterial pathogen *Xoo* was observed in transgenic rice plants overexpressing *OsPBZ1* (also named

OsPR1a) (Huang *et al.,* 2016). Transgenic Arabidopsis plants constitutively expressing *OsPBZ1* exhibited resistance against bacterial blight (*Xoo*) and fungal (*Xanthomonas campestris pv. campestris*) pathogens (Huang *et al*., 2016). Finally, constitutive overexpression of *JIOsPR10* in rice enhanced resistance to rice blast fungus (Wu et al. 2016). At present, however, the specific role of *OsPBZ1* in the *M. oryzae*-rice pathosystem has not been characterized yet.

Knowing the relevance of the Pi status in the rice plant in determining a phenotype of resistance (low and sufficient Pi conditions) or susceptibility (High-Pi conditions), we examined in more detail the conditions used by other authors when assaying pathogen resistance in plants overexpressing *OsPBZ1*. Huang *et al*. (2016) supplied the rice plants with MS medium, while in our study the rice plants were supplied with half-strength Hoagland's solution. Specifically, the MS medium contains 1.25 mM of KH2PO4, a condition that falls between our sufficient and high Pi regimes. As the Pi content was not determined in the rice plants assayed by Huang *et al*. (2016), it is difficult to explain differences in blast resistance (present study; Huang *et al*., 2016) based solely on the Pi condition used to grow the rice plants. Also, differences in components of the two fertirrigation solutions other than Pi (Huang *et al.,* 2016; present work) make it challenging to directly compare results observed on blast resistance in *OsPBZ1* overexpressor plants and CRISPR/Cas9 plants. For instance, the MS medium contains 100 µM Fe (Huang *et al*., 2016), whereas our half-strength Hoagland's solution contains 11 µM Fe (present work). As previously reported by our group, exposure of rice plants to high Fe (1 mM Fe) confers resistance to infection by the blast fungus in rice (Sánchez-Sannuy *et al*., 2022). Nitrogen (N) is another crucial nutrient that has an impact on blast resistance in rice (Nitrogen-Induced Susceptibility, NIS), and N conditions also differed in blast resistance assays in *OsPBZ1*

overexpressor plants (Huang *et al*., 2016) and CRISPRPBZ1 plants (present work) (20 mM and 0.5 mM NH_4NO_3 in the MS and half-strength Hoagland's solution, respectively). From this, it is clear that understanding mechanisms underlying *OsPBZ1*-mediated resistance to infection by the rice blast fungus requires first to standardize experimental conditions, including nutrient supply. As an additional complexity, there is the possibility that PBZ1 functioning might be dependent on the lifestyle of the pathogen, e.g., biotrophic, necrotrophic, hemibiotrophic pathogens. Both *Xoo* and *X. campestris* have a necrotrophic lifestyle (Huang *et al*. 2016), whereas *M. oryzae* has a hemibiotrophic lifestyle (present work).

Collectively, results obtained on expression analyses and CRISPR*PBZ1* rice lines support that *OsPBZ1* expression is regulated by both Pi and pathogen infection. Pi content in rice leaves is an important factor in determining *OsPBZ1* function and outcome of the rice/*M. oryzae* interaction.

Regarding the biochemical function of PBZ1, it has been proposed that this protein exhibits RNase activity *in vitro* (Kim *et al*., 2008; Kim *et al*., 2011; Huang *et al*., 2016). Although RNase activity can be exhibited by distinct PR10 proteins, it is not believed to be a universal characteristic (McBride *et al.*, 2019). In other studies, Kim *et al.* (2011) described that a recombinant PBZ1 protein causes cell death *in vitro* in rice suspension culture cells and *in planta* in *N. benthamiana* leaves. These observations correlated well with degrading RNA activity, which is a well-accepted hallmark feature of the programmed cell death in plants. PR10 proteins have been also shown to exhibit RNase activity against pathogens, leading to a cytotoxic effect on cells and inhibition of pathogen growth by degrading the pathogen's cells (Dos Santos & Franco, 2023). At present, however, the specific biochemical function of PBZ1 in plant cell death is still a matter of debate.

Regarding the subcellular localization of PBZ1, our findings in transient expression assays on the heterologous system of *N. benthamiana* leaves revealed that PBZ1 resides in the cytoplasm. Although members of the PR10 family have been found in the cytoplasm, there are also exceptions in which the PR10 protein localizes in the nucleus, cell membrane or forming complexes with other proteins in the apoplast and mitochondria (dos Santos *et al.,* 2023). In this respect, earlier research postulated that interactions of PBZ1 with other proteins might alter its subcellular localization which, in turn, might have an impact on its function in disease resistance (Lopes *et al*., 2023). During bacterial infection of pepper plants, it was reported that PR10 is phosphorylated by an unknown kinase, thereby increasing its RNase activity and contributing to antibacterial resistance (Choi *et al*., 2012). In line with this, our phosphoproteome analysis **(Section 3)** indicated that PR10 proteins, in particular RSOsPR10 (and most probably also PBZ1), undergo phosphorylation. Further studies are needed to clarify whether phosphorylation and/or interaction with other proteins determines subcellular localization of PBZ1 in rice.

Collectively, results obtained in this PhD Thesis demonstrated that Pi excess negatively affects blast resistance. **Figure 8** depicts a conceptual model elucidating the potential regulatory role of Pi and protein phosphorylation in modulating defense responses against *M. oryzae* in rice plants, thereby influencing blast resistance or susceptibility. According to this conceptual framework, defense-related proteins tend to accumulate in the apoplast of rice plants cultivated under low-Pi conditions, even in the absence of infection. These proteins include peroxidases, catalases, pathogenesis-related proteins (PRs), peptidases, among others.

Similarly, the phosphorylation status of proteins in low-Pi plants resembles that observed during infection. In contrast, high-Pi plants

undergo a notable change in their phosphorylation status when exposed to *M. oryzae* infection. Additionally, the hydration of the apoplast and the influence of proteins related to abscisic acid (ABA) may contribute to susceptibility to *M. oryzae* under conditions of Pi excess. While the specific role of PBZ1 remains unclear, its phosphorylation status appears to be significant in the context of infection, as evidenced by its dependency on the phosphate levels in the plant. The intricate interplay of these factors leads to a susceptible phenotype in high-Pi plants.

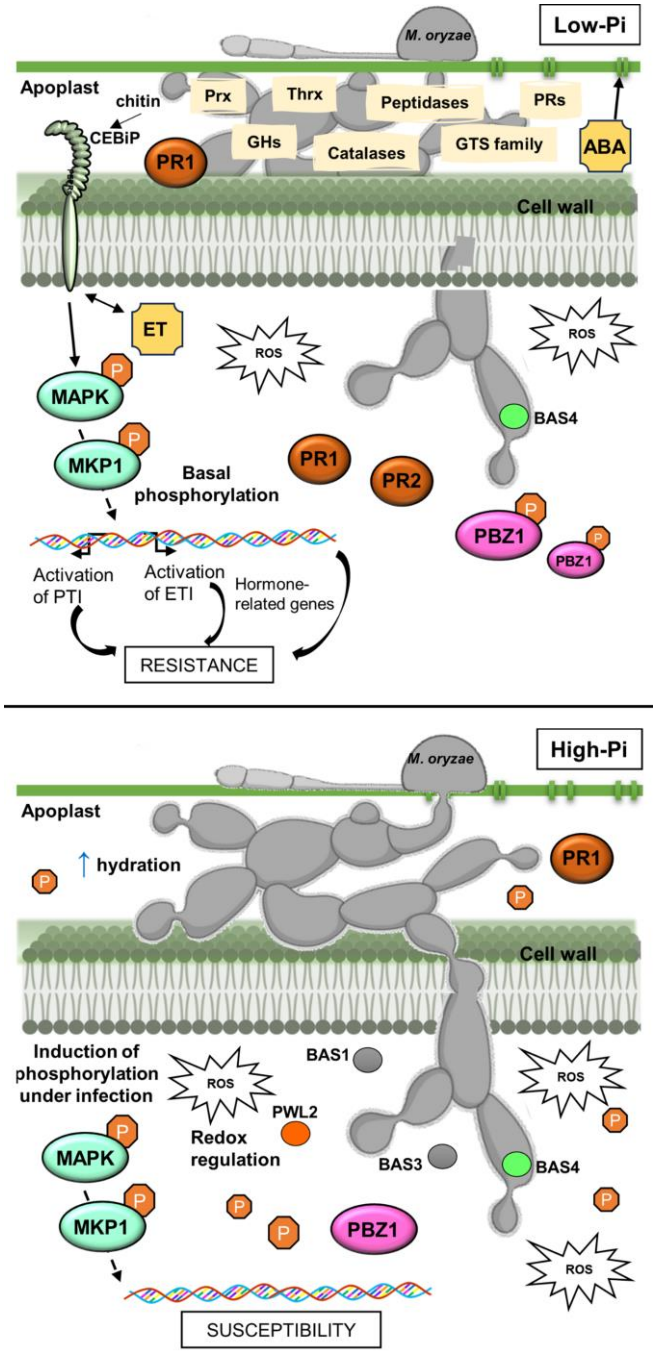

Figure 8. Theoretical model depicting the Pi-responsive components in the response of rice plants to *M. oryzae* infection. Abbreviations: peroxidases (Prx), thioredoxins (Thrx), Glycosyl hydrolases (GHs), glutathione transferase (GTS), Pathogenesis-related protein (PR), abscisic acid (ABA), chitin elicitor binding protein (CEBiP), ethylene (ET), reactive oxygen species (ROS), mitogen-activated protein kinases (MAPK) PAMP-triggered immunity (PTI), effector-triggered immunity (ETI), phosphate (P).

Due to the importance of Pi in plant nutrition and immunity, the development of Pi biosensors is of great interest. In this work, we generated rice (*O. sativa spp. japonica* cv Tainung 67) plants expressing a FLIPPi sensor which were then successfully used to monitor changes in Pi content in rice roots in response to treatment with Pi or elicitors. These results are presented in **Section 5**. FLIPPI sensors have been previously used for live imaging of Pi in Arabidopsis plants with cellular and subcellular resolution, but their usefulness to monitor Pi content in rice tissues was unknown. Life imaging of roots from Pi-treated cpFLIPPi rice lines showed FRET ratio changes that varied according to the Pi condition in which the plants are grown. Furthermore, we could observe that Pi replenishment in rice roots occurs during the first hours of treatment (experiments in which the plants were grown under Low-Pi condition and then supplied with High-Pi by passive diffusion). The FRET ratio decreased, hence the Pi concentration increased in rice roots, by 1 hour following addition of High-Pi solution. These findings point to a rapid uptake of Pi from the medium into the rice roots. In Arabidopsis, Sahu *et al.* (2020) also described rapid changes in FRET ratios in response to Pi. Differences in Pi content were not observed in plants supplied with Pi concentrations at a concentration above 0,25mM Pi (sufficient Pi), which can be explained by substrate binding saturation. This phenomenon has been previously described in *Arabidopsis* (Banerjee *et al*., 2016).

Additionally, the FLIPPi sensor rice lines were used to examine alterations in Pi content in response to treatment with elicitors (chitin, fungal elicitors). The effect of elicitor treatment was better seen in plants that have been grown under Pi limiting conditions where the FRET ratio decreased (indicating that the Pi concentration increased) in root cells during elicitor treatment.

The use of FLIPPi sensors represents an useful tool to monitor changes in Pi content in rice roots, as FRET responses can be easily monitored and correlated with the Pi status in the root. Live-imaging of rice plants expressing a FLIPPi sensor opens new avenues to investigate mechanisms involved in Pi homeostasis in rice, also in the context of disease resistance. From the practical point of view, FLIPPi sensors could also be used in crop research to develop more sustainable Pi fertilization practices.

Currently, fertilizers and pesticides are routinely used to optimize yield and to prevent losses caused by *M. oryzae* infection. However, the indiscriminate use of fertilizers might have undesirable effects not only on the environment but also on severity of rice blast, making necessary to increase pesticide use. The information gained in this Ph. D. Thesis might lay a foundation for rationally optimizing fertilizer and pesticide use in rice production. For this, a better knowledge of the molecular mechanisms underlying crosstalk between Pi signaling and immune signaling is still needed.

Conclusions

1. Phosphate content in rice leaves has a dual impact on both the rice plant and the fungal pathogen *M. oryzae*. The accumulation of Pi negatively influences the accumulation of Pathogenesis-Related (PR) proteins in the plant, resulting in a susceptible phenotype, while simultaneously there is a stimulation of the expression of fungal effectors.

2. The leaf apoplast of Low-Pi plants is notably enriched in proteins associated with plant defense reactions. This enrichment aligns with the observed resistance phenotype in Low-Pi rice plants against *M. oryzae*. At the same time, the increased hydration in the apoplast of High-Pi plants might promote *M. oryzae* growth compared to Low-Pi plants. This enhancement may occur through the facilitation of water and nutrient uptake from the apoplast.

3. Phosphoproteomic analysis indicates the involvement of diverse phosphorylation events during *M. oryzae* infection. The phosphorylation status of crucial proteins remains consistent in Low-Pi plants, irrespective of mock conditions or infection. In contrast, High-Pi plants undergo many modifications in protein phosphorylation. Rice PR10 proteins, including RSOsPR10 and PBZ1, also appear to be regulated by phosphorylation.

4. Functional characterization of *OsPBZ1* reveals its pivotal role in rice's defense against *M. oryzae* which is dependent on Pi content in the plant. *OsPBZ1* exhibits differential expression patterns under low-Pi conditions and during *M. oryzae* infection. CRISPR/Cas9-mediated mutagenesis of *OsPBZ1* results in altered blast resistance, suggesting

a complex interplay between *OsPBZ1* functioning, Pi availability, and blast susceptibility. Further investigations are required to understand the precise molecular interactions and signaling pathways involving *OsPBZ1* in rice's defense.

5. FRET-live imaging sensors serve as valuable tools for real-time detection of Pi in live cell imaging, facilitating the study of cellular processes at the organ level. We demonstrated the utility of these sensors in rice plants, showcasing their effectiveness in monitoring phosphate changes induced by various stimuli such as alterations in phosphate supply or elicitor treatment.

Materials and Methods

Materials and methods

Plant and fungal material

Rice plants (*O. sativa* cv. Nipponbare and Tainung 67) were grown at 28 °C with a 14 h/10 h light/ dark cycle in soil consisting in a 1:1 (w/w) mixture of inert substrate (vermiculite 33% and 66% peat supplemented with 1 g/L CaCO3) and dorsolite (0.6 a 1.2 mm grain diameter). Plants were irrigated with water for one week and with half-strength Hoagland solution during two weeks (2.5 mM KNO_3, 2.5 mM $Ca(NO_3)_2 \cdot 4H_2O$, 1 mM $MgSO_4 \cdot 7H_2O$, 0.5 mM NH_4NO_3, 0.25 mM KH_2PO_4, 23.15 µM H_3BO_3, 4.55 µM $MnCl_2 \cdot 4H_2O$, 0.38 µM $ZnSO_4 \cdot 7H_2O$, 0.1 µM $CuSO_4 \cdot 5H_2O$, 0.14 µM $Na_2MoO_4 \cdot 2H_2O$, 50 µM Fe-EDDHA, pH 5.5).

M. oryzae (strain Guy 11) was grown in Complete Media Agar (CMA, 9 cm plates, containing 30 mg/L chloramphenicol) for 15 days at 28 °C under a 16 h/8 h light/dark photoperiod condition. *M. oryzae* spores were collected by adding sterile water to the surface of the mycelium and adjusted to the appropriate concentration (Campo *et al.,* 2013).

Infection assays

Soil-grown rice plants at the three to four-leaf stage were spray-inoculated with a suspension of *M. oryzae* spores ($5x10^5$ spores/ml sterile water containing 0.02% Tween; 2 ml/plant) using an aerograph at 2 atm of pressure. Infected plants, as well as mock-inoculated plants, were maintained overnight in the dark under high humidity (plastic bags) and allowed to continue growth under controlled conditions (plant growth chamber) at 28ºC, 80% relative humidity and a 12-hour day

length. The progress of disease symptoms was followed with time. After 5-7 days post-infection, when disease symptoms become apparent, rice leaves were photographed with a Nikon Z50 digital camera, and the percentage of diseased leaf area was determined by using the APS Assess 2.0 program (Lamari, 2008). Quantification of fungal DNA biomass was carried out by real-time PCR using specific primers for the *M. oryzae* 28S gene and normalized to the rice *Ubiquitin1* as an internal control **(Supplemental Table S1)** (Qi & Yang, 2002).

Pi treatment and measurement of Pi content

For Pi treatment, plants were grown for 1 week with water and then fertilized for two weeks with modified Hoagland half-strength solution containing the desired concentration of Pi: 0,025 mM for Low-Pi, 0,25 mM for Suff-Pi and 2,5 mM for High-Pi supply. The Pi content of rice leaves was determined as previously described (Ames, 1966; Versaw & Harrison, 2002). For each Pi condition, three technical replicates of three biological replicates (each replicate is a pool of three plants) were analyzed and statistically significant differences were determined by *t-test*.

Gene expression analysis by RT-qPCR

Total RNA was extracted using TRIzol reagent (Invitrogen). For quantitative RT-PCR (RT-qPCR), the first complementary DNA was synthesized from DNAse-treated total RNA (1 µg) with reverse transcriptase and oligo-dT (High-Capacity cDNA reverse transcription kit, Applied Biosystems). qPCR was performed in optical 384-well plates using SYBR® green in a Light Cycler 480 (Roche) using the following program: 10 min at 95°C, 45 cycles of 95°C for 10 s and 60°C for 30 s,

and an additional cycle of dissociation curves to ensure a unique amplification. Primers were designed using Primer-Blast (https://www.ncbi.nlm.nih.gov/tools/primerblast/) and are listed in **Supplemental Table S1**. Unless otherwise stated, three biological replicates each one from a pool of four different plants, and three technical replicates for each biological replicate were analyzed. The *Ubiquitin1* gene (Os06g0681400) was used to normalize transcript levels of *O. sativa* genes. For *M. oryzae* genes, the *actin* gene (MGG_03982) was used to normalize the transcript level in each sample. The average cycle threshold (Ct) obtained were normalized to the average Ct values for the control gene from the same RNA preparations, yielding the ΔCt value or normalized expression (relative expression). The 2–ΔΔCt method was used to analyze relative changes in gene expression. Statistically significant differences were determined by *t-test*.

Agroinfiltration and transient expression in *N. benthamiana* leaves

Agroinfiltration and transient expression assays were carried out in *N. benthamiana* leaves to examine the subcellular localization of fluorescently-tagged PBZ1 proteins. For this, the pGWB5-PBZ1 and pGWB6-PBZ1 plasmids were generated. The nucleotide sequence of *OsPBZ1* (LOC_Os12g36880.1) was obtained from the Rice Genome Annotation Project (RGAP) database. The *OsPBZ1* exon sequences were amplified using the forward MR_OsPBZ1_F and reverse MR_OsPBZ1_ws-R / MR_OsPBZ1_R primers from gDNA. The full-length *OsPBZ1* cDNA sequence lacking stop codon was obtained by overlapping PCR. The PCR product was cloned into pENTR™/D-TOPO™ (Invitrogen). The resulting entry clones were used to obtain the expression vectors designed for the production of C-terminal and N-

terminal GFP-tagged fusion proteins in *N. benthamiana* leaves (the pGWB5 and pGWB6 plasmids, respectively). Expression of GFP fusion genes was driven by the 35S Cauliflower mosaic virus (35SCaMV) promoter contained in pGWB56 plasmid with the Gateway system (Karimi *et al*., 2002). Constructs containing the quimeric genes were used to transform *A. tumefaciens* EAH105 strain and then used in transient expression assays. The *A. tumefaciens* strain GV3101 carrying the pAN589-mCherry-AtPIP2 plasmid was kindly provided by Javier Quintero (Seville, Spain). Primers and plasmids used in this study are listed in **Supplemental Table S2**.

For transient expression assays, the transformed *A. tumefaciens* strain carrying the construct of interest was grown for 24h at 28ºC, centrifugated at 4000 rpm for 15 min, Bacterial cells were resuspended in Induction buffer (10mM $MgSO_4$, 10mM MES, pH 5.6, 0,15mM Acetosyringone) and incubated for 2 hours. *Agrobacterium* cultures (approximately 5 mL) of bacterial cultures (optical density at 600nm of 0.5) were applied with a syringe to the underside of three leaves of 3-week-old *N. benthamiana* plants. To boost transgene expression, the potent silencing suppressor HcPro from the *Plum pox virus* (PPV) was co-expressed along with the GFP fusion gene under study. Samples of leaf patches infiltrated with *Agrobacterium* were collected at 3 days after infiltration for western blot analysis.

Experiments for co-expression of the fluorescently labelled *PBZ1-GFP* with organelle markers fused to the Red Fluorescent protein (RFP) were also carried out. Leaves of *N. benthamiana* were co-infiltrated with mixed *Agrobacterium* cultures, listed in **Supplemental Table S3**.

Confocal laser scanning microscopy (CLSM) of agroinfiltrated leaves was carried out on a Leica SP5-X microscope (Leica Microsystems), with an 40x oil/immersion objective, using excitation Argon laser 20%

power. The excitation wavelength was 488 nm for GFP and 561 nm for RFP. The emission window was set at 500 to 549 nm for GFP and 570 to 670 for RFP.

CRISPR/Cas9 design and rice transformation

The vector used for CRISPR/Cas9-mediated mutagenesis of *OsPBZ1* was based on the pH-Ubi-cas9-7 and pOs-sgRNA plasmids described by Miao *et al.* (2013) in which Cas9 expression is driven by the maize *Ubiquitin3* promoter (*Ubi3*). The pH-Ubicas9-7 vector contains the hygromycin resistance gene (*hptII*, *hygromycin phosphotransferase II*) as the selectable marker for rice transformation. The pOs-sgRNA plasmid was used to introduce the single guide RNA (sgRNA). Computational prediction of the sgRNA site, target site sequences and prediction of potential off-target sites were performed using the CRISPRP software (http://cbi.hzau.edu.cn/crispr/) (Lei *et al*., 2014). To generate the CRISPR*OsPBZ1* construct, the sgRNA sequence for the *OsPBZ1* coding sequence was PCR amplified using the following primers: Fw: 5'- GGCAAAGCACATACAAGACCCGGG-3' and Rv: 5'- AAACCCCGGGTCTTGTATGTGCTT-3' and cloned into the *BsaI* and *BsmBI* restriction sites of the entry vector (pOs-sgRNA). The DNA fragment containing the sgRNA, and the *maize U3 promoter* was cloned into the *attR1* and *attR2* recombinant sites of the pH-Ubi-cas9-7 plasmid containing the *Cas9* gene. For identification of mutant transgenic lines, genomic DNA was extracted from hygromycin-resistant T0 plants which was then used for PCR analysis using primers designed to amplify the DNA fragment across the target site in the *OsPBZ1* sequence (Fw: 5'- ACAAGCAGCTCTAGCTAGCTAC-3' and Rv: 5'- TCACGGACTCAAACGCCAC-3'). The transgenic lines were also examined by PCR using Cas9-specific primers (Fw: 5'-

GAGACAGCCGAGGCTACAA-3'; Rv: 5'-ATGGTCGGGTACTTCTCGTC-3') and hygromycin-specific primers (Fw: 5'-GCCGATGGTTTCTACAAAGA-3'; Rv: 5'-GAAGAAGATGTTGGCGACCT-3'). All the PCR products were subjected to DNA sequencing.

Transgenic rice (*Oryza sativa* cv. Nipponbare) plants were produced by *Agrobacterium*-mediated transformation of embryogenic calli derived from mature embryos. For rice transformation, the constructs were introduced into *Agrobacterium tumefaciens* strain *EHA105*. PCR analysis using primers designed to specifically amplify *Cas9* and *hptII* sequences confirmed the integration of the CRISPR/Cas9 system in the genome of the regenerated rice lines. To confirm the specificity and efficiency of DNA cutting, the targeted region was PCR amplified from genomic DNA and sequenced. Similarly, primer sets were used to amplify predicted off-target sites in the rice genome.

The progeny of T0 mutant plants was genotyped by PCR and DNA sequencing for the identification of heterozygous and homozygous lines (T1 to T3 generations).

Preparation of total protein extracts and immunoblotting

For preparation of total protein extracts, the third leaves of three-weeks old rice plants (a pool of three plants) were grinded to a fine powder under liquid nitrogen and stored at -80°C until use. The powder was thawed and homogenized in denaturation/loading buffer (125 mM Tris-HCl, pH 7.5, 2% SDS, 6 M urea, 4% glycerol, 1mM DTT). Samples were homogenized for 30 min at 4ºC and centrifuged to separate cell debris. Protein concentration of total extracts was determined by Bradford's method (Bradford, 1976). Total protein extracts were subjected to SDS-PAGE (12% acrylamide), and electroblotted to

nitrocellulose membranes. Ponceau red staining was used to verify equivalent loading of total proteins in each sample. Blots were probed with the primary antibody at 4ºC overnight. Antibodies (and dilutions) used in this work were: anti-PR1 (1:2000 dilution; Agrisera), anti-PR2 (1:2000 dilution; Agrisera), anti-PR10e (1:2000 dilution; Agrisera), anti-GFP (1:5000 dilution; Proteintech Group, Inc.). Blots were then incubated with the secondary antibody, horse rabbit peroxidase (HRP)-labelled donkey anti-Rabbit IgG (H+L) (Thermo Fisher Scientific) at a dilution of 1:20000 for 1 hour at room temperature. Serological reactions were visualized by using the Clarity ECL Western Blotting substrate for enhanced chemiluminescence detection (Bio-Rad) on an Amersham ImageQuant™ 800 CCD imaging system.

Isolation of apoplastic proteins

Apoplastic fluid extraction from rice leaves was carried out using the extraction buffer (CA buffer: 200 mM CaCl2, 5 mM Na-acetate, pH 4.3 adjusted with glacial acetic acid, containing 0.1 mM TPCK and 0.1 mM PMSF) and vacuum-infiltration and centrifugation (CA-VIC) extraction method (Kim *et al*., 2013). Briefly, 1 g of leaf pieces of aprox. 5 cm were placed in a 50 mL Falcon tube containing 30 mL of CA buffer and kept on ice under constant agitation for 1 hour. Then, vacuum was applied for 30 minutes and leaves were removed and carefully dried. Dried leaves were rolled and placed in a tube for apoplast washing fluid (AWF) recovery. Leaves were centrifuged a 3000 rpm, 15 minutes at 4ºC. The apoplastic fluid was recovered from the bottom of the tube and kept in -20 until use.

The malate dehydrogenase (MDH) activity assay was used to assess that the apoplastic fluid was devoid of cytoplasmic contaminants. For each material, the MDH activity value in the apoplast samples was

compared with that of total protein extracts. For this, total protein extracts were prepared from rice leaves using MOPS as the extraction buffer (1 mM MOPS, pH 7.5, 5 mM NaCl, containing the protease inhibitors TPCK and PMSF, 0.1 mM each). Protein concentration of total and apoplastic fluid extracts was determined by Bradford's method (Bradford 1976). For MDH assay, protein samples (10 µl of either total protein or apoplastic fluid extracts, at 0.1 µg/µl) were added to the reaction mixture (0.4 mM β-Nicotinamide adenine dinucleotide, 0.2 mM oxaloacetic acid, 1mM MOPS, pH 7.5) in 96 micro titer plates. The absorbance at 340nm at 25ºC was recorded during 10 minutes. MDH activity was calculated as U/µg: (Δabsorbance/time) / (molar extinction coefficient x path length x 1 µmol x µg).

To calculate the dilution of apoplast during AWF extraction, parallel AWF extractions were performed with and without 50 µM indigo carmine in the infiltration fluid. Ratios of absorbance at A_{610} were used to calculate the apoplast dilution factor as described previously (O'Leary *et al*., 2014).

Apoplastic proteins were separated by 12,5% SDS–PAGE and visualized by silver staining following the procedure described by Merril 1983 with minor modifications. Gels were fixed for 1 hour with 40% ethanol and 10% acetic acid and then washed with mq$H_2$0. Sensitizing was performed with 0.02% sodium thiosulfate for 2 minutes. After washing, the staining solution (0.1% silver nitrate solution + 0.02% formaldehyde) was applied for 40 min at 4ºC. Finally, the gel was washed again and revealed with 3% sodium carbonate + 0.05% formaldehyde. Gels were kept at 4 ºC in 1% acetic for storage.

Proteomic analysis of apoplastic proteins

Liquid chromatography-tandem mass spectrometry (LC-MS/MS) analyses were carried out at the Barcelona Science Park (PCB) proteomics platform from Barcelona University (UB). The protein samples were adjusted to pH 7.0 (by adding 100 mM NH_4HCO_3, pH 8), reduced with dithiothreitol (DTT) (20mM DTT in 50 mM NH_4HCO_3, pH 8 ;30 min, 60ºC), and alkylated (iodoacetamide 55mM in 50mM NH_4HCO_3, pH 8; 25ºC, 30 min, in the dark). Trypsin digestion of protein samples (sequence grade modified Trypsin, Promega) was carried out for 2 h at 37ºC. A new aliquot of enzyme was added, and the digestion was allowed to continue overnight at 37ºC. The resulting peptide mixtures were cleaned up with a C18 tip (PolyLC Inc.) following the manufacturer´s instructions. Finally, the cleaned-up peptide solutions were dried-down and stored at -20ºC until the LC-MS analyses.

For LC-MS/MS, the dried-down peptide mixtures were analyzed in a nanoAcquity liquid chromatographer (Waters) coupled to a LTQ-Orbitrap Velos (Thermo Scientific) mass spectrometer. The tryptic digests were resuspended in 1% formic acid solution and an aliquot per sample was injected for chromatographic separation. Peptides were trapped on a Symmetry C18TM trap column (5µm 180µm x 20mm; Waters) and separated using a C18 reverse phase capillary column (ACQUITY UPLC BEH column; 130Å, 1.7µm, 75 µm x250 mm, Waters). The gradient used for the elution of the peptides was 1 to 35 % B in 175 minutes, followed by a gradient from 40% to 60% in 10 min. (A: 0.1% formic acid B: 100% acetonitrile, 0.1%FA; flow rate: 250 nL/min). Column temperature: 40ºC.

Eluted peptides were subjected to electrospray ionization in a stainless steel emitter (Thermo Fisher Scientific) with an applied voltage of 2000V. Peptide masses (m/z 300-1600) were analyzed in data

dependent mode where a full Scan MS was acquired in the Orbitrap with a resolution of 60,000 FWHM at 400m/z. Up to the 15th most abundant peptides (minimum intensity of 500 counts) were selected from each MS scan and then fragmented in the linear ion trap using collision-induced dissociation (38% normalized collision energy) with helium as the collision gas. Ions selected for MS/MS fragmentation were dynamically excluded for 30s. The scan time settings were: Full MS: 250 ms (1 microscan) and MSn: 120 ms. Generated .raw data files were collected with Thermo Xcalibur (v.2.2).

For data analysis, a Database search and protein ID database was created by merging all entries for *O. sativa* with all entries for *M. oryzae* contained in the public database Uniprot (v.21/9/21). A small database containing laboratory contaminants was also added. The data files obtained in the mass spectrometry analyses were used to perform database search with Sequest HT search engine using Thermo Proteome Discoverer (v.1.4.1.14) against the database described above. For this, the following search parameters were applied:

Database/Taxonomy:
uniprot_Osativa_tax_4530_Moryzae_tax_318829_210921_cont.fasta;
Enzyme: Trypsin (semi); Missed cleavage: 2; Fixed modifications: Carbamidomethyl of cysteine; Variable modifications: Oxidation of methionine, deamidation of asparagine, deamidation of glutamine; Peptide tolerance: 10 ppm and 0.6 Da (respectively for MS and MS/MS spectra); Percolator:Target FDR (Strict): 0.01. Target FDR (Relaxed): 0.05. Validation based on q-Value.

To improve the sensitivity of the database search, Percolator (semi-supervised learning machine) was used to discriminate correct from incorrect peptide spectrum matches. Percolator assigns a q-value to each spectrum, which is defined as the minimal FDR at which the

identification is deemed correct. These q-values are estimated using the distribution of scores from the decoy database search.

The search results obtained with the Sequest HT search were visualized in Proteome Discoverer (v.1.4.1.14) and exported to Excel as lists of identified proteins. The results have been filtered so only proteins identified with at least 2 peptides (FDR ≤ 5%) are included in the lists.

Preparation of proteins for phosphoproteome analysis

Proteins were extracted from rice leaves (500 mg of fresh weight) that had been inoculated with a *M.oryzae* spore suspension, or mock inoculated, following the whole-plant infection method (10^5 spores/ml, 0.2 ml/plant, at 40- hpi). Rice plants were grown under Low-P or High-Pi conditions as described above. Protein extraction was carried out under non-denaturing conditions using 50mM Tris-HCl, pH 7,5 containing 150 mM NaCl as the extraction buffer. After homogenization in a rotor in cool chamber, samples were treated with 0.1% Protamine Sulfate (w/v, in deionized water) for 30 min to enrich the low-abundance proteins (e.g. RUBISCO depletion). After homogenization, samples were centrifugated at 12,000×g for 5 min at 4 °C to separate supernatant and pellet. Supernatant proteins were precipitated in cold 12.5% (v/v) trichloroacetic acid-acetone solution containing 0.05% DTT. The homogenate was stored at -20ºC overnight and proteins were recovered by centrifugation at 10 000xg for 15 min. The pellet was washed twice with cold acetone. Then, pellets were resuspended in 50mM Tris-HCl, pH 7,5 containing150 mM NaCl and kept at -20ºC until analysis.

Phosphopeptide enrichment and LC/MS/MS analysis

Protein samples (180 µg, each sample) were reduced with DTT (20 mM DTT in 50 mM ammonium bicarbonate pH 8, for 60min at 56ºC. Samples were then alkylated with iodoacetamide (55mM of Iodoacetamide in 50 mM ammonium bicarbonate buffer pH 8) and incubated in the dark for 30 min at room temperature. Digestion was done in two steps: an initial digestion with 1:30 (w/w) trypsin 0.2 µg/µL (Sequence grade modified trypsin, Promega) for 16h at 37ºC followed by a digestion with 1:30 (w/w) trypsin (0.2 µg/µL) for 2h at 37ºC. The resulting peptide mixtures were extracted from the gel matrix with 5% formic acid in 50% acetonitrile, and 100 % acetonitrile, and concentrated in a SpeedVac vacuum system (Eppendorf). Peptides were cleaned up with C18 tips (P200 top tip, PolyLC Inc.). Briefly, peptides were loaded in the tip columns (previously washed with 70% acetonitrile in 0.1 % formic acid and equilibrated with 0.1% formic acid by centrifugation (350 g for 2 min). Columns were washed twice with 100 µL 0.1% formic acid by centrifugation (350 g for 2 min). Peptides were eluted in 2 x 80 µL of 70% acetonitrile / 0.1% formic acid by centrifugation (350 g for 2 min and 900 g for 1 min).

Phosphopeptide enrichment was carried out with TiO2 following the manufacturer's instructions (ThermoScientific High SelectTM TiO2 Phosphopeptide Enrichment Kit). Briefly, samples were resuspended in 150 µL of binding buffer and loaded onto the spin columns previously equilibrated by centrifugation at 1000g for 5 min. After binding and washing steps, phosphopeptides were eluted with phosphopeptide elution buffer. All samples were dried-down in Speed Vacuum (Eppendorf) and stored at -20ºC until LC-MS analysis.

LC-MS/MS analysis was performed at the Institut for Research in Biomedicine (IRB), Mass Spectrometry and Proteomics Core Facility. The dried-down peptides were analyzed in a Thermo Scientific Dionex

Ultimate 3000 coupled to a Orbitrap Fusion Lumos™ Tribrid (Thermo Scientific) mass spectrometer. Enriched phophopeptides samples were resuspended in 1% formic acid solution and subjected to chromatography. Peptides were trapped on a μ-precolumn 300 μm (i.d. × 5 mm PepMap100, 5 μm, 100 Å, C18; ThermoScientific) and separated using a NanoEase MZ HSS T3 column (75 μm × 250 mm, 1.8 μm, 100 Å) (Waters). The gradient used for peptide elution was 3 to 35 % B (60 minutes), followed by gradient from 35% to 50% in 5 min (A: 0.1% formic acid; B: 100% acetonitrile, 0.1% formic acid), with a 250 nL/min flow rate, at 40ºC. Eluted peptides were subjected to electrospray ionization in an Advion Triversa Nanomate (Advion BioSciences, Ithaca, NY, USA) nESI through chip technology with an applied voltage of 1700V. Peptide masses were analyzed in data dependent mode using collision energy of 28% for the HCD fragmentations. For that, a full Scan MS was carried out in the Orbitrap with a resolution of 120k for MS1 and 30Kfor MS2, (375-1500 m/z range).

Generated raw data files were collected with Thermo Xcalibur (v.4.2). All Raw data were processed with Thermo Proteome Discoverer software (v_2.5). The spectra were searched using SequestHT search engine, against the Uniprot_OSativa_MOryzae_221220.fasta database (v_221220) including contaminants. The following parameters were used: i) fixed modifications: carbamidomethylation of cysteins (C); ii) variable modifications: Serine, threonine and tyrosine (STY) phosphorylation, methionine (M) oxidation, asparagine and glutamine (NQ) deamidation and protein N-terminus acetylation; and iii) enzyme: trypsin; maximum allowed missed cleavage. Other non-specified parameters were left as default. For label-free quantification (LFQ) (Cox *et al*., 2014), the minimum ratio count was set to 1 and both razor and unique peptides were used for quantitation. False discovery rate (FDR)

was set to 1% for both protein and peptide spectrum match (PSMs) levels.

Data processing of label-free quantitavie data was carried out using Thermo Proteome Discoverer software (v. 2.5). To test for significant varying proteins within the study groups, one-way ANOVA was applied to the curated proteins dataset (p-value) and corrected for multiple-testing by FDR method (q-value, Benjamini & Hochberg, 1995). Tukey's Honest Significant Difference (HSD) test (Tukey, 1949) was applied to discriminate for those significant comparisons over the three study groups.

Production of transgenic rice lines expressing a Pi sensor (FLIPPi lines) and life imaging of Pi levels

FRET (Föster Resonance Energy Transfer)-based Pi biosensors have been successfully used to monitor cytoplasmic Pi dynamics in Arabidopsis (known as FLIPPi sensors). In this work, transgenic rice lines expressing the cpFLIPPI 5.3m sensor or the cpFLIPPI-null constructs were generated and used for life imaging of Pi levels. Plasmids for of the FLIPPi sensors in Arabidopsis were kindly provided by Dr. W. K. Versaw (Texas A & M University, USA) (Mukerjee *et al*., 2015). They consist of a cyanobacterial Pi binding protein (PiBP) fused to enhanced cyan fluorescent protein (eCFP) and a circularly permuted (cp) form of the fluorescent protein Venus (cpVenus). In the cpFLIPPi-5.3m sensor plasmid (CFP::PiBP::cpVenus) the expression of the Pi sensor is driven by the Arabidopsis *Ubiquitin10* (UBQ10) promoter (designed for live imaging of Pi in *Arabidopsis*) (Mukherjee *et al*., 2015). To replace the Arabidopsis *UBQ10* promoter, a modified pCAMBIA1300 plasmid carrying *OsUBI* promoter (cloned into the *BamHI* and *SmaI* sites of pCAMBIA1300, plasmid pSONI) was digested with *BamHI* and *SmaI*.

FLIPPi sensor was amplified from cpFLIPPi-5.3m and cpFLIPPi-null sensor plasmids using BV_Ubi10p_fw and BV_tNOS_Rv primers located upstream the *BamHI* and *SmaI* restriction sites **(Supplemental Table 1)**. Purified PCR products were digested with *BamHI* and *SmaI* and purified using a GeneJET Gel Extraction Kit (ThermoFisher Scientific). Ligation of purified PCR products and BamHI/SmaI-digested pCAMBIA1300 vector was performed using T4 DNA polymerase.

Transgenic rice (cv Tainung 67) lines harbouring the *pC1300::ubi1::cpFLIPPi::nos* or the *pC1300::ubi1::cpFLIPPi-null::nos* construct were produced by *Agrobacterium*-mediated transformation of embryogenic calli derived from mature embryos (Sallaud *et al.,* 2003). The parent pCAMBIA 1300 vector already contained the *hptII* (*hygromycinphosphotransferase*) gene encoding hygromycin resistance in the T-DNA region. Transgene expression was confirmed by RT-qPCR analysis of primary T0 transformants. The stability of transgene expression was monitored in the selected transgenic lines at the T1 and T2 generations.

For FRET response analysis, the rice plants were grown *in vitro* at 28 ºC with a 14 h/10 h light/ dark cycle on modified half-strength Hoagland medium containing the desired concentration of Pi (0,025 mM, 0,25 mM and 2,5 mM KH_2PO_4), for 7 – 10 days. For cpFLIPPi-sensors imaging, rice roots were cut and imaged with Super-resolution Confocal Microscope ZEISS LSM 980 (Carl Zeiss Microscopy), with a 25× water immersion objective, using excitation laser at 445-nm. The emission settings were recorder for CFP (481-/34-nm), cpVenus (543-/23-nm), and transmission (bright field). Azygous seedlings were used to establish background fluorescence values and to adjust laser intensity and exposure settings, that were kept constant. All image analyses were done using Zeiss Zen 3.7 software. FRET ratio was

calculated as eCFP/cpVenus intensities as previously described (Mukerjee *et al.,* 2015).

To assess the effect of treatment with either *Fusarium fujikuroi (teleomorph Gibberella fujikuroi)* elicitors or chitin, the rice plants were grown *in vitro* in half-strength Hoagland medium containing one or another elicitor. *F. fujikuroi* elicitors were prepared as described by Casacuberta *et al.* (1992) and used at a final concentration of 300 µg/ml. Chitin (Sigma C7170) solution was used in a final concentration of 0,1 mg/mL. Treatment with elicitors was carried out for 3 hours.

Supplemental material

Supplemental Table S1. Oligonucleotides used in this study.

Oligo name	Sequence	Gene name	Gene ID
PiBP_qPCR_F	GACTACCCAATCGTGGGCTT	*PiBP*	--
PiBP_qPCR_R	GTGATGGCTTGACCCTCTGG		
MoBAS3-qPCR-F	TAACTTGGGAGCAGTGGCCTA	*MoBAS3*	MGG_11610
MoBAS3-qPCR-R	GCTCAAACTTCCAACCTCCCC		
MoBAS4-qPCR-F	CCGACTCGCACCAGAATCTT	*MoBAS4*	MGG_10914
MoBAS4-qPCR-R	CTGTTGTTGTCGGGGTAGGT		
MoPWL2-qPCR-F	GACAAAGGCGAAAGAGAGGG	*MoPWL2*	MGG_13863 MGG_04301
MoPWL2-qPCR-R	CCAGGATAACTGGGGCCATA		
MoBAS1-qPCR-F	GCCGACCAAGGTTCTAACACA	*MoBAS1*	MGG_04795
MoBAS1-qPCR-R	TGTTTTTCCTCACGAATCGGTC		
OsPR10b-qPCR-F	TCAGTATTGTGTTTTTGCTTCACG	*OsPR10b*	LOC_Os12g36850
OsPR10b-qPCR-R	ACACTGATCCACAATCTTCCAT		
3'-OsPBZ1-qPCR-F	GCGTTTGAGTCCGTGAGAGT	*OsPBZ1*	LOC_Os12g36880
3'-OsPBZ1-qPCR-R	GCAGAACACATTCAGACTTGCC		
5'_OsPBZ1-qPCR-F.2	ACGACATTGCGGTCGAGG		
5'_OsPBZ1-qPCR-R.2	TTCATGGTGTAGATGGTGCC		
RSOsPR10-qPCR-F	TGAGCCACGACAAATCCAATC	*ROsPR10*	LOC_Os12g36830
RSOsPR10-qPCR-R	AGCCTTTGTAGTGATCTCCCA		
OsPR10e-qPCR-F	ACCAACACAATCCATGGCTGA	*OsPR10e*	LOC_Os12g36860
OsPR10e-qPCR-R	AGCTAGGCACATACAACACAAT		
OsChib3a-qRT-R	TCTACGACGTGCAGAACAACTTCAG	*Class III Chitinase*	LOC_Os01g47070
OsChib3a-qRT-R	TCCAACTCAACCACTGTGCAAGTAA		
MB_OsMAPK5_qPCR_F	AGCTGATCTTCAACGAAGCGA	*OsMAPK5*	LOC_Os03g17700
MB_OsMAPK5_qPCR_R	GCAGGTATAGACGGGATCTCA		
OsPR1a_RT_F	CTGCAAGCTGGAGCACTCG	*OsPR1a*	LOC_Os07g03710
OsPR1a_RT_R	AAGATGTTCTCGCCGTACTTCC		
OsUbi1_F	TTCCCCAATGGAGCTATGGTT	*OsUbi*	LOC_Os06g46770
OsUbi1_R	AAACGGGACACGACCAAGG		
Cas9-F	GAGACAGCCGAGGCTACAA	*cas9*	--
Cas9-R	ATGGTCGGGTACTTCTCGTC		
Act_Magna_ F	TTCATGTTACTTTCGCGGCC	*MoAct*	MGG_03982
Act_Magna_ R	CTAGCGACTCCGGTAAAGCG		
MR_sgRNA_PBZ1_F	GGCAAAGCACATACAAGACCCGGG	*sgRNA-PBZ1*	
MR_sgRNA_PBZ1_R	AAACCCCGGGTCTTGTATGTGCTT		
Hygro_F	GCCGATGGTTTCTACAAAGA	*Hygromicine*	
Hygro_R	GAAGAAGATGTTGGCGACCT		
OsPR10a-F-gDNA	ACAAGCAGCTCTAGCTAGCTAC	*OsPBZ1*	LOC_Os12g36880
OsPR10a-R-gDNA	TCACGGACTCAAACGCCAC		
MR_OsPR10a_F_TOPO	caccATGgctccggcctgc		
MR_OsPR10a_F	ATGgctccggcctgc		
MR_OsPR10a_ws-R	GGCGTATTCGGCAGGGT		
MR_OsPR10a_R	TTAGGCGTATTCGGCAGGGT		
MR_OsPR10e_F	ACACCGCTGATTTTTTCGTAT	*OsPR10e*	LOC_Os12g36860
MR_OsPR10e_R	GGCGAATTCGGCAGGGTGA		
Mo28S-qPCR-F	TACGAGAGGAACCGCTCATTCAGATAATTA	*28S Ribosomal DNA*	--
Mo28S-qPCR-R	TCAGCAGATCGTAACGATAAAGCTACTC		
BV_Ubi10p_fw	TGGTGTTAGTTTCTAGTTTGTGCG	*FLIPPi*	---
BV_tNOS_Rv	TAATCATCGCAAGACCGGCA		

Supplemental Table S2. Plasmids used in this study.

Plasmid	Strain	Resistance
pGWB5	*A. tumefaciens* EHA105	Kanamycin, Hygromycin, Rifampicin
pGWB6	*A. tumefaciens* EHA105	Kanamycin, Hygromycin, Rifampicin
pGWB6::PBZ1	*A. tumefaciens* EHA105	Kanamycin, Hygromycin, Rifampicin
pGWB5::PBZ1	*A. tumefaciens* EHA105	Kanamycin, Hygromycin, Rifampicin
pGWB655 (Cyt:RFP)	*A. tumefaciens* EHA105	Spectinomycin, Hygromycin, Rifampicin
pAN589-mCherry-AtPIP2	*A. tumefaciens* EHA105	Kanamycin, Rifampicin
pH UbiCas9-7	*E. coli* Top10	Spectinomycin
pOsgRNA	*E. coli* Top10	Kanamycin
pH UbiCas9-7 + pOsgRNA + PBZ1 sgRNAs	*A. tumefaciens* EHA105	Spectinomycin, Hygromycin
pFLIPPi	*A. tumefaciens* EHA105	Kanamycin, Rifampicin
pFLIPPi_null	*A. tumefaciens* EHA105	Kanamycin, Rifampicin
pC1300::OsUbi	*E. coli* Top10	Kanamycin

Supplemental Table S3. Agroinfiltration mixtures used in this study.

Agroinfiltration mixture	Silencing suppresor	Plasmid	Coexpressor plasmid
GFP	HcPro	pGWB5	-
GFP		pGWB6	-
GFP:PBZ1		pGWB6::PBZ1	-
PBZ1:GFP		pGWB5::PBZ1	-
PBZ1:GFP / Cyt:RFP		pGWB5::PBZ1	pGWB655
PBZ1:GFP / AtPIP2-mCherry		pGWB5::PBZ1	pAN589-mCherry-AtPIP2

Annex I. Pi-responsive proteins in apoplast rice leaves identified by LC-MS/MS proteomic analysis.
https://docs.google.com/spreadsheets/d/1gkyLoyOlUPfA1ckZLWsT_YwYEl8ZqCD9/edit?usp=drive_link&ouid=109681529839304639484&rtpof=true&sd=true

Annex II. Whole list of rice phosphoproteins regulated by Pi treatment and *M.oryzae* infection in rice leaves.
https://docs.google.com/spreadsheets/d/1s6MjDJ4KxXkpyVOZjpjFM7IhwjptXJdX/edit?usp=drive_link&ouid=109681529839304639484&rtpof=true&sd=true

Annex III. Rice phosphoproteins regulated by Pi treatment in rice leaves.
https://docs.google.com/spreadsheets/d/1bTiEfzhk9eL_Sb5l9WKVLg_ux0CGkeeu/edit?usp=drive_link&ouid=109681529839304639484&rtpof=true&sd=true

Annex IV. Rice phosphoproteins regulated by *M. oryzae* infection in Low-Pi rice plants.
https://docs.google.com/spreadsheets/d/1XQmG5ashf7yoMBxvgRBrFND-Nsur9Acu/edit?usp=drive_link&ouid=109681529839304639484&rtpof=true&sd=true

Annex V. Rice phosphoproteins regulated by *M. oryzae* infection in High-Pi rice plants.
https://docs.google.com/spreadsheets/d/1h7usla4tlFq-bt0mxlmc4SMwwR1hRR-0/edit?usp=drive_link&ouid=109681529839304639484&rtpof=true&sd=true

References

Aerts N, Pereira Mendes M, Van Wees SCM. 2021. Multiple levels of crosstalk in hormone networks regulating plant defense. Plant J 105(2):489-504.

Agarwal P and Agarwal PK. 2014. Pathogenesis related-10 proteins are small, structurally similar but with diverse role in stress signaling. Mol Biol Rep 41(2):599-611.

Agrawal GK, Rakwal R, Jwa N, Agrawal VP. 2001. Signalling molecules and blast pathogen attack activates rice OsPR1a and OsPR1b genes: A model illustrating components participating during defence/stress response. Plant Physiology and Biochemistry 39(12):1095-103.

Agrawal GK, Jwa N, Lebrun M, Job D, Rakwal R. 2010. Plant secretome: Unlocking secrets of the secreted proteins. Proteomics 10(4):799-827.

Ahluwalia O, Singh PC, Bhatia R. 2021. A review on drought stress in plants: Implications, mitigation and the role of plant growth promoting rhizobacteria. Resources, Environment and Sustainability 5:100032.

Alexander D, Goodman RM, Gut-Rella M, Glascock C, Weymann K, Friedrich L, Maddox D, Ahl-Goy P, Luntz T, Ward E. 1993. Increased tolerance to two oomycete pathogens in transgenic tobacco expressing pathogenesis-related protein 1a. Proc Natl Acad Sci U S A 90(15):7327-31.

Alexandersson E, Danielson JÅ, Råde J, Moparthi VK, Fontes M, Kjellbom P, Johanson U. 2010. Transcriptional regulation of aquaporins in accessions of arabidopsis in response to drought stress. The Plant Journal 61(4):650-60.

Ali S, Ganai BA, Kamili AN, Bhat AA, Mir ZA, Bhat JA, Tyagi A, Islam ST, Mushtaq M, Yadav P, et al. 2018. Pathogenesis-related proteins and peptides as promising tools for engineering plants with multiple stress tolerance. Microbiol Res 212-213:29-37.

Almagro L, Gómez Ros LV, Belchi-Navarro S, Bru R, Ros Barceló A, Pedreño MA. 2009. Class III peroxidases in plant defence reactions. J Exp Bot 60(2):377-90.

Ames BN. 1966. [10] Assay of inorganic phosphate, total phosphate and phosphatases. In: Methods in enzymology. Elsevier. 115 p.

Antoniw JF, Ritter CE, Pierpoint WS, Van Loon LCY1. 1980. Comparison of three pathogenesis-related proteins from plants of two cultivars of tobacco infected with TMV. Journal of General Virology, 47(1):79-87.

Arouna A, Lokossou JC, Wopereis MCS, Bruce-Oliver S, Roy-Macauley H. 2017. Contribution of improved rice varieties to poverty reduction and food security in sub-saharan africa. Global Food Security 14:54-60.

Assunção AGL, Gjetting SK, Hansen M, Fuglsang AT, Schulz A. 2020. Live imaging of phosphate levels in *Arabidopsis* root cells expressing a FRET-based phosphate sensor. Plants (Basel) 9(10):1310.

Atwell BJ, Wang H, Scafaro AP. 2014. Could abiotic stress tolerance in wild relatives of rice be used to improve oryza sativa? Plant Science 215:48-58.

Aung K, Lin S, Wu C, Huang Y, Su C, Chiou T. 2006. Pho2, a phosphate overaccumulator, is caused by a nonsense mutation in a microRNA399 target gene. Plant Physiol 141(3):1000-11.

Bakare OO, Gokul A, Keyster M. 2021. PR1-like protein as a potential target for the identification of fusarium oxysporum: An in silico approach. BioTech 10(2).

Ballini E, Nguyen TT, Morel J. 2013. Diversity and genetics of nitrogen-induced susceptibility to the blast fungus in rice and wheat. Rice (N Y) 6(1):32-.

Banerjee S, Garcia LR, Versaw WK. 2016. Quantitative imaging of FRET-based biosensors for cell- and organelle-specific analyses in plants. Microsc Microanal 22(2):300-10.

Beattie GA. 2011. Water relations in the interaction of foliar bacterial pathogens with plants. Annu Rev Phytopathol 49:533-55.

Beckers GJM, Jaskiewicz M, Liu Y, Underwood WR, He SY, Zhang S, Conrath U. 2009. Mitogen-activated protein kinases 3 and 6 are required for full priming of stress responses in arabidopsis thaliana. Plant Cell 21(3):944-53.

Benjamini Y and Hochberg Y. 1995. Controlling the false discovery rate: A practical and powerful approach to multiple testing. Journal of the Royal Statistical Society: Series B (Methodological) 57(1):289-300.

Bhadouria J and Giri J. 2022. Purple acid phosphatases: Roles in phosphate utilization and new emerging functions. Plant Cell Rep 41(1):33-51.

Bhadouria J, Mehra P, Verma L, Pazhamala LT, Rumi R, Panchal P, Sinha AK, Giri J. 2023. Root-expressed rice PAP3b enhances secreted APase

activity and helps utilize organic phosphate. Plant Cell Physiol 64(5):501-18.

Bharath P, Gahir S, Raghavendra AS. 2021. Abscisic acid-induced stomatal closure: An important component of plant defense against abiotic and biotic stress. Front Plant Sci 12:615114.

Blom N, Sicheritz-Pontén T, Gupta R, Gammeltoft S, Brunak S. 2004. Prediction of post-translational glycosylation and phosphorylation of proteins from the amino acid sequence. Proteomics 4(6):1633-49.

Bradford MM. 1976. A rapid and sensitive method for the quantitation of microgram quantities of protein utilizing the principle of protein-dye binding. Anal Biochem 72:248-54.

Brar DS and Singh K. 2011. Oryza. In: Wild crop relatives: Genomic and breeding resources: Cereals. Kole C, editor. Berlin, Heidelberg: Springer Berlin Heidelberg. 321 p.

Brodersen P, Sakvarelidze-Achard L, Bruun-Rasmussen M, Dunoyer P, Yamamoto YY, Sieburth L, Voinnet O. 2008. Widespread translational inhibition by plant miRNAs and siRNAs. Science 320(5880):1185-90.

Broglie R and Broglie K. 1993. Chitinase gene expression in transgenic plants: A molecular approach to understanding plant defence responses. Philosophical Transactions: Biological Sciences 342(1301):265-70.

Buchel AS LH. 1999. In: PR1: A group of plant proteins induced upon pathogen infection. in: Pathogenesis-related proteins in plants. CRC Press;21.

Bucher M and Fabiańska I. 2016. Long-sought vacuolar phosphate transporters identified. Trends Plant Sci 21(6):463-6.

Campo S, Peris-Peris C, Siré C, Moreno AB, Donaire L, Zytnicki M, Notredame C, Llave C, San Segundo B. 2013. Identification of a novel microRNA (miRNA) from rice that targets an alternatively spliced transcript of the Nramp6 (natural resistance-associated macrophage protein 6) gene involved in pathogen resistance. New Phytol 199(1):212-27.

Campos-Soriano L, Bundó M, Bach-Pages M, Chiang S, Chiou T, San Segundo B. 2020. Phosphate excess increases susceptibility to pathogen infection in rice. Mol Plant Pathol 21(4):555-70.

Cao J, Yang C, Li L, Jiang L, Wu Y, Wu C, Bu Q, Xia G, Liu X, Luo Y, et al. 2016. Rice plasma membrane proteomics reveals magnaporthe oryzae promotes susceptibility by sequential activation of host hormone signaling pathways. Mol Plant Microbe Interact 29(11):902-13.

Cao W, Yu Y, Li M, Luo J, Wang R, Tang H, Huang J, Wang J, Zhang H, Bao Y. 2019. OsSYP121 accumulates at fungal penetration sites and mediates host resistance to rice blast. Plant Physiol 179(4):1330-42.

Casacuberta JM, Raventós D, Puigdoménech P, San Segundo B. 1992. Expression of the gene encoding the PRlike protein PRms in germinating maize embryos. Mol Gen Genet 234(1):97-104.

Castrillo G, Teixeira PJPL, Paredes SH, Law TF, de Lorenzo L, Feltcher ME, Finkel OM, Breakfield NW, Mieczkowski P, Jones CD, et al. 2017. Root microbiota drive direct integration of phosphate stress and immunity. Nature 543(7646):513-8.

Cejudo FJ, Sandalio LM, Van Breusegem F. 2021. Understanding plant responses to stress conditions: Redox-based strategies. J Exp Bot 72(16):5785-8.

Chan C, Liao Y, Chiou T. 2021. The impact of phosphorus on plant immunity. Plant Cell Physiol 62(4):582-9.

Chaudhuri B, Hörmann F, Frommer WB. 2011. Dynamic imaging of glucose flux impedance using FRET sensors in wild-type arabidopsis plants. J Exp Bot 62(7):2411-7.

Chaudhuri B, Hörmann F, Lalonde S, Brady SM, Orlando DA, Benfey P, Frommer WB. 2008. Protonophore- and pH-insensitive glucose and sucrose accumulation detected by FRET nanosensors in arabidopsis root tips. Plant J 56(6):948-62.

Chen E, Huang X, Tian Z, Wing RA, Han B. 2019. The genomics of oryza species provides insights into rice domestication and heterosis. Annu Rev Plant Biol 70:639-65.

Chen J, Wang L, Yuan M. 2021. Update on the roles of rice MAPK cascades. International Journal of Molecular Sciences 22(4).

Chen Z, Truong TM, Ai H. 2017. Illuminating brain activities with fluorescent protein-based biosensors. Chemosensors 5(4).

Chien P, Chiang C, Leong SJ, Chiou T. 2018. Sensing and signaling of phosphate starvation: From local to long distance. Plant Cell Physiol 59(9):1714-22.

Chiou T and Lin S. 2011. Signaling network in sensing phosphate availability in plants. Annu Rev Plant Biol 62:185-206.

Chiou T, Aung K, Lin S, Wu C, Chiang S, Su C. 2006. Regulation of phosphate homeostasis by MicroRNA in arabidopsis. Plant Cell 18(2):412-21.

Choi JY, Platts AE, Fuller DQ, Hsing Y, Wing RA, Purugganan MD. 2017. The rice paradox: Multiple origins but single domestication in asian rice. Mol Biol Evol 34(4):969-79.

Civáň P and Brown TA. 2017. Origin of rice (oryza sativa L.) domestication genes. Genet Resour Crop Evol 64(6):1125-32.

Cordell D, Rosemarin A, Schroder JJ, Smit AL. 2011. Towards global phosphorus security: A systems framework for phosphorus recovery and reuse options. Chemosphere 84(6):747-58.

Couch BC, Fudal I, Lebrun M, Tharreau D, Valent B, van Kim P, Nottéghem J, Kohn LM. 2005. Origins of host-specific populations of the blast pathogen magnaporthe oryzae in crop domestication with subsequent expansion of pandemic clones on rice and weeds of rice. Genetics 170(2):613-30.

Cox J, Hein MY, Luber CA, Paron I, Nagaraj N, Mann M. 2014. Accurate proteome-wide label-free quantification by delayed normalization and maximal peptide ratio extraction, termed MaxLFQ. Mol Cell Proteomics 13(9):2513-26.

Custers JHHV, Harrison SJ, Sela-Buurlage MB, van Deventer E, Lageweg W, Howe PW, van der Meijs PJ, Ponstein AS, Simons BH, Melchers LS, et al. 2004. Isolation and characterisation of a class of carbohydrate oxidases from higher plants, with a role in active defence. Plant J 39(2):147-60.

Dalio RJD, Paschoal D, Arena GD, Magalhães DM, Oliveira TS, Merfa MV, Maximo HJ, Machado MA. 2021. Hypersensitive response: From NLR pathogen recognition to cell death response. Ann Appl Biol 178(2):268-80.

Darino M, Kanyuka K, Hammond-Kosack KE. 2022. Apoplastic and vascular defences. Essays Biochem 66(5):595-605.

Dean R, Van Kan JAL, Pretorius ZA, Hammond-Kosack KE, Di Pietro A, Spanu PD, Rudd JJ, Dickman M, Kahmann R, Ellis J, et al. 2012. The top 10 fungal pathogens in molecular plant pathology. Mol Plant Pathol 13(4):414-30.

Dean RA, Talbot NJ, Ebbole DJ, Farman ML, Mitchell TK, Orbach MJ, Thon M, Kulkarni R, Xu J, Pan H, et al. 2005. The genome sequence of the rice blast fungus magnaporthe grisea. Nature 434(7036):980-6.

Delaunois B, Jeandet P, Clément C, Baillieul F, Dorey S, Cordelier S. 2014. Uncovering plant-pathogen crosstalk through apoplastic proteomic studies. Front Plant Sci 5:249.

Derksen H, Rampitsch C, Daayf F. 2013. Signaling cross-talk in plant disease resistance. Plant Science 207:79-87.

Deslandes L and Rivas S. 2012. Catch me if you can: Bacterial effectors and plant targets. Trends Plant Sci 17(11):644-55.

Deuschle K, Chaudhuri B, Okumoto S, Lager I, Lalonde S, Frommer WB. 2006. Rapid metabolism of glucose detected with FRET glucose nanosensors in epidermal cells and intact roots of arabidopsis RNA-silencing mutants. Plant Cell 18(9):2314-25.

Devanna BN, Jain P, Solanke AU, Das A, Thakur S, Singh PK, Kumari M, Dubey H, Jaswal R, Pawar D, et al. 2022. Understanding the dynamics of blast resistance in rice-magnaporthe oryzae interactions. Journal of Fungi 8(6).

Ding L, Li Y, Wu Y, Li T, Geng R, Cao J, Zhang W, Tan X. 2022. Plant disease resistance-related signaling pathways: Recent progress and future prospects. Int J Mol Sci 23(24):16200.

Dixon MH, Cowles KN, Zaacks SC, Marciniak IN, Barak JD. 2022. Xanthomonas infection transforms the apoplast into an accessible and habitable niche for salmonella enterica. Appl Environ Microbiol 88(22):e0133022,22. Epub 2022 Oct 31.

Dong Z, Li W, Liu J, Li L, Pan S, Liu S, Gao J, Liu L, Liu X, Wang G, et al. 2019. The rice phosphate transporter protein OsPT8 regulates disease resistance and plant growth. Sci Rep 9(1):5408-9.

Dos Santos C and Franco OL. 2023. Pathogenesis-related proteins (PRs) with enzyme activity activating plant defense responses. Plants (Basel) 12(11):2226.

Du Z, Arias T, Meng W, Chye M. 2016. Plant acyl-CoA-binding proteins: An emerging family involved in plant development and stress responses. Prog Lipid Res 63:165-81.

Ekanayake G, Gohmann R, Mackey D. 2022. A method for quantitation of apoplast hydration in arabidopsis leaves reveals water-soaking activity of effectors of pseudomonas syringae during biotrophy. Sci Rep 12(1):18363-x.

El Kasmi F, Horvath D, Lahaye T. 2018. Microbial effectors and the role of water and sugar in the infection battle ground. Curr Opin Plant Biol 44:98-107.

Epple P, Apel K, Bohlmann H. 1995. An arabidopsis thaliana thionin gene is inducible via a signal transduction pathway different from that for pathogenesis-related proteins. Plant Physiol 109(3):813-20.

Erickson J, Weckwerth P, Romeis T, Lee J. 2022. What's new in protein kinase/phosphatase signalling in the control of plant immunity? Essays Biochem 66(5):621-34.

Estudillo JP, Kijima Y, Sonobe T. 2023. Introduction: Agricultural development in asia and africa. In: Agricultural development in asia and africa: Essays in honor of keijiro otsuka. Estudillo JP, Kijima Y,Sonobe T, editors. Singapore: Springer Nature Singapore. 1 p.

Fakhar A, Gul B, Rafique M, Ortas I. 2022. Use of biostimulants to increase heavy metal tolerance in cereals. In: Sustainable remedies for abiotic stress in cereals. Abdel Latef AAH, editor. Singapore: Springer Nature Singapore. 575 p.

Fernandes H, Michalska K, Sikorski M, Jaskolski M. 2013. Structural and functional aspects of PR10 proteins. Febs J 280(5):1169-99.

Fernandez J and Orth K. 2018. Rise of a cereal killer: The biology of magnaporthe oryzae biotrophic growth. Trends Microbiol 26(7):582-97.

Fiyaz RA, Krishnan SG, Rajashekara H, Yadav AK, Bashyal BM, Bhowmick PK, Singh NK, Prabhu KV, Singh AK. 2014. Development of high throughput screening protocol and identification of novel sources of resistance against bakanae disease in rice (oryza sativa L.). Indian J Genet Plant Breed 74(04):414-22.

Freeman BC and Beattie GA. 2009. Bacterial growth restriction during host resistance to pseudomonas syringae is associated with leaf water loss and localized cessation of vascular activity in arabidopsis thaliana. Mol Plant-Microbe Interact 22(7):857-67.

Friso G and van Wijk KJ. 2015. Posttranslational protein modifications in plant metabolism. Plant Physiol 169(3):1469-87.

Fu J, Liu H, Li Y, Yu H, Li X, Xiao J, Wang S. 2010. Manipulating broad-spectrum disease resistance by suppressing pathogen-induced auxin accumulation in rice. Plant Physiol 155(1):589-602.

Fujii H, Chiou T, Lin S, Aung K, Zhu J. 2005. A miRNA involved in phosphate-starvation response in arabidopsis. Curr Biol 15(22):2038-43.

Fukamizo T. 2000. Chitinolytic enzymes: Catalysis, substrate binding, and their application. Curr Protein Pept Sci 1(1):105-24.

Gamir J, Darwiche R, Van't Hof P, Choudhary V, Stumpe M, Schneiter R, Mauch F. 2017. The sterol-binding activity of PATHOGENESIS-RELATED PROTEIN 1 reveals the mode of action of an antimicrobial protein. Plant J 89(3):502-9.

Gao J, Agrawal GK, Thelen JJ, Xu D. 2009. P3DB: A plant protein phosphorylation database. Nucleic Acids Res 37(Database issue):960.

Garcia N, Kalicharan RE, Kinch L, Fernandez J. 2023. Regulating death and disease: Exploring the roles of metacaspases in plants and fungi. International Journal of Molecular Sciences 24(1).

García-Olmedo F, Molina A, Segura A, Moreno M. 1995. The defensive role of nonspecific lipid-transfer proteins in plants. Trends Microbiol 3(2):72-4.

Garris AJ, Tai TH, Coburn J, Kresovich S, McCouch S. 2005. Genetic structure and diversity in oryza sativa L. Genetics 169(3):1631-8.

Gaupels F, Durner J, Kogel K. 2017. Production, amplification and systemic propagation of redox messengers in plants? the phloem can do it all! New Phytol 214(2):554-60.

Gentzel I, Giese L, Ekanayake G, Mikhail K, Zhao W, Cocuron J, Alonso AP, Mackey D. 2022. Dynamic nutrient acquisition from a hydrated apoplast supports biotrophic proliferation of a bacterial pathogen of maize. Cell Host Microbe 30(4):502,517.e4.

Gho Y, Choi H, Moon S, Song MY, Park HE, Kim D, Ha S, Jung K. 2020. Phosphate-starvation-inducible S-like RNase genes in rice are involved in phosphate source recycling by RNA decay. Front Plant Sci 11:585561.

Gilroy S, Białasek M, Suzuki N, Górecka M, Devireddy AR, Karpiński S, Mittler R. 2016. ROS, calcium, and electric signals: Key mediators of rapid systemic signaling in plants. Plant Physiol 171(3):1606-15.

Giraldo MC and Valent B. 2013. Filamentous plant pathogen effectors in action. Nat Rev Microbiol 11(11):800-14.

Gjetting SK, Ytting CK, Schulz A, Fuglsang AT. 2012. Live imaging of intra- and extracellular pH in plants using pHusion, a novel genetically encoded biosensor. J Exp Bot 63(8):3207-18.

Goff SA, Ricke D, Lan T, Presting G, Wang R, Dunn M, Glazebrook J, Sessions A, Oeller P, Varma H, et al. 2002. A draft sequence of the rice genome (oryza sativa L. ssp. japonica). Science 296(5565):92-100.

Gorshkov V and Tsers I. 2022. Plant susceptible responses: The underestimated side of plant-pathogen interactions. Biol Rev Camb Philos Soc 97(1):45-66.

Green TR and Ryan CA. 1972. Wound-induced proteinase inhibitor in plant leaves: A possible defense mechanism against insects. Science 175(4023):776-7.

Gu H, Lalonde S, Okumoto S, Looger LL, Scharff-Poulsen AM, Grossman AR, Kossmann J, Jakobsen I, Frommer WB. 2006. A novel analytical method for in vivo phosphate tracking. FEBS Lett 580(25):5885-93.

Gu P, Tao W, Tao J, Sun H, Hu R, Wang D, Zong G, Xie X, Ruan W, Xu G, et al. 2023. The D14-SDEL1-SPX4 cascade integrates the strigolactone and phosphate signalling networks in rice. New Phytol 239(2):673-86.

Guo J and Cheng Y. 2022. Advances in fungal elicitor-triggered plant immunity. Int J Mol Sci 23(19):12003.

Guo R, Zhang Q, Qian K, Ying Y, Liao W, Gan L, Mao C, Wang Y, Whelan J, Shou H. 2023. Phosphate-dependent regulation of vacuolar trafficking of OsSPX-MFSs is critical for maintaining intracellular phosphate homeostasis in rice. Mol Plant 16(8):1304-20.

Guo X, Zhong D, Xie W, He Y, Zheng Y, Lin Y, Chen Z, Han Y, Tian D, Liu W, et al. 2019. Functional identification of novel cell death-inducing effector proteins from magnaporthe oryzae. Rice 12(1):59.

Gupta R, Lee SE, Agrawal GK, Rakwal R, Park S, Wang Y, Kim ST. 2015. Understanding the plant-pathogen interactions in the context of proteomics-generated apoplastic proteins inventory. Front Plant Sci 6:352.

Ham B, Chen J, Yan Y, Lucas WJ. 2018. Insights into plant phosphate sensing and signaling. Curr Opin Biotechnol 49:1-9.

Hanafy MS, El-Banna A, Schumacher HM, Jacobsen H, Hassan FS. 2013. Enhanced tolerance to drought and salt stresses in transgenic faba bean (vicia faba L.) plants by heterologous expression of the PR10a gene from potato. Plant Cell Rep 32(5):663-74.

Hashimoto M, Kisseleva L, Sawa S, Furukawa T, Komatsu S, Koshiba T. 2004. A novel rice PR10 protein, RSOsPR10, specifically induced in roots by biotic and abiotic stresses, possibly via the jasmonic acid signaling pathway. Plant and Cell Physiology 45(5):550-9.

He S, Jiang J, Chen B, Kuo C, Ho S. 2018. Overexpression of a constitutively active truncated form of OsCDPK1 confers disease resistance by affecting OsPR10a expression in rice. Sci Rep 8(1):403-2.

Helliwell EE, Wang Q, Yang Y. 2016. Ethylene biosynthesis and signaling is required for rice immune response and basal resistance against magnaporthe oryzae infection. Mol Plant-Microbe Interact 29(11):831-43.

Hinsinger P, Betencourt E, Bernard L, Brauman A, Plassard C, Shen J, Tang X, Zhang F. 2011. P for two, sharing a scarce resource: Soil phosphorus

acquisition in the rhizosphere of intercropped species. Plant Physiol 156(3):1078-86.

Hönig M, Roeber VM, Schmülling T, Cortleven A. 2023. Chemical priming of plant defense responses to pathogen attacks. Front Plant Sci 14:1146577.

Hsieh L, Lin S, Shih AC, Chen J, Lin W, Tseng C, Li W, Chiou T. 2009. Uncovering small RNA-mediated responses to phosphate deficiency in arabidopsis by deep sequencing. Plant Physiol 151(4):2120-32.

Hu X, Wang C, Fu Y, Liu Q, Jiao X, Wang K. 2016. Expanding the range of CRISPR/Cas9 genome editing in rice. Mol Plant 9(6):943-5.

Huang H, Nguyen Thi Thu T, He X, Gravot A, Bernillon S, Ballini E, Morel J. 2017. Increase of fungal pathogenicity and role of plant glutamine in nitrogen-induced susceptibility (NIS) to rice blast. Front Plant Sci 8:265.

Huang L, Lin K, He S, Chen J, Jiang J, Chen B, Hou Y, Chen R, Hong C, Ho S. 2016. Multiple patterns of regulation and overexpression of a ribonuclease-like pathogenesis-related protein gene, OsPR10a, conferring disease resistance in rice and arabidopsis. PLoS One 11(6):e0156414.

Huang X and Han B. 2015. Rice domestication occurred through single origin and multiple introgressions. Nat Plants 2:15207.

Iqbal M, Javed N, Sahi S, Cheema N. 2011. Genetic management of bakanae disease of rice and evaluation of various fungicides against fusarium moniliforme in vitro. 23:103-7.

Iwai T, Seo S, Mitsuhara I, Ohashi Y. 2007. Probenazole-induced accumulation of salicylic acid confers resistance to magnaporthe grisea in adult rice plants. Plant Cell Physiol 48(7):915-24.

Jach G, Görnhardt B, Mundy J, Logemann J, Pinsdorf E, Leah R, Schell J, Maas C. 1995. Enhanced quantitative resistance against fungal disease by combinatorial expression of different barley antifungal proteins in transgenic tobacco. Plant J 8(1):97-109.

Jacquemin J, Bhatia D, Singh K, Wing RA. 2013. The international oryza map alignment project: Development of a genus-wide comparative genomics platform to help solve the 9 billion-people question. Curr Opin Plant Biol 16(2):147-56.

Jagodzik P, Tajdel-Zielinska M, Ciesla A, Marczak M, Ludwikow A. 2018. Mitogen-activated protein kinase cascades in plant hormone signaling. Front Plant Sci 9:1387.

Jalmi SK and Sinha AK. 2015. ROS mediated MAPK signaling in abiotic and biotic stress- striking similarities and differences. Front Plant Sci 6:769.

Jiang C, Liu X, Liu X, Zhang H, Yu Y, Liang Z. 2017. Stunted growth caused by blast disease in rice seedlings is associated with changes in phytohormone signaling pathways. Frontiers in Plant Science 8:1558.

Jiang C, Shimono M, Sugano S, Kojima M, Liu X, Inoue H, Sakakibara H, Takatsuji H. 2013. Cytokinins act synergistically with salicylic acid to activate defense gene expression in rice. Mol Plant Microbe Interact 26(3):287-96.

Jiang L, Chen Y, Luo L, Peck SC. 2018. Central roles and regulatory mechanisms of dual-specificity MAPK phosphatases in developmental and stress signaling. Front Plant Sci 9:1697.

Jones JDG and Dangl JL. 2006. The plant immune system. Nature 444(7117):323-9.

Jwa N and Hwang BK. 2017. Convergent evolution of pathogen effectors toward reactive oxygen species signaling networks in plants. Front Plant Sci 8:1687.

Kadota Y, Shirasu K, Zipfel C. 2015. Regulation of the NADPH oxidase RBOHD during plant immunity. Plant Cell Physiol 56(8):1472-80.

Kankanala P, Czymmek K, Valent B. 2007. Roles for rice membrane dynamics and plasmodesmata during biotrophic invasion by the blast fungus. Plant Cell 19(2):706-24.

Karimi M, Inzé D, Depicker A. 2002. GATEWAY vectors for agrobacterium-mediated plant transformation. Trends Plant Sci 7(5):193-5.

Katz E, Fon M, Eigenheer RA, Phinney BS, Fass JN, Lin D, Sadka A, Blumwald E. 2010. A label-free differential quantitative mass spectrometry method for the characterization and identification of protein changes during citrus fruit development. Proteome Sci 8:68-.

Kaur A, Kaur S, Kaur A, Navraj KS, Sharma D. 2022. Pathogenesis-related proteins and their transgenic expression for developing disease-resistant crops: Strategies progress and challenges. In: Breeding strategies and cases for several major plants. Haiping Wang, editor. Rijeka: IntechOpen.

Kaur G and Pati PK. 2016. Analysis of cis-acting regulatory elements of respiratory burst oxidase homolog (rboh) gene families in arabidopsis and rice provides clues for their diverse functions. Computational Biology and Chemistry 62:104-18.

Kerbler SM and Wigge PA. 2023. Temperature sensing in plants. Annu Rev Plant Biol 74:341-66.

Khan A, Numan M, Khan AL, Lee I, Imran M, Asaf S, Al-Harrasi A. 2020. Melatonin: Awakening the defense mechanisms during plant oxidative stress. Plants 9(4).

Khang CH, Berruyer R, Giraldo MC, Kankanala P, Park S, Czymmek K, Kang S, Valent B. 2010. Translocation of magnaporthe oryzae effectors into rice cells and their subsequent cell-to-cell movement. Plant Cell 22(4):1388-403.

Kieu NP, Aznar A, Segond D, Rigault M, Simond-Côte E, Kunz C, Soulie M, Expert D, Dellagi A. 2012. Iron deficiency affects plant defence responses and confers resistance to dickeya dadantii and botrytis cinerea. Mol Plant Pathol 13(8):816-27.

Kim JY, Wu J, Kwon SJ, Oh H, Lee SE, Kim SG, Wang Y, Agrawal GK, Rakwal R, Kang KY, et al. 2014. Proteomics of rice and cochliobolus miyabeanus fungal interaction: Insight into proteins at intracellular and extracellular spaces. Proteomics 14(20):2307-18.

Kim SG, Kim ST, Wang Y, Yu S, Choi I, Kim YC, Kim WT, Agrawal GK, Rakwal R, Kang KY. 2011. The RNase activity of rice probenazole-induced protein1 (PBZ1) plays a key role in cell death in plants. Mol Cells 31:25-31.

Kim SG, Wang Y, Lee KH, Park Z, Park J, Wu J, Kwon SJ, Lee Y, Agrawal GK, Rakwal R, et al. 2013. In-depth insight into in vivo apoplastic secretome of rice-magnaporthe oryzae interaction. J Proteomics 78:58-71.

Kim ST, Cho KS, Yu S, Kim SG, Hong JC, Han C, Bae DW, Nam MH, Kang KY. 2003. Proteomic analysis of differentially expressed proteins induced by rice blast fungus and elicitor in suspension-cultured rice cells. Proteomics 3(12):2368-78.

Kim ST, Kang YH, Wang Y, Wu J, Park ZY, Rakwal R, Agrawal GK, Lee SY, Kang KY. 2009. Secretome analysis of differentially induced proteins in rice suspension-cultured cells triggered by rice blast fungus and elicitor. Proteomics 9(5):1302-13.

Kim ST, Kim SG, Kang YH, Wang Y, Kim J, Yi N, Kim J, Rakwal R, Koh H, Kang KY. 2008. Proteomics analysis of rice lesion mimic mutant (spl1) reveals tightly localized probenazole-induced protein (PBZ1) in cells undergoing programmed cell death. J Proteome Res 7(4):1750-60.

Kim YJ, Lee HM, Wang Y, Wu J, Kim SG, Kang KY, Park KH, Kim YC, Choi IS, Agrawal GK, et al. 2013. Depletion of abundant plant RuBisCO protein using the protamine sulfate precipitation method. Proteomics 13(14):2176-9.

Konishi H, Ishiguro K, Komatsu S. 2001. A proteomics approach towards understanding blast fungus infection of rice grown under different levels of nitrogen fertilization. Proteomics 1(9):1162-71.

Kou Y, Qiu J, Tao Z. 2019. Every coin has two sides: Reactive oxygen species during Rice⁻Magnaporthe oryzae interaction. Int J Mol Sci 20(5):1191.

Lagrimini LM, Burkhart W, Moyer M, Rothstein S. 1987. Molecular cloning of complementary DNA encoding the lignin-forming peroxidase from tobacco: Molecular analysis and tissue-specific expression. Proc Natl Acad Sci U S A 84(21):7542-6.

Lalonde S, Ehrhardt DW, Frommer WB. 2005. Shining light on signaling and metabolic networks by genetically encoded biosensors. Curr Opin Plant Biol 8(6):574-81.

Lamari L. 2008. Assess 2.0: Image analysis software for plant disease quantification.[computer program]. St. Paul, MN, USA. APS Press: .

Lee GH, Min CW, Jang JW, Wang Y, Jeon J, Gupta R, Kim ST. 2023. Analysis of post-translational modification dynamics unveiled novel insights into rice responses to MSP1. Journal of Proteomics 287:104970.

Lee S, Völz R, Lim Y, Harris W, Kim S, Lee Y. 2023. The nuclear effector MoHTR3 of magnaporthe oryzae modulates host defence signalling in the biotrophic stage of rice infection. Mol Plant Pathol 24(6):602-15.

Lei Y, Lu L, Liu H, Li S, Xing F, Chen L. 2014. CRISPRP: A web tool for synthetic single-guide RNA design of CRISPRsystem in plants. Mol Plant 7(9):1494-6.

Lenman M, Sörensson C, Andreasson E. 2008. Enrichment of phosphoproteins and phosphopeptide derivatization identify universal stress proteins in elicitor-treated arabidopsis. Mol Plant Microbe Interact 21(10):1275-84.

Li J, Wang J, Zeigler RS. 2014. The 3,000 rice genomes project: New opportunities and challenges for future rice research. Gigascience 3:8,8. eCollection 2014.

Li P and Liu J. 2021. Protein phosphorylation in plant cell signaling. In: Plant phosphoproteomics: Methods and protocols. Wu XN, editor. New York, NY: Springer US. 45 p.

Lin S, Chen L, Tao H, Huang J, Xu C, Li L, Ma S, Tian T, Liu W, Xue L, et al. 2016. Impact of SNPs on protein phosphorylation status in rice (oryza sativa L.). Int J Mol Sci 17(11):1738.

Lin S, Santi C, Jobet E, Lacut E, El Kholti N, Karlowski WM, Verdeil J, Breitler JC, Périn C, Ko S, et al. 2010. Complex regulation of two target genes encoding SPX-MFS proteins by rice miR827 in response to phosphate starvation. Plant Cell Physiol 51(12):2119-31.

Lin W, Lin Y, Chiang S, Syu C, Hsieh L, Chiou T. 2018. Evolution of microRNA827 targeting in the plant kingdom. New Phytol 217(4):1712-25.

Lin Y, Xu M, Hsu C, Damei FA, Lee H, Tsai W, Hoang CV, Chiang Y, Ma L. 2023. Ustilago maydis PR1-like protein has evolved two distinct domains for dual virulence activities. Nature Communications 14(1):5755.

Linthorst HJM and Van Loon LC. 1991. Pathogenesis-related proteins of plants. Crit Rev Plant Sci 10(2):123-50.

Liu N, Qi L, Huang M, Chen D, Yin C, Zhang Y, Wang X, Yuan G, Wang R, Yang J, et al. 2022. Comparative secretome analysis of magnaporthe oryzae identified proteins involved in virulence and cell wall integrity. Genomics Proteomics Bioinformatics 20(4):728-46.

Liu T, Huang T, Tseng C, Lai Y, Lin S, Lin W, Chen J, Chiou T. 2012. PHO2-dependent degradation of PHO1 modulates phosphate homeostasis in arabidopsis. Plant Cell 24(5):2168-83.

Liu T, Huang T, Yang S, Hong Y, Huang S, Wang F, Chiang S, Tsai S, Lu W, Chiou T. 2016. Identification of plant vacuolar transporters mediating phosphate storage. Nat Commun 7:11095.

Liu X, Huang B, Lin J, Fei J, Chen Z, Pang Y, Sun X, Tang K. 2006. A novel pathogenesis-related protein (SsPR10) from solanum surattense with ribonucleolytic and antimicrobial activity is stress- and pathogen-inducible. J Plant Physiol 163(5):546-56.

Liu Z, Zhu Y, Shi H, Qiu J, Ding X, Kou Y. 2021. Recent progress in rice broad-spectrum disease resistance. Int J Mol Sci 22(21):11658.

Llave C, Xie Z, Kasschau KD, Carrington JC. 2002. Cleavage of scarecrow-like mRNA targets directed by a class of arabidopsis miRNA. Science 297(5589):2053-6.

Lo S, Fan M, Hsing Y, Chen L, Chen S, Wen I, Liu Y, Chen K, Jiang M, Lin M, et al. 2016. Genetic resources offer efficient tools for rice functional genomics research. Plant Cell Environ 39(5):998-1013.

Lopes NDS, Santos AS, de Novais DPS, Pirovani CP, Micheli F. 2023. Pathogenesis-related protein 10 in resistance to biotic stress: Progress in elucidating functions, regulation and modes of action. Front Plant Sci 14:1193873.

Lowder LG, Zhang D, Baltes NJ, Paul JW3, Tang X, Zheng X, Voytas DF, Hsieh T, Zhang Y, Qi Y. 2015. A CRISPR/Cas9 toolbox for multiplexed plant genome editing and transcriptional regulation. Plant Physiol 169(2):971-85.

Lu Y, Li M, Cheng K, Tan CM, Su L, Lin W, Shih H, Chiou T, Yang J. 2014. Transgenic plants that express the phytoplasma effector SAP11 show altered phosphate starvation and defense responses. Plant Physiol 164(3):1456-69.

Lynch J. 1995. Root architecture and plant productivity. Plant Physiol 109(1):7-13.

Malik K and Maqbool A. 2020. Transgenic crops for biofortification. Frontiers in Sustainable Food Systems 4.

Manna M, Rengasamy B, Sinha AK. 2023. Revisiting the role of MAPK signalling pathway in plants and its manipulation for crop improvement. Plant Cell Environ 46(8):2277-95.

Marcec MJ, Gilroy S, Poovaiah BW, Tanaka K. 2019. Mutual interplay of ca(2+) and ROS signaling in plant immune response. Plant Sci 283:343-54.

Matton DP and Brisson N. 1989. Cloning, expression, and sequence conservation of pathogenesis-related gene transcripts of potato. Mol Plant Microbe Interact 2(6):325-31.

Mauch F, Mauch-Mani B, Boller T. 1988. Antifungal hydrolases in pea tissue : II. inhibition of fungal growth by combinations of chitinase and beta-1,3-glucanase. Plant Physiol 88(3):936-42.

McBride JK, Cheng H, Maleki SJ, Hurlburt BK. 2019. Purification and characterization of pathogenesis related class 10 panallergens. Foods 8(12):609.

McGee JD, Hamer JE, Hodges TK. 2001. Characterization of a PR10 pathogenesis-related gene family induced in rice during infection with magnaporthe grisea. Mol Plant Microbe Interact 14(7):877-86.

McGoldrick S, O'Sullivan SM, Sheehan D. 2005. Glutathione transferase-like proteins encoded in genomes of yeasts and fungi: Insights into evolution of a multifunctional protein superfamily. FEMS Microbiol Lett 242(1):1-12.

Megeressa M, Siraj B, Zarina S, Ahmed A. 2020. Structural characterization and in vitro lipid binding studies of non-specific lipid transfer protein 1 (nsLTP1) from fennel (foeniculum vulgare) seeds. Scientific Reports 10(1):21243.

Melchers LS, Apotheker-de Groot M, van der Knaap JA, Ponstein AS, Sela-Buurlage MB, Bol JF, Cornelissen BJ, van den Elzen PJ, Linthorst HJ. 1994. A new class of tobacco chitinases homologous to bacterial exo-chitinases displays antifungal activity. Plant J 5(4):469-80.

Meng Q, Gupta R, Min CW, Kim J, Kramer K, Wang Y, Park S, Finkemeier I, Kim ST. 2019. A proteomic insight into the MSP1 and flg22 induced signaling in oryza sativa leaves. J Proteomics 196:120-30.

Mentlak TA, Kombrink A, Shinya T, Ryder LS, Otomo I, Saitoh H, Terauchi R, Nishizawa Y, Shibuya N, Thomma BPHJ, et al. 2012. Effector-mediated suppression of chitin-triggered immunity by magnaporthe oryzae is necessary for rice blast disease. Plant Cell 24(1):322-35.

Merril CR, Goldman D, Van Keuren ML. 1983. Silver staining methods for polyacrylamide gel electrophoresis. Methods Enzymol 96:230-9.

Métraux JP, Streit L, Staub T. 1988. A pathogenesis-related protein in cucumber is a chitinase. Physiol Mol Plant Pathol 33(1):1-9.

Miao J, Guo D, Zhang J, Huang Q, Qin G, Zhang X, Wan J, Gu H, Qu L. 2013. Targeted mutagenesis in rice using CRISPRcas system. Cell Res 23(10):1233-6.

Midoh N and Iwata M. 1996. Cloning and characterization of a probenazole-inducible gene for an intracellular pathogenesis-related protein in rice. Plant Cell Physiol 37(1):9-18.

Moselhy S, Asami T, Abualnaja K, Al-Malki A, Yamano H, Akiyama T, Wada R, Yamagishi T, Hikosaka M, Iwakawa J, et al. 2016. Spermidine, a polyamine, confers resistance to rice blast. Journal of Pesticide Science 41.

Mosquera G, Giraldo MC, Khang CH, Coughlan S, Valent B. 2009. Interaction transcriptome analysis identifies magnaporthe oryzae BAS1-4 as biotrophy-associated secreted proteins in rice blast disease. Plant Cell 21(4):1273-90.

Mukherjee P, Banerjee S, Wheeler A, Ratliff LA, Irigoyen S, Garcia LR, Lockless SW, Versaw WK. 2015. Live imaging of inorganic phosphate in plants with cellular and subcellular resolution. Plant Physiol 167(3):628-38.

Munkvold GP. 2017. Fusarium species and their associated mycotoxins. Methods Mol Biol 1542:51-106.

Nahar K, Kyndt T, Nzogela YB, Gheysen G. 2012. Abscisic acid interacts antagonistically with classical defense pathways in rice–migratory nematode interaction. New Phytol 196(3):901-13.

Naseem M, Kunz M, Dandekar T. 2017. Plant–pathogen maneuvering over apoplastic sugars. Trends Plant Sci 22(9):740-3.

Ning Y, Xie Q, Wang G. 2011. OsDIS1-mediated stress response pathway in rice. Plant Signaling & Behavior 6:1684-6.

Niño-Liu DO, Ronald PC, Bogdanove AJ. 2006. Xanthomonas oryzae pathovars: Model pathogens of a model crop. Mol Plant Pathol 7(5):303-24.

Nobori T and Tsuda K. 2019. The plant immune system in heterogeneous environments. Curr Opin Plant Biol 50:58-66.

Oda T, Hashimoto H, Kuwabara N, Akashi S, Hayashi K, Kojima C, Wong HL, Kawasaki T, Shimamoto K, Sato M, et al. 2010. Structure of the N-terminal regulatory domain of a plant NADPH oxidase and its functional implications*. J Biol Chem 285(2):1435-45.

Okumoto S, Jones A, Frommer WB. 2012. Quantitative imaging with fluorescent biosensors. Annu Rev Plant Biol 63:663-706.

Okushima Y, Koizumi N, Kusano T, Sano H. 2000. Secreted proteins of tobacco cultured BY2 cells: Identification of a new member of pathogenesis-related proteins. Plant Mol Biol 42(3):479-88.

O'Leary BM, Rico A, McCraw S, Fones HN, Preston GM. 2014. The infiltration-centrifugation technique for extraction of apoplastic fluid from plant leaves using phaseolus vulgaris as an example. J Vis Exp (94):52113.

Pandey N. 2018. Role of plant nutrients in plant growth and physiology. Plant Nutrients and Abiotic Stress Tolerance :51-93.

Park C, Chen S, Shirsekar G, Zhou B, Khang CH, Songkumarn P, Afzal AJ, Ning Y, Wang R, Bellizzi M, et al. 2012. The magnaporthe oryzae effector AvrPiz-t targets the RING E3 ubiquitin ligase APIP6 to suppress pathogen-associated molecular pattern-triggered immunity in rice. Plant Cell 24(11):4748-62.

Pastor-Fernández J, Sánchez-Bel P, Flors V, Cerezo M, Pastor V. 2023. Small signals lead to big changes: The potential of peptide-induced resistance in plants. Journal of Fungi 9(2).

Paul S, Datta SK, Datta K. 2015. miRNA regulation of nutrient homeostasis in plants. Front Plant Sci 6:232.

Paz-Ares J, Puga MI, Rojas-Triana M, Martinez-Hevia I, Diaz S, Poza-Carrión C, Miñambres M, Leyva A. 2022. Plant adaptation to low phosphorus availability: Core signaling, crosstalks, and applied implications. Mol Plant 15(1):104-24.

Peck SC. 2003. Early phosphorylation events in biotic stress. Curr Opin Plant Biol 6(4):334-8.

Pel MJC and Pieterse CMJ. 2013. Microbial recognition and evasion of host immunity. J Exp Bot 64(5):1237-48.

Pendin D, Greotti E, Lefkimmiatis K, Pozzan T. 2017. Exploring cells with targeted biosensors. J Gen Physiol 149(1):1-36.

Peris-Peris C, Serra-Cardona A, Sánchez-Sanuy F, Campo S, Ariño J, San Segundo B. 2017. Two NRAMP6 isoforms function as iron and manganese transporters and contribute to disease resistance in rice. Mol Plant Microbe Interact 30(5):385-98.

Puga MI, Rojas-Triana M, de Lorenzo L, Leyva A, Rubio V, Paz-Ares J. 2017. Novel signals in the regulation of pi starvation responses in plants: Facts and promises. Curr Opin Plant Biol 39:40-9.

Qi M and Yang Y. 2002. Quantification of magnaporthe grisea during infection of rice plants using real-time polymerase chain reaction and northern blot/phosphoimaging analyses. Phytopathology 92(8):870-6.

Rafiei V, Vélëz H, Tzelepis G. 2021. The role of glycoside hydrolases in phytopathogenic fungi and oomycetes virulence. International Journal of Molecular Sciences 22(17).

Raj T, Muthukumar A, Renganathan P, Kumar R, Suji H. 2019. Biological control of sheath blight of rice caused by rhizoctonia solani kuhn using marine associated bacillus subtilis.

Rakwal R, Agrawal GK, Yonekura M. 1999. Separation of proteins from stressed rice (oryza sativa L.) leaf tissues by two-dimensional polyacrylamide gel electrophoresis: Induction of pathogenesis-related and cellular protectant proteins by jasmonic acid, UV irradiation and copper chloride. Electrophoresis 20(17):3472-8.

Ram H, Soni P, Salvi P, Gandass N, Sharma A, Kaur A, Sharma TR. 2019. Insertional mutagenesis approaches and their use in rice for functional genomics. Plants (Basel) 8(9):310.

Ravelo-Ortega G, Pelagio-Flores R, López-Bucio J, Campos-García J, Reyes de la Cruz H, López-Bucio JS. 2022. Early sensing of phosphate deprivation triggers the formation of extra root cap cell layers via SOMBRERO through a process antagonized by auxin signaling. Plant Mol Biol 108(1-2):77-91.

Rhee SG, Woo HA, Kil IS, Bae SH. 2012. Peroxiredoxin functions as a peroxidase and a regulator and sensor of local peroxides. J Biol Chem 287(7):4403-10.

Sachdev S, Ansari SA, Ansari MI. 2023. ROS as signaling molecule under unfavorable conditions. In: Reactive oxygen species in plants: The right balance. Sachdev S, Ansari SA,Ansari MI, editors. Singapore: Springer Nature Singapore. 203 p.

Sahu A, Banerjee S, Raju AS, Chiou T, Garcia LR, Versaw WK. 2020. Spatial profiles of phosphate in roots indicate developmental control of uptake, recycling, and sequestration. Plant Physiol 184(4):2064-77.

Saijo Y and Loo EP. 2020. Plant immunity in signal integration between biotic and abiotic stress responses. New Phytol 225(1):87-104.

Saini LK, Bheri M, Pandey GK. 2023. Protein phosphatases and their targets: Comprehending the interactions in plant signaling pathways. Adv Protein Chem Struct Biol 134:307-70.

Sallaud C, Meynard D, van Boxtel J, Gay C, Bès M, Brizard JP, Larmande P, Ortega D, Raynal M, Portefaix M, et al. 2003. Highly efficient production and characterization of T-DNA plants for rice (*oryza sativa* L.) functional genomics. Theor Appl Genet 106(8):1396-408.

Sánchez-Sanuy F, Mateluna-Cuadra R, Tomita K, Okada K, Sacchi GA, Campo S, San Segundo B. 2022. Iron induces resistance against the rice blast fungus magnaporthe oryzae through potentiation of immune responses. Rice (N Y) 15(1):68-w.

Secco D, Wang C, Arpat BA, Wang Z, Poirier Y, Tyerman SD, Wu P, Shou H, Whelan J. 2012. The emerging importance of the SPX domain-containing proteins in phosphate homeostasis. New Phytol 193(4):842-51.

Selitrennikoff CP. 2001. Antifungal proteins. Appl Environ Microbiol 67(7):2883-94.

Shahzad A, Ullah S, Dar AA, Sardar MF, Mehmood T, Tufail MA, Shakoor A, Haris M. 2021. Nexus on climate change: Agriculture and possible solution to cope future climate change stresses. Environ Sci Pollut Res Int 28(12):14211-32.

Sharma JK, Sihmar M, Santal AR, Singh NP. 2019. Impact assessment of major abiotic stresses on the proteome profiling of some important crop plants: A current update. Biotechnol Genet Eng Rev 35(2):126-60.

Sharma M, Sudheer S, Usmani Z, Rani R, Gupta P. 2020. Deciphering the omics of plant-microbe interaction: Perspectives and new insights. Curr Genomics 21(5):343-62.

Shenton MR, Berberich T, Kamo M, Yamashita T, Taira H, Terauchi R. 2012. Use of intercellular washing fluid to investigate the secreted proteome of the rice-magnaporthe interaction. J Plant Res 125(2):311-6.

Shimizu T, Nakano T, Takamizawa D, Desaki Y, Ishii-Minami N, Nishizawa Y, Minami E, Okada K, Yamane H, Kaku H, et al. 2010. Two LysM receptor molecules, CEBiP and OsCERK1, cooperatively regulate chitin elicitor signaling in rice. Plant J 64(2):204-14.

Shukla D, Rinehart CA, Sahi SV. 2017. Comprehensive study of excess phosphate response reveals ethylene mediated signaling that negatively regulates plant growth and development. Scientific Reports 7(1):3074.

Simhadri CG and Kondaveeti HK. 2023. Automatic recognition of rice leaf diseases using transfer learning. Agronomy 13(4).

Singh P, Mazumdar P, Harikrishna JA, Babu S. 2019. Sheath blight of rice: A review and identification of priorities for future research. Planta 250(5):1387-407.

Singh R and Sunder S. 2012. Foot rot and bakanae of rice: An overview. Rev. Pl. Pathol.:565-604.

Singh S and Srivastava S. 2023. Recent advances in arsenic mitigation in rice through biotechnological approaches. Int J Phytoremediation 25(3):305-13.

Sinha RK, Verma SS, Rastogi A. 2020. Role of pathogen-related protein 10 (PR 10) under abiotic and biotic stresses in plants. *Phyton-International Journal of Experimental Botany* 89(2).

Somssich IE, Schmelzer E, Bollmann J, Hahlbrock K. 1986. Rapid activation by fungal elicitor of genes encoding "pathogenesis-related" proteins in cultured parsley cells. Proc Natl Acad Sci U S A 83(8):2427-30.

Sooriyaarachchi S, Jaber E, Covarrubias AS, Ubhayasekera W, Asiegbu FO, Mowbray SL. 2011. Expression and β-glucan binding properties of scots pine (pinus sylvestris L.) antimicrobial protein (sp-AMP). Plant Mol Biol 77(1-2):33-45.

Stein JC, Yu Y, Copetti D, Zwickl DJ, Zhang L, Zhang C, Chougule K, Gao D, Iwata A, Goicoechea JL, et al. 2018. Genomes of 13 domesticated and wild rice relatives highlight genetic conservation, turnover and innovation across the genus oryza. Nat Genet 50(2):285-96.

Suzuki N, Rivero RM, Shulaev V, Blumwald E, Mittler R. 2014. Abiotic and biotic stress combinations. New Phytol 203(1):32-43.

Tabata R and Sawa S. 2014. Maturation processes and structures of small secreted peptides in plants. Front Plant Sci 5:311.

Tadano T and Sakai H. 1991. Secretion of acid phosphatase by the roots of several crop species under phosphorus-deficient conditions. Soil Sci Plant Nutr 37(1):129-40.

Terras FR, Eggermont K, Kovaleva V, Raikhel NV, Osborn RW, Kester A, Rees SB, Torrekens S, Van Leuven F, Vanderleyden J. 1995. Small cysteine-rich antifungal proteins from radish: Their role in host defense. Plant Cell 7(5):573-88.

Trost B and Kusalik A. 2013. Computational phosphorylation site prediction in plants using random forests and organism-specific instance weights. Bioinformatics 29(6):686-94.

Torres MA. 2010. ROS in biotic interactions. Physiol Plantarum 138(4):414-29.

Tukey JW. 1949. Comparing individual means in the analysis of variance. Biometrics :99-114.

Val-Torregrosa B, Bundó M, San Segundo B. 2021. Crosstalk between nutrient signalling pathways and immune responses in rice. Agriculture 11(8).

Val-Torregrosa B, Bundó M, Martín-Cardoso H, Bach-Pages M, Chiou T, Flors V, Segundo BS. 2022. Phosphate-induced resistance to pathogen infection in arabidopsis. Plant J 110(2):452-69.

van Loon LC. 1982. Regulation of changes in proteins and enzymes associated with active defence against virus infection. In: Active defense mechanisms in plants. Wood RKS, editor. Boston, MA: Springer US. 247 p.

van Loon LC, Pierpoint WS, Boller TH, Conejero V. 1994. Recommendations for naming plant pathogenesis-related proteins. Plant Mol Biol Rep 12:245-64.

van Loon LC. 1985. Pathogenesis-related proteins. Plant Mol Biol 4(2):111-6.

Vera P and Conejero V. 1988. Pathogenesis-related proteins of tomato : P-69 as an alkaline endoproteinase. Plant Physiol 87(1):58-63.

Veresoglou SD, Barto EK, Menexes G, Rillig MC. 2013. Fertilization affects severity of disease caused by fungal plant pathogens. Plant Pathol 62(5):961-9.

Verma D, Bhagat PK, Sinha AK. 2021. A dual-specificity phosphatase, MAP kinase phosphatase 1, positively regulates blue light-mediated seedling development in arabidopsis. Planta 253(6):131-6.

Versaw WK and Garcia LR. 2017. Intracellular transport and compartmentation of phosphate in plants. Curr Opin Plant Biol 39:25-30.

Versaw WK and Harrison MJ. 2002. A chloroplast phosphate transporter, PHT2;1, influences allocation of phosphate within the plant and phosphate-starvation responses. Plant Cell 14(8):1751-66.

Vu LD, Gevaert K, De Smet I. 2018. Protein language: Post-translational modifications talking to each other. Trends Plant Sci 23(12):1068-80.

Wang C, Han G, Yang Z, Li Y, Wang B. 2022. Plant salinity sensors: Current understanding and future directions. Frontiers in Plant Science 13.

Wang C, Huang W, Ying Y, Li S, Secco D, Tyerman S, Whelan J, Shou H. 2012. Functional characterization of the rice SPX-MFS family reveals a key role of OsSPX-MFS1 in controlling phosphate homeostasis in leaves. New Phytol 196(1):139-48.

Wang J, Zhou L, Shi H, Chern M, Yu H, Yi H, He M, Yin J, Zhu X, Li Y, et al. 2018. A single transcription factor promotes both yield and immunity in rice. Science 361(6406):1026-8.

Wang L, Jin J, Li L, Qu S. 2020. Long non-coding RNAs responsive to blast fungus infection in rice. Rice (N Y) 13(1):77-w.

Wang N, Long T, Yao W, Xiong L, Zhang Q, Wu C. 2013. Mutant resources for the functional analysis of the rice genome. Mol Plant 6(3):596-604.

Wang Y, Wu J, Kim SG, Tsuda K, Gupta R, Park S, Kim ST, Kang KY. 2016. Magnaporthe oryzae-secreted protein MSP1 induces cell death and elicits defense responses in rice. Mol Plant Microbe Interact 29(4):299-312.

Wang Y, Li H, Chen S. 2010. Advances in quantitative proteomics. Frontiers in Biology 5(3):195-203.

Wang Z, Ruan W, Shi J, Zhang L, Xiang D, Yang C, Li C, Wu Z, Liu Y, Yu Y, et al. 2014. Rice SPX1 and SPX2 inhibit phosphate starvation responses through interacting with PHR2 in a phosphate-dependent manner. Proceedings of the National Academy of Sciences 111(41):14953-8.

Wei F, Droc G, Guiderdoni E, Hsing YC. 2013. International consortium of rice mutagenesis: Resources and beyond. Rice (N Y) 6(1):39-.

Wei L, Wang D, Gupta R, Kim ST, Wang Y. 2023. A proteomics insight into advancements in the rice-microbe interaction. Plants (Basel) 12(5):1079.

Wei Y, Zhang Z, Andersen CH, Schmelzer E, Gregersen PL, Collinge DB, Smedegaard-Petersen V, Thordal-Christensen H. 1998. An epidermis/papilla-specific oxalate oxidase-like protein in the defence response of barley attacked by the powdery mildew fungus. Plant Mol Biol 36(1):101-12.

Wild R, Gerasimaite R, Jung J, Truffault V, Pavlovic I, Schmidt A, Saiardi A, Jessen HJ, Poirier Y, Hothorn M, et al. 2016. Control of eukaryotic phosphate homeostasis by inositol polyphosphate sensor domains. Science 352(6288):986-90.

Wilson RA and Talbot NJ. 2009. Under pressure: Investigating the biology of plant infection by magnaporthe oryzae. Nat Rev Microbiol 7(3):185-95.

Woo HA, Yim SH, Shin DH, Kang D, Yu D, Rhee SG. 2010. Inactivation of peroxiredoxin I by phosphorylation allows localized H(2)O(2) accumulation for cell signaling. Cell 140(4):517-28.

Wright CA and Beattie GA. 2004. Pseudomonas syringae pv. tomato cells encounter inhibitory levels of water stress during the hypersensitive response of arabidopsis thaliana. Proceedings of the National Academy of Sciences 101(9):3269-74.

Wu J, Kim SG, Kang KY, Kim J, Park S, Gupta R, Kim YH, Wang Y, Kim ST. 2016. Overexpression of a pathogenesis-related protein 10 enhances biotic and abiotic stress tolerance in rice. Plant Pathol J 32(6):552-62.

Wu Y, Xiao N, Chen Y, Yu L, Pan C, Li Y, Zhang X, Huang N, Ji H, Dai Z, et al. 2019. Comprehensive evaluation of resistance effects of pyramiding lines with different broad-spectrum resistance genes against magnaporthe oryzae in rice (oryza sativa L.). Rice (N Y) 12(1):11-3.

Xie K, Chen J, Wang Q, Yang Y. 2014. Direct phosphorylation and activation of a mitogen-activated protein kinase by a calcium-dependent protein kinase in rice. Plant Cell 26(7):3077-89.

Xie Y, Chen Z, Brown RL, Bhatnagar D. 2010. Expression and functional characterization of two pathogenesis-related protein 10 genes from zea mays. J Plant Physiol 167(2):121-30.

Ya Ma L, Lu Y, Cheng J, Wan Q, Ge J, Wang Y, Li Y, Feng F, Li M, Yu X. 2023. Functional characterization of rice (oryza sativa) thioredoxins for detoxification and degradation of atrazine. Gene 877:147540.

Yamada K, Saijo Y, Nakagami H, Takano Y. 2016. Regulation of sugar transporter activity for antibacterial defense in arabidopsis. Science 354(6318):1427-30.

Yamamoto T, Yoshida Y, Nakajima K, Tominaga M, Gyohda A, Suzuki H, Okamoto T, Nishimura T, Yokotani N, Minami E, et al. 2018. Expression of RSOsPR10 in rice roots is antagonistically regulated by jasmonate/ethylene and salicylic acid via the activator OsERF87 and the repressor OsWRKY76, respectively. Plant Direct 2(3):e00049.

Yang F, Li W, Derbyshire M, Larsen MR, Rudd JJ, Palmisano G. 2015. Unraveling incompatibility between wheat and the fungal pathogen zymoseptoria tritici through apoplastic proteomics. BMC Genomics 16(1):362.

Yang H, Bogner M, Stierhof Y, Ludewig U. 2010. H+-independent glutamine transport in plant root tips. Plos One 5(1):e8917.

Yazawa K, Jiang C, Kojima M, Sakakibara H, Takatsuji H. 2012. Reduction of abscisic acid levels or inhibition of abscisic acid signaling in rice during the early phase of magnaporthe oryzae infection decreases its susceptibility to the fungus. Physiol Mol Plant Pathol 78:1-7.

Yi M and Valent B. 2013. Communication between filamentous pathogens and plants at the biotrophic interface. Annu Rev Phytopathol 51:587-611.

Yu J, Hu S, Wang J, Wong GK, Li S, Liu B, Deng Y, Dai L, Zhou Y, Zhang X, et al. 2002. A draft sequence of the rice genome (oryza sativa L. ssp. indica). Science 296(5565):79-92.

Yuan M, Chu Z, Li X, Xu C, Wang S. 2010. The bacterial pathogen xanthomonas oryzae overcomes rice defenses by regulating host copper redistribution. Plant Cell 22(9):3164-76.

Zandvakili N, Zamani M, Motallebi M, Moghaddassi Jahromi Z. 2017. Cloning, overexpression and in vitro antifungal activity of zea mays PR10 protein. Iran J Biotechnol 15(1):42-9.

Zhang H. 2023. Plant latent defense response against compatibility. The ISME Journal 17(6):787-91.

Zhang S and Xu J. 2014. Effectors and effector delivery in magnaporthe oryzae. PLoS Pathog 10(1):e1003826.

Zhang S, Deng YZ, Zhang L. 2018. Phytohormones: The chemical language in magnaporthe oryzae-rice pathosystem. Mycology 9(3):233-7.

Zhang WJ, Zhou Y, Zhang Y, Su YH, Xu T. 2023. Protein phosphorylation: A molecular switch in plant signaling. Cell Rep 42(7):112729.

Zhang Z, Collinge DB, Thordal-Christensen H. 1995. Germin-like oxalate oxidase, a H2O2-producing enzyme, accumulates in barley attacked by the powdery mildew fungus. The Plant Journal 8(1):139-45.

Zhou J and Zhang Y. 2020. Plant immunity: Danger perception and signaling. Cell 181(5):978-89.